UNITED STATES DEPARTMENT OF THE INTERIOR
GEOLOGICAL SURVEY

Petrography of some Ambrosia Lake, New Mexico prefault uranium ores, and implications for their genesis

By

James D. Webster

Open-File Report 83-8
1983

Contents

Page

Abstract....1
Introduction....1
Acknowledgements....2
Methods of Analysis....2
Chemical Analyses....2
Geologic Setting and Stratigraphy....8
Ages and Structural Relationships....11
Geology and Geochemistry of the Ores....12
Characteristics of the host-rocks of the ores of this study....12
Characteristics of the ores of the present study....15
Prefault versus postfault ore....15
Observed ore characteristics....16
Ore characteristics of the Section 30, Section 30-W, and Section 23 mines....16
Characteristics of the detrital phases of this study....17
Characteristics of the ore-related phases of this study....20
Pyrite and marcasite....20
Clausthalite....23
Titanium phases....25
Organic matter....35
Other matrix phases....47
Uranium-bearing phases....47
Discussion....52
Metals and their source....52
Paragenetic model for uranium deposition....53
Summary and conclusions....58
References....59
Appendix....64

Illustrations

Figure 1. Index map of Ambrosia Lake, New Mexico....3
2. Geologic map of the Grants District, New Mexico....9
3. Stratigraphic section of Ambrosia Lake, New Mexico....10
4. Photomicrograph of a barren sandstone sample....13
5. Photomicrograph of organic matrix in an ore sample....14
6. Photomicrograph of an altered titanomagnetite....19
7. Photomicrograph of pyrite replacing an altered titanomagnetite....21
8. Photomicrograph of the V-Ti phase within an altered titanomagnetite....22
9. Photomicrograph of clausthalite and organic matter....24
10. Photomicrograph of anatase replacing an altered titanomagnetite....26
11. Photomicrograph of banded V-Ti phase, silica and organic matter....27
12. Photomicrograph of organic matter replacing an altered titanomagnetite in sample S30W-A2....28
13. Photomicrograph of organic matter replacing an altered titanomagnetite in sample S30-A5....30

Illustrations--continued

Page

14. Photomicrograph of organic matter and ilmenite replacing an altered titanomagnetite.....31
15. Photomicrograph of ilmenite and silica replacing an altered titanomagnetite.....32
16. Photomicrograph of radiating rutile crystals.....33
17. Photomicrograph of a single rutile crystal within zoned matter.....34
18. Photomicrograph of the V-Ti phase replacing an altered titanomagnetite.....36
19. Photomicrograph of organic matter replacing an altered titanomagnetite grain.....37
20. SEM photomicrograph of highly zoned organic matter.....39
21. Sketch displaying the textural differences between light and dark, zoned organic matter.....40
22. Photomicrograph of folded, zoned organic matter.....41
23. SEM photomicrograph of zoned organic matter.....43
24. SEM X-ray map for U of the same region seen in figure 23.....44
25. SEM photomicrograph of zoned organic matter.....45
26. SEM X-ray map for U of the same region seen in figure 25.....46
27. Photomicrograph of the chert rosette.....48
28. Photomicrograph of the matrix of a low grade ore sample.....50
29. Fission track map of the low grade sample seen in figure 28 showing the U distribution in the sandstones matrix.....51
30. Photomicrograph of compressed and folded organic matter which is strongly zoned.....56

Tables

Page

Table I. Chemical analyses of samples from Sections 30, 30W, and 23 mines in Ambrosia Lake uranium mining district showing selected major and trace elements.....4
Table II. Chemical analyses from Ambrosia Lake uranium mining district showing major elements of oxides, carbon, sulfur, molybdenum, selenium, and vanadium.....7

ABSTRACT

Petrographic and chemical study of prefault uranium ores from the Section 30, Section 30-west, and Section 23 mines in the Ambrosia Lake mining district, New Mexico has revealed that prefault ores commonly contain several authigenic phases including a new V-Ti mineral, which formed from destruction and remobilization of primary constituents in Ti-magnetites. High-grade ore samples also contain diagenetic clausthalite. Microprobe and SEM/EDS study indicate high U concentrations along the contacts of organic matter and surrounding detrital grains. The cores of the organic matter which fill pore spaces are commonly very low in U, as well as Si, Al, V, and Fe. Petrographic relationships as well as the chemistry and U distribution of the titanomagnetite grains and organic matter imply that the U was introduced to the sediments after the organic matter was emplaced and before the sediments were compacted.

INTRODUCTION

Arkosic sandstones of the Jurassic Morrison Formation in the Grants Mineral Belt, New Mexico contain the largest uranium reserves in the United States. Granger (1963) was the first to distinguish prefault ore from postfault ore in Ambrosia Lake. The prefault ore is intimately intergrown with organic matter. Post-fault ore is secondary or redistributed ore which is never associated with organic matter but is controlled by Laramide and later faulting, may have a roll-front geometry and is located at redox interfaces. Unfortunately, the extremely fine grain size of the uraniferous phases, which are intermixed with authigenic organic matter, clays, and silica, has inhibited the identification of the uranium minerals. Granger (1963) reports coffinite peaks in X-ray patterns of prefault ore samples, but little coffinite has been petrographically identified. Coffinite and uraninite are easily identified in postfault ore samples, however. The purpose of this study was to observe the occurrence of the primary prefault uranium ores in Ambrosia Lake, and to determine the nature of the uranium phases. Therefore, this study will address only post-fault ore in the general discussion of the introduction. This report is concerned only with primary ore.

There are three important questions which concern the Ambrosia Lake prefault ores. 1) What are the relationships of the organic matter to U-mineralization? 2) What is the timing of the U-mineralization? 3) What are the U-phases which make up the mineralization? This study shows that uranium is not homogeneously distributed within the organic matrix, but is, instead, concentrated along the organic boundary with surrounding detrital grains. Based on the microscale zonations of U and the colloform textures of the U-bearing organic matter, the mineralization event must have occurred before the sediments were greatly compacted and subsequently dewatered. The prefault U-phases include minor coffinite and much U adsorbed to the organics, clays, silica, and Fe-Ti oxides of the matrix.

Acknowledgements

I would like to thank Ralph Christian for help with the electron microprobe, James Nishi for teaching me the use of the SEM/EDS, and Robert A. Zielinski for help with the fission-track maps. Joel S. Leventhal helped greatly in the interpretation of the chemical data. My greatest appreciation goes to Craig Simmons, Harry C. Granger and Kenneth R. Ludwig for many hours of stimulating discussion.

Ore samples for this study were collected from the Section 30, Section 30-W and Section 23 mines in Ambrosia Lake, as shown in figure 1. The Section 30 and 30-W mines are the property of Kerr-McGee Corporation and the Section 23 mine belongs to United Nuclear-Homestake Partners. The sampling sites in the Section 30 mine were located with the help of Robert Malone and Charles Lafkoff. Steve Huddlestone helped in sampling of the Section 30-W mine, and William Harrison and Phil Gray helped in the Section 23 mine.

Methods of analysis

Thirty-three polished thin sections and nine polished sections were prepared from 2 barren and 18 ore samples collected in the Sections 30, 30 west (abbreviated 30W), and Section 23 mines in the Westwater Canyon Member of the Morrison Formation. The petrographic descriptions and photomicrographs in this report are the result of the petrographic study of samples using a Zeiss-transmitted and reflected light microscope equipped with a photomicrographic camera. Chemical analyses, both qualitative and quantitative, were performed with the scanning electron microscope equipped with an energy-dispersive X-ray fluorescence analyzer (abbreviated SEM/EDS) and the electron microprobe. The changes in concentration of U, Si, Al, Fe, V, K, S and Pb within the matrix were observed through X-ray fluorescence mapping and line scans on both the SEM/EDS and electron microprobe (at the one-half percent limit of detection). The electron beam was run across the surface of the matrix, between detrital grains, and any corresponding changes in elemental concentrations were recorded. Fission-track maps showed which matrix regions were high in U and which regions were low. By varying the nuclear reactor irradiation time of the ore samples, the optimum fission-track density for samples was determined. Muscovite was used as the fission track detector which was taped to the surface of the polished thin section before irradiation. After irradiation, the muscovite detector was etched in hydrofluoric acid, rinsed and mounted on a glass slide.

Chemical analyses

The major elements Table I, reported in parts per million, were measured by X-ray fluorescence (XRF) after ashing the samples at 900°C. The samples were ashed at 900°C to measure the loss-on-ignition (LOI), reported in weight percent (Table II). Selenium was measured semi-quantitatively by XRF on a separate sample split without ashing at 900°C. Major-element, LOI, and Se analyses were performed by J. S. Wahlberg, J. Taggart, and J. Baker of the Branch of Analytical Laboratories, U.S. Geological Survey, Denver, Colorado.

All trace elements reported in Table I except Mo, V, and Se were measured semi-quantitatively by inductively coupled plasma optical emission spectroscopy (Taggart, Lichte and Wahlberg, 1981). All of the trace elements,

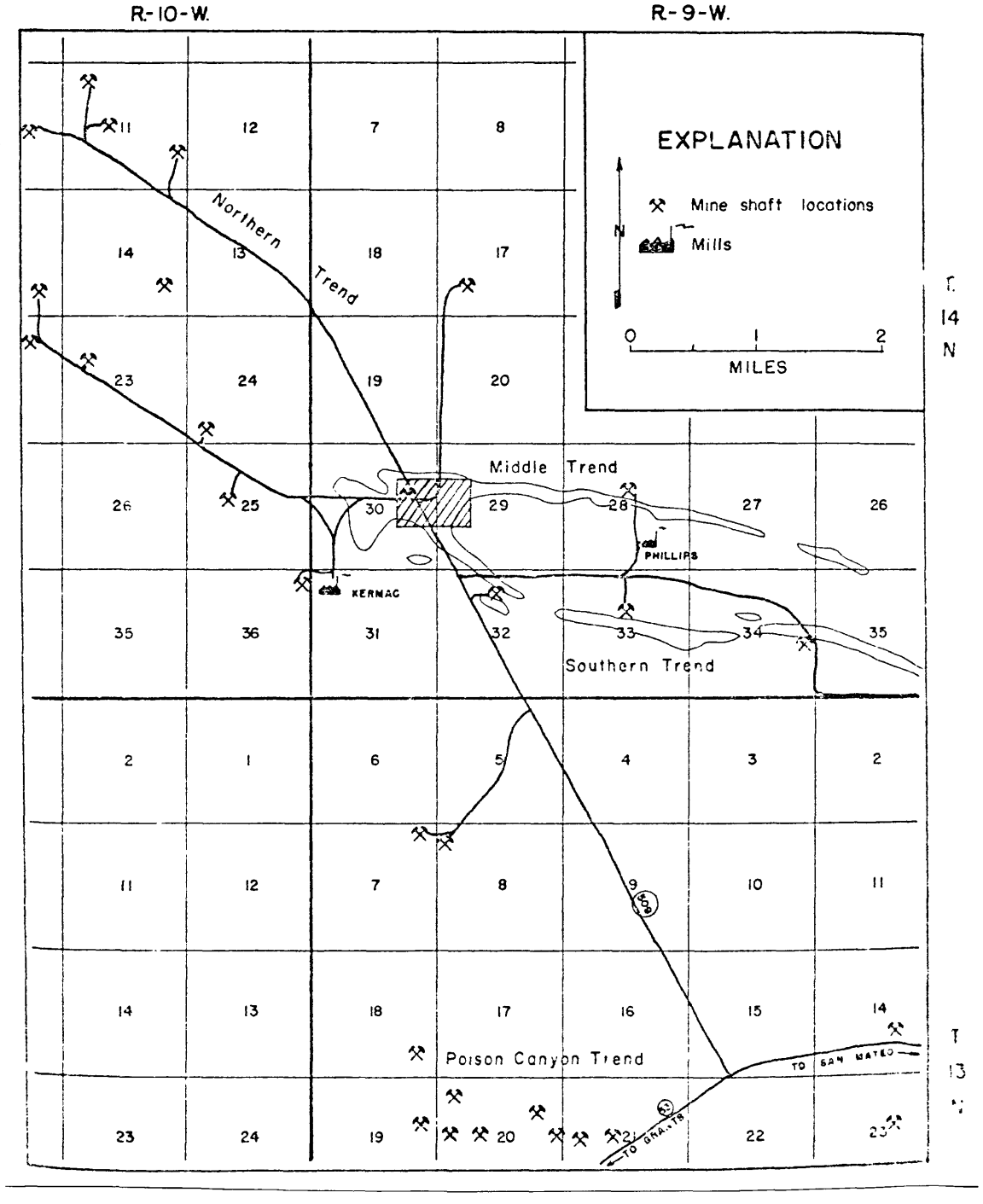

Figure 1.--Location map of part of the Ambrosia Lake area (modified from Clary and others, 1963).

Table I.--Chemical analyses of samples from Sections 30, 30W, and 23 mines in the Ambrosia Lake uranium mining district showing selected major and trace elements.

LAB NO.		D-230325	D-230326	D-230327	D-230328	D-230329	D-230330	D-230331	D-230332
FIELD NO.		S30-NM-A4	S23-A2	S30W-A1	S23-A5	S30W-A3M	S23-NM-A1	S23-A4	S30W-A2
FE	%-S	0.58	0.97	1.5	2.7	2.0	1.4	3.7	3.0
MG	%-S	0.16	0.12	0.20	0.07	0.32	0.20	0.50	0.38
CA	%-S	7.6	2.4	6.0	31.	0.87	0.64	0.34	0.19
TI	%-S	0.07	0.14	0.03	0.01	0.09	0.19	0.08	0.10
MN	PPM-S	1100.	590.	940.	1400.	180.	340.	390.	300.
AG	PPM-S	-	-	-	-	-	-	-	-
AU	PPM-S	-	-	-	-	-	-	-	-
BA	PPM-S	360.	450.	510.	60.	40.	200.	90.	150.
BE	PPM-S	<2.	<2.	<2.	7.	<2.	<2.	2.	2.
BI	PPM-S	<20.	<20.	<20.	<20.	<20.	<20.	<20.	<20.
CD	PPM-S	<5.	<5.	<5.	<5.	<5.	<5.	<5.	<5.
CO	PPM-S	<2.	<2.	<2.	<2.	2.	2.	3.	2.
CR	PPM-S	5.	30.	20.	5.	4.	20.	16.	12.
CU	PPM-S	3.	6.	7.	<2.	2.	4.	8.	<2.
LA	PPM-S	13.	20.	30.	80.	20.	30.	30.	40.
MO	PPM-S	- *1	- *1	- *1	- *1	- *1	- *1	- *1	- *1
NB	PPM-S	8.	17.	20.	10.	25.	30.	20.	55.
NI	PPM-S	19.	4.	<2.	<2.	<2.	<2.	<2.	<2.
PB	PPM-S	14.	19.	60.	110.	55.	20.	60.	150.
SC	PPM-S	<2.	<2.	<2.	<2.	<2.	<2.	4.	<2.
SN	PPM-S	<9.	<9.	<9.	<9.	<9.	<9.	<9.	12.
SR	PPM-S	140.	110.	150.	1600.	90.	85.	80.	70.
U	PPM-S	120.	260.	3000.	1500.	2600.	4700.	5300.	13000.
V	PPM-S	- *1	- *1	- *1	- *1	- *1	- *1	- *1	- *1
W	PPM-S	<10.	<10.	<10.	<10.	<10.	<10.	<10.	<10.
Y	PPM-S	20.	7.	6.	80.	20.	14.	80.	11.
ZN	PPM-S	24.	40.	20.	30.	20.	14.	55.	28.
AL	%-S	3.0	3.0	3.6	0.28	2.7	3.0	3.7	3.1
NA	%-S	0.60	1.0	0.95	0.33	0.58	0.90	0.71	0.65
K	%-S	2.0	1.4	2.0	0.75	1.2	0.95	1.5	1.1
P	%-S	0.01	0.01	0.01	11.0	0.17	0.03	0.02	0.02
CE	PPM-S	<20.	40.	20.	70.	110.	50.	100.	70.
GA	PPM-S	<4.	9.	30.	15.	25.	40.	50.	100.
GE	PPM-S	<2.	<2.	4.	6.	<2.	7.	<2.	20.
LI	PPM-S	8.	15.	20.	10.	20.	10.	30.	30.
TA	PPM-S	<10.	<10.	<10.	<10.	<10.	<10.	<10.	<10.
TH	PPM-S	7.	5.	5.	50.	5.	6.	<5.	20.
YB	PPM-S	<1.	<1.	<1.	6.	<1.	<1.	3.	<1.
ZR	PPM-S	<10.	<10.	<10.	40.	20.	20.	30.	10.
ND	PPM-S	<5.	20.	<5.	30.	20.	20.	80.	30.
SM	PPM-S	11.	10.	9.	25.	6.	6.	15.	<5.
EU	PPM-S	<5.	<5.	<5.	<5.	<5.	<5.	<5.	<5.
GD	PPM-S	<10.	<10.	20.	<10.	20.	25.	40.	80.
TB	PPM-S	<10.	<10.	20.	<10.	<10.	<10.	20.	40.
DY	PPM-S	<10.	<10.	<10.	<10.	<10.	<10.	<10.	<10.
HO	PPM-S	<5.	<5.	<5.	<5.	<5.	<5.	<5.	<5.
ER	PPM-S	<5.	<5.	<5.	-	<5.	<5.	<5.	<5.
TM	PPM-S	<5.	<5.	<5.	<5.	<5.	<5.	<5.	<5.
YB	PPM-S	-	-	-	-	-	-	-	-

All trace elements in ppm.
*(-*1) signifies trace trace elements measured by quantitative emission spectroscopy.
*(-) signifies trace elements not measured.
0(<10) signifies the measured values were below thelimit of detection, in this case the limit of detection is 10 ppm.

Table I.--Chemical analyses of samples from Sections 30, 30W, and 23 mines in the Ambrosia Lake uranium mining district showing selected major and trace elements.--continued

LAB NO.		D-230333	D-230334	D-230335	D-230336	D-230337	D-230338	D-230339	D-230340
FIELD NO.		S30-A8	S30-A10-3	S30-A9	S30-A10-2	S30-A10-1	S30-NM-A10-4	S30-A10-5	S30-A6
FE	%-S	2.1	2.6	2.0	2.8	2.3	2.0	1.6	3.8
MG	%-S	0.47	0.70	0.43	0.58	0.65	0.66	0.48	1.0
CA	%-S	0.38	0.34	0.34	0.35	0.34	0.34	0.33	0.51
TI	%-S	0.21	0.21	0.24	0.20	0.20	0.22	0.19	0.07
MN	PPM-S	550.	880.	530.	660.	730.	890.	800.	890.
AG	PPM-S	-	-	-	-	-	-	-	-
AU	PPM-S	-	-	-	-	-	-	-	-
BA	PPM-S	100.	160.	100.	100.	50.	80.	60.	110.
BE	PPM-S	6.	8.	5.	6.	8.	10.	8.	20.
BI	PPM-S	<20.	<20.	<20.	<20.	<20.	<20.	<20.	<20.
CD	PPM-S	<5.	<5.	<5.	<5.	<5.	<5.	<5.	<5.
CO	PPM-S	6.	3.	10.	4.	3.	3.	5.	30.
CR	PPM-S	20.	70.	30.	50.	40.	60.	70.	10.
CU	PPM-S	3.	15.	4.	<2.	<2.	<2.	<2.	<2.
LA	PPM-S	100.	80.	110.	80.	70.	60.	100.	40.
MO	PPM-S	- *1	- *1	- *1	- *1	- *1	- *1	- *1	- *1
NB	PPM-S	300.	490.	270.	330.	460.	540.	410.	2300.
NI	PPM-S	5.	9.	6.	<2.	5.	6.	<2.	20.
PB	PPM-S	140.	120.	120.	160.	150.	110.	190.	160.
SC	PPM-S	2.	<2.	<2.	<2.	<2.	<2.	<2.	4.
SN	PPM-S	<9.	14.	10.	<9.	<9.	<9.	12.	22.
SR	PPM-S	170.	170.	170.	170.	160.	170.	160.	180.
U	PPM-S	-	24000.	18000.	20000.	25000.	26000.	30000.	52000.
V	PPM-S	- *1	- *1	- *1	- *1	- *1	- *1	- *1	- *1
W	PPM-S	<10.	<10.	<10.	<10.	<10.	<10.	<10.	<10.
Y	PPM-S	90.	15.	30.	20.	14.	14.	30.	660.
ZN	PPM-S	6.	60.	35.	50.	65.	80.	60.	70.
AL	%-S	4.3	4.5	4.4	4.5	4.4	4.5	4.3	3.9
NA	%-S	1.2	0.99	1.2	1.1	1.0	1.0	1.1	0.15
K	%-S	1.8	1.8	1.7	1.3	1.6	1.4	1.7	2.1
P	%-S	0.02	0.01	0.02	0.01	0.01	0.01	<0.01	0.06
CE	PPM-S	200.	100.	160.	170.	110.	100.	170.	160.
GA	PPM-S	130.	140.	120.	120.	150.	150.	200.	150.
GE	PPM-S	<2.	<2.	<2.	<2.	<2.	<2.	5.	<2.
LI	PPM-S	40.	50.	30.	50.	50.	50.	40.	60.
TA	PPM-S	<10.	<10.	<10.	<10.	<10.	<10.	<10.	<10.
TH	PPM-S	26.	30.	20.	20.	30.	30.	40.	70.
YB	PPM-S	3.	<1.	<1.	<1.	<1.	<1.	<1.	50.
PR	PPM-S	30.	15.	20.	20.	15.	<10.	30.	12.
ND	PPM-S	100.	50.	70.	60.	50.	50.	100.	100.
SM	PPM-S	13.	<5.	<5.	7.	<5.	<5.	9.	<5.
EU	PPM-S	<5.	<5.	<5.	<5.	<5.	<5.	<5.	<5.
GD	PPM-S	110.	110.	100.	100.	110.	120.	170.	170.
TP	PPM-S	40.	40.	30.	40.	30.	50.	60.	40.
DY	PPM-S	10.	<10.	<10.	<10.	<10.	<10.	<10.	50.
HO	PPM-S	<5.	<5.	<5.	<5.	<5.	<5.	<5.	<5.
ER	PPM-S	-	-	<5.	20.	<5.	<5.	20.	-
TM	PPM-S	<5.	<5.	<5.	<5.	<5.	<5.	<5.	<5.
LU	PPM-S	-	-	-	-	-	-	-	-

Table I.--Chemical analyses of samples from Sections 30, 30W, and 23 mines in the Ambrosia Lake uranium mining district showing selected major and trace elements.--continued

LAB NO.		D-230341	D-230342	D-230343
FIELD NO.		S30-A7	S30-A5	NM-1S30W-A2
FE	%-S	0.74	1.6	3.1
MG	%-S	0.28	0.59	0.39
CA	%-S	0.35	0.41	0.18
TI	%-S	0.11	0.15	0.11
MN	PPM-S	540.	600.	300.
AG	PPM-S	-	-	-
AU	PPM-S	-	-	-
BA	PPM-S	160.	210.	100.
BE	PPM-S	8.	14.	3.
BI	PPM-S	23.	<20.	<20.
CD	PPM-S	<5.	<5.	<5.
CO	PPM-S	6.	20.	3.
CR	PPM-S	15.	16.	13.
CU	PPM-S	<2.	<2.	3.
LA	PPM-S	130.	50.	40.
MO	PPM-S	- *1	- *1	- *1
NB	PPM-S	320.	1000.	80.
NI	PPM-S	4.	18.	<2.
PB	PPM-S	480.	380.	160.
SC	PPM-S	<2.	<2.	<2.
SN	PPM-S	16.	17.	9.
SR	PPM-S	170.	170.	75.
U	PPM-S	52000.	52000.	15000.
V	PPM-S	- *1	- *1	- *1
W	PPM-S	<10.	<10.	<10.
Y	PPM-S	30.	15.	12.
ZN	PPM-S	60.	45.	30.
AL	%-S	3.9	4.3	3.1
NA	%-S	1.1	0.83	0.65
K	%-S	1.8	1.5	1.2
P	%-S	0.01	0.04	0.02
CE	PPM-S	230.	160.	60.
GA	PPM-S	350.	300.	130.
GE	PPM-S	120.	<2.	24.
LI	PPM-S	30.	40.	30.
TA	PPM-S	<10.	<10.	<10.
TH	PPM-S	50.	60.	20.
YB	PPM-S	<1.	<1.	<1.
PR	PPM-S	19.	16.	<10.
ND	PPM-S	120.	90.	40.
SM	PPM-S	6.	<5.	<5.
EU	PPM-S	<5.	<5.	<5.
GD	PPM-S	300.	250.	90.
TB	PPM-S	120.	100.	40.
DY	PPM-S	<10.	<10.	<10.
HO	PPM-S	<5.	<5.	<5.
ER	PPM-S	15.	30.	<5.
TM	PPM-S	<5.	<5.	<5.
LU	PPM-S	-	-	-

Table II.--Chemical analyses of samples from Ambrosia Lake uranium mining district showing major elements of oxides, carbon, sulfur, molybdenum, selenium, and vanadium

MAJOR ELEMENTS*

Field Number	NM-S30-A4	NM-S23-A2	NM-S30W-A1	NM-S23-A5	NM-S30W-A3R	NM-S23-A1	NM-S23-A4	NM-S30W-A2	NM-S30-A8	NM-S30-A10-3	NM-S30-A9	NM-S30-A10-2	NM-S30-A10-1	NM-S30-A10-4	NM-S30-A10-5	NM-S30-A7	NM-S30-A5	NM-S30-A6
SiO_2	70.4	80.9	67.9	2.1	87.1	84.4	77.2	79.7	70.2	67.7	74.1	69.3	68.5	68.4	69.3	64.7	64.7	25.8
Al_2O_3	4.9	6.57	6.99	0.4	5.13	5.88	7.48	5.96	8.28	8.69	8.32	8.61	8.38	8.32	7.98	7.63	7.94	6.92
Fe_2O_3	0.81	1.33	2.26	3.91	2.79	1.83	5.52	4.24	2.81	3.54	2.76	3.82	3.15	2.71	2.07	0.89	1.93	4.61
MgO	0.3	0.2	0.4	0.3	0.57	0.4	0.93	0.65	0.84	1.3	0.78	1.1	1.2	1.2	0.85	0.54	1.0	1.8
CaO	11.7	3.49	9.49	49.6	0.71	0.81	0.45	0.24	0.51	0.48	0.47	0.48	0.48	0.47	0.46	0.51	0.56	0.69
Na_2O	0.8	1.3	1.2	0.4	0.7	1.1	0.9	0.9	1.5	1.3	1.5	1.5	1.3	1.3	1.4	1.4	1.1	0.3
K_2O	1.77	1.91	2.41	0.07	1.60	1.83	2.06	1.80	2.45	2.35	2.46	2.31	2.35	2.46	2.49	2.63	2.56	2.68
TiO_2	0.13	0.32	0.04	<0.02	0.18	0.42	0.16	0.19	0.37	0.36	0.43	0.34	0.34	0.35	0.32	0.21	0.25	0.10
P_2O_5	<0.1	<0.1	<0.1	25.8	<0.1	<0.1	<0.1	<0.1	<0.1	<0.1	<0.1	<0.1	<0.1	<0.1	<0.1	<0.1	0.1	0.2
MnO	0.13	0.06	0.11	0.14	<0.02	0.03	0.04	0.02	0.05	0.09	0.05	0.07	0.07	0.09	0.08	0.05	0.05	0.08
LOI	9.21	3.01	7.31	8.78	1.95	1.46	3.61	3.84	7.18	9.26	5.00	7.91	9.12	8.85	8.62	11.6	8.76	41.9

*All major elements and loss-on-ignition (LOI) reported in weight percent.

CARBON AND SULFUR*

Field Number	NM-S30-A4	NM-S23-A2	NM-S30W-A1	NM-S23-A5	NM-S30W-A3R	NM-S23-A1	NM-S23-A4	NM-S30W-A2	NM-S30-A8	NM-S30-A10-3	NM-S30-A9	NM-S30-A10-2	NM-S30-A10-1	NM-S30-A10-4	NM-S30-A10-5	NM-S30-A7	NM-S30-A5	NM-S30-A6
Total S	0.14	0.51	0.76	3.63	0.49	0.44	1.08	0.94	1.80	1.51	1.48	1.92	1.38	1.01	0.99	0.57	0.82	3.29
Total C	2.35	0.72	2.11	3.84	0.46	0.14	0.85	1.48	2.80	4.35	1.47	3.34	4.26	4.39	4.45	6.61	3.55	26.5
Organic C	0.01	0.04	0.39	0.76	0.46	0.07	1.03	1.49	2.8	4.2	1.5	3.3	4.3	4.4	4.5	6.6	3.6	26.2

*All C and S data reported in weight percent.

ADDITIONAL TRACE ELEMENTS[0]

Field Number	NM-S30-A4	NM-S23-A2	NM-S30W-A1	NM-S23-A5	NM-S30W-A3R	NM-S23-A1	NM-S23-A4	NM-S30W-A2	NM-S30-A8	NM-S30-A10-3	NM-S30-A9	NM-S30-A10-2	NM-S30-A10-1	NM-S30-A10-4	NM-S30-A10-5	NM-S30-A7	NM-S30-A5	NM-S30-A6
Mo	3.0	<2.0	<2.0	200.0	40.0	<2.0	<2.0	30.0	2000.0	220.0	410.0	1060.0	260.0	90.0	1180.0	1760.0	1600.0	6170.0
Se	0.6	1.4	75.0	130.0	74.0	59.0	270.0	180.0	280.0	160.0	120.0	310.0	110.0	63.0	120.0	260.0	310.0	870.0
V	13.0	45.0	180.0	220.0	270.0	210.0	170.0	500.0	4500.0	8000.0	4100.0	5100.0	7300.0	8750.0	6250.0	4100.0	16500.0	40200.0

[0]Mo, Se and V reported in parts per million (ppm).

including Mo, V, and Se are reported in parts per million (ppm). The Mo and V were quantitatively measured by quantitative emission spectroscopy. All trace-element analyses, except for Se, were performed by F. E. Lichte and G. Shipley of the Branch of Analytical Laboratories, U.S. Geological Survey, Denver, Colorado.

All S and C values are reported in weight percent in Table II. Total C, organic C, and total S analyses, by LECO, were performed by Mark Stanton of the Branch of Uranium and Thorium, U.S. Geological Survey, Golden, Colorado. Percent organic carbon was measured by ashing at 450°C. The loss on ignition (LOI) is also reported, and is equivalent to 100 percent minus ash percent.

The chemical concentrations reported in Tables I and II are listed by field numbers. The first sample, NM-S30-A4, was collected in New Mexico (NM), from the Section 30 mine (-30-) and is sample number (A4) from that mine. This method of cataloging is used for barren and ore samples. Only 2 samples were barren. These are samples NM-S30-A4 and NM-S23-A2. The remaining 17 samples are sufficiently concentrated in U to have been mined as ore.

Geologic setting and stratigraphy

The Grants mineral belt, which contains the Laguna, Ambrosia Lake, and Gallup mining districts (Hilpert, 1963), parallels the southern margin of the San Juan Basin (fig. 2). The belt extends east-west for approximately 160 km between Gallup and Canoncito and is approximately 40 km wide. The Ambrosia Lake district is situated approximately 14 km north of Grants. The Ambrosia Lake ore deposits occur dominantly in the Westwater Canyon Member of the Morrison Formation and the Todilto Limestone both of Jurassic age (fig. 2). Todilto uranium ores are contained in the limestone and are localized by structures interpreted as either biogenic reefs or as soft-sediment deformational features (Perry, 1963; McLaughlin, 1963; Green, 1981). The U occurs as primary pitchblende and as secondary uranyl vanadates and silicates (McLaughlin, 1963).

Todilto Limestone is overlain by the Summerville Formation, the Bluff Sandstone and the Morrison Formation, all of Jurassic age. Minor amounts of ore in the Summerville are associated with orebodies immediately below in the Todilto Limestone. No uranium ore is known in the Bluff Sandstone. Conformably overlying the Bluff is the Morrison Formation, the major ore producer of the Grants mineral belt.

Although the Morrison Formation consists of four members elsewhere on the Colorado Plateau, locally the Morrison Formation consists only of the Recapture, Westwater Canyon, and Brushy Basin Members (fig. 3). The Recapture consists of quartzose sandstones and intercalated mudstones which are interpreted as overbank and floodplain deposits (Cadigan, 1967). The Recapture also contains significant devitrified and argillized remnants of volcanic ash (Granger and others, 1980; Galloway, 1980). Green (1975) states that the upper one-third of the Recapture (predominantly first-cycle arkosic to subarkosic, conglomeratic sandstones) was probably derived from a source area south-southwest of Gallup. Granger and others (1980) support a source in west-central Arizona. Cadigan's (1967) detailed petrographic study delineates

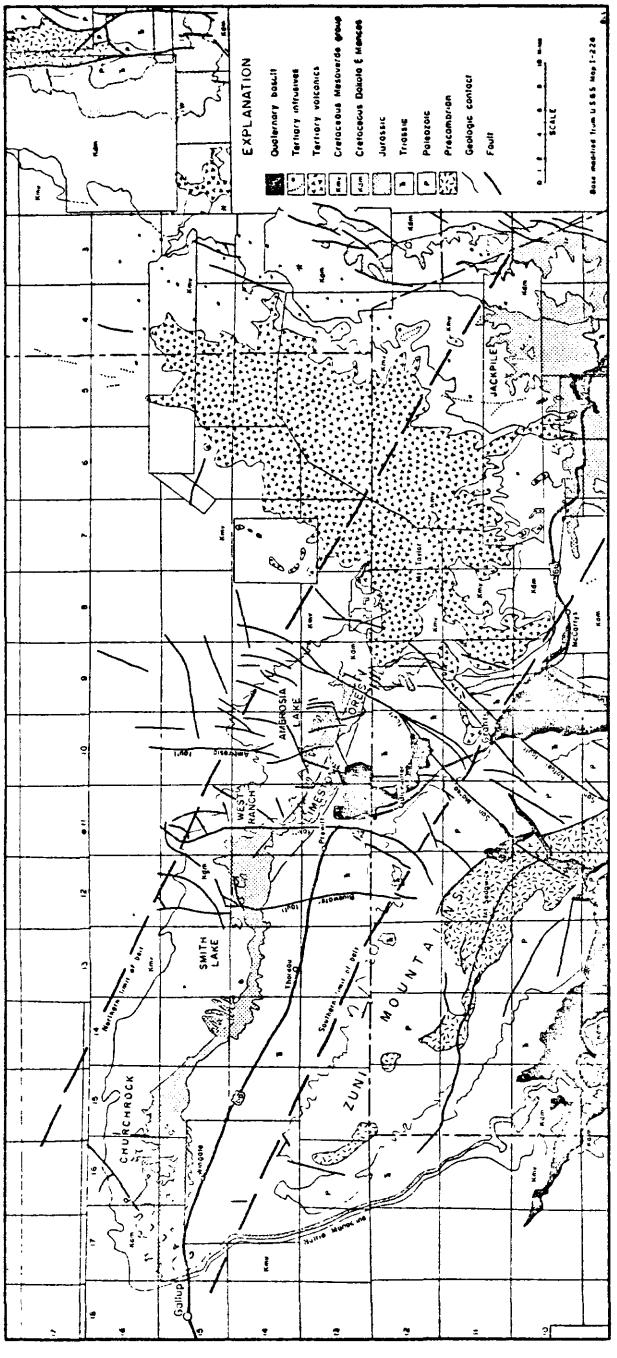

Figure 2.--Geologic map of the Grants region, showing the Grants mineral belt, the limestone ore trend, and mining areas (from Laverty and others, 1963).

Stratigraphic section,
Ambrosia Lake area, McKinley and Valencia Counties, New Mexico

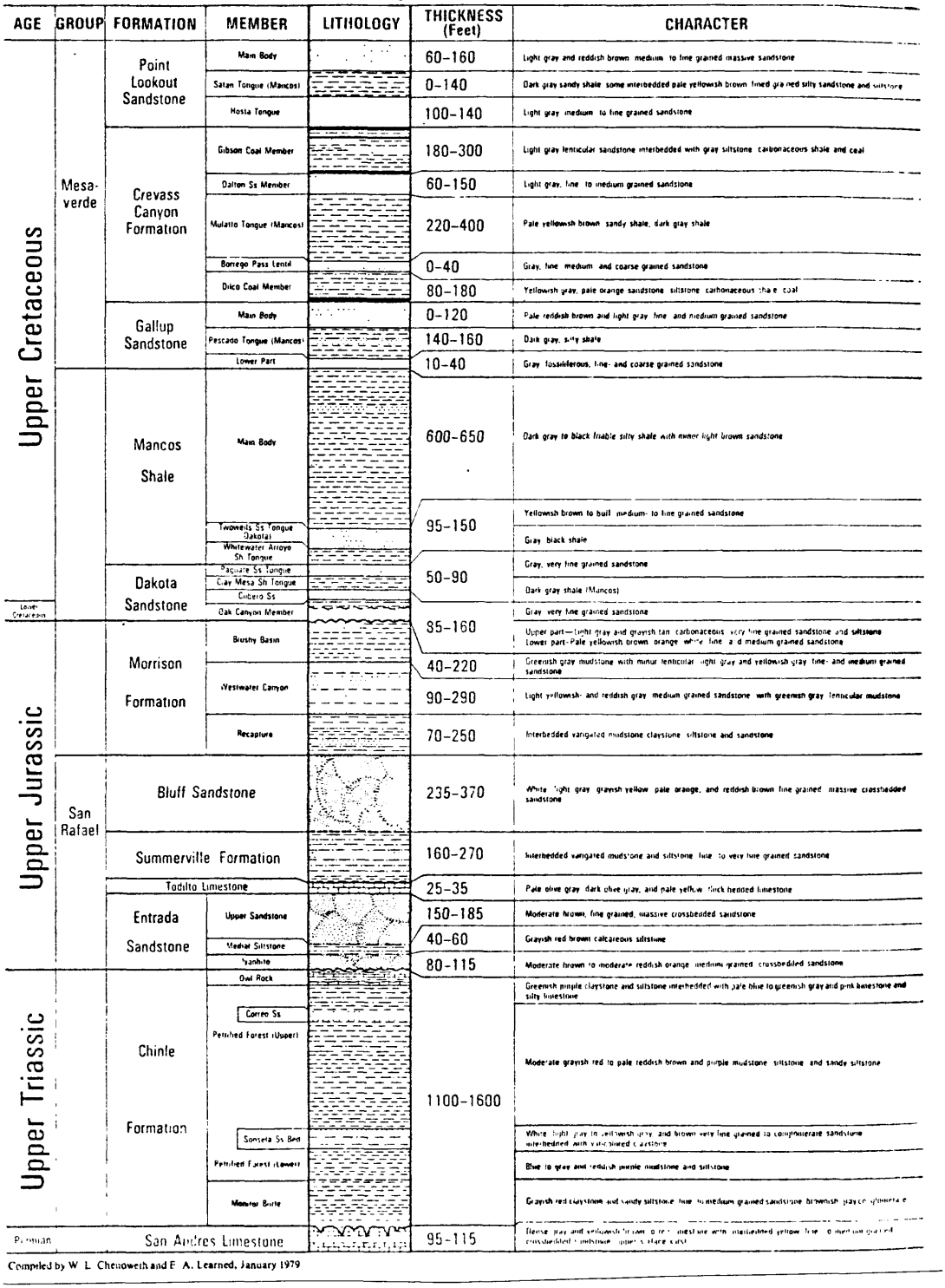

Figure 3.--Stratigraphic column for the Ambrosia Lake mining district (from Chenoweth and Learned, 1979).

the sources for the major constituent detritus as including Utah, Arizona and central New Mexico. The Recapture has only a few minor uranium deposits located only in the upper one-third of the member in Ambrosia Lake.

The Westwater Canyon Member, deposited from braided streams on a wedge-shaped alluvial fan complex, is the predominant ore-bearing member in the Morrison Formation (Granger and others, 1980). The Westwater Canyon Member ranges in thickness from 15 m to 76 m (Fitch, 1980) and is gradationally distinct from the underlying Recapture (Cadigan, 1967). The sands of the Westwater Canyon Member are mostly gray to yellow-brown, fine- to coarse-grained, poorly-sorted, and are cross-bedded with minor intercalated seams of gray mudstone and siltstone (Cadigan, 1967). Silicified, carbonized and uranium-bearing plant and tree fragments occur throughout the member. Cross-bedding trends are to the southeast in the lower part of the Westwater Canyon Member, whereas the foresets dip more to the northeast higher in the member (Cadigan, 1967).

The uppermost member of the Morrison Formation is the Brushy Basin Member. Granger and others (1980), Cadigan (1967), Hilpert (1963), and Squyres (1969), (1980) all support the view that the predominantly montmorillonitic clays and zeolites are the altered remnants of volcanic ash, and consider the Brushy Basin Member as a possible source of uranium in the underlying Westwater Canyon. Interfingered with the bentonitic shales are lenticular sandstone bodies, one of which is the major ore carrier in the Laguna district, the Jackpile sandstone. The sandstone lenses in the Brushy Basin appear to have been deposited in small flexures which resulted from penecontemporaneous folding (Adams and others, 1978).

The Dakota Sandstone, the Mancos Shale and Mesaverde Group, all of Cretaceous age overlie the Morrison Formation. No ore has been located in the Mancos Shale or Mesaverde Group, to date, but a large quantity of ore has been mined from the Dakota. These units are also important sources of oil and coal.

Ages and structural relations

Isotopic dating of the ores and host sediments in the Grants region includes Rb-Sr dates on associated clays and chlorite by Brookins (1980), U-Pb dates by Miller and Kulp (1963), and U-Pb dates by Berglof (1970). Brookins (1980) gives a Rb-Sr apparent age of 139± 24 million years (at the 95 percent confidence limit) to what he terms chlorite-rich ore-zone material in the Westwater Canyon and Brushy Basin sandstones. For the Jackpile ore, Brookins gives a 110 and 115 million year age. The validity of Brookins' ages are, however, dependent on whether or not chlorite is syn-depositional with the ore and whether or not the parent-daughter relationship has remained a closed system since formation. Miller and Kulp (1963) report $^{207}Pb/^{235}U$ ages of 107 ± 6 m.y. for an ore sample from the Todilto Limestone of Ambrosia Lake, whereas Berglof (1970) reports a 94 ± 3 m.y. age for an ore sample from the Jackpile sandstone.

The Ambrosia Lake District is centered on a major fault zone of the Grants mineral belt, is bounded on to the east by the Mt. Taylor volcanic

field and to the south by the Zuni Mountains. Chronologically the mineralization events (both prefault and postfault) fit into a geological scheme including: 1) pre-Dakota intraformational folding; 2) prefault mineralization; 3) post-Dakota folding and faulting, including uplift of the Zuni Mountains, formation of the San Juan basin, Acoma sag and McCartys syncline, as well as the major faults (the San Rafael, San Mateo, Ambrosia Lake, Zuni, and Bluewater-figure 2); 4) Eocene uplift and erosion; 5) possible postfault remobilization of ores; 6) Pliocene rejuvenation of the New Mexico Rocky Mountains, subsidence of the Rio Grande trough, and the first eruptions of the Mt. Taylor volcanic field; and 7) a second possible period of ore remobilization (Hilpert and Moench, 1960; Kelley, 1963; Moench, 1963; Moench and Schlee, 1967; Santos, 1970; Brookins, 1980; Saucier, 1980; and Adams and others, 1978).

Folding of the sediments while they were being deposited is indicated by soft-sediment slump breccias, intraformational folds and by cylindrical, sandstone pipes (Kelley, 1963). Intraformational folds within the Todilto served to localize Todilto ores. Sandstone pipes penetrate both the Bluff Sandstone and the Morrison Formation. The Woodrow pipe in the Laguna mining district is mineralized, however, most pipes are not (Wylie, 1963). The sandstone cylinders are as large as 100 m in diameter and 100 m in height, and are believed to be a result of sediment subsidence due to karst-type solution of underlying limestone (Schlee, 1963). Schlee (1963) gives an excellent description of their characteristics and occurrence, and Nash (1968) reports that over 600 sandstone pipes have been found in northwest New Mexico. Within the Laguna district, sandstone pipes tend to occur along the flanks of the larger pre-Dakota folds (Schlee, 1963).

GEOLOGY AND GEOCHEMISTRY OF THE ORES

Characteristics of the host-rocks of the ores of the present study

The sandstones of the Westwater Canyon Member of the Morrison Formation are the ore host in the Section 30, Section 30-W, and Section 23 mines. The following discussion is based on my petrographic observations. With 40 to 80 percent quartz and 10 to 40 percent feldspar, the sandstones range from sub-arkosic to arkosic. An example of a calcite-cemented sandstone is seen in figure 4. Cements include organic material, chert, calcite, and pyrite. The dominant cementing agents are chert and organic material (fig. 5). The matrix, which consists of various amounts of organic matter, clays, silica (as chert and fine dust-like crystals of silica), anatase, iron oxides and pyrite, can make up to 20 percent of the sandstones. The usual well-sorted nature of the arkoses commonly requires the matrix to be less than 5 percent of the sandstone. Detrital accessory minerals observed in the barren and prefault ore samples include: biotite, volcanic rock fragments, chert fragments, silicified-limestone fragments, zircon, pyroxenes, apatite, muscovite, sphene and epidote. Authigenic, epigenetic, and diagenetic constituents are montmorillonite, chlorite, kaolinite, anatase, ilmenite, rutile, V-Ti phase, clausthalite, coffinite (uraninite in postfault ores), and jordisite.

Commonly the arkoses are moderately sorted to well-sorted, fine- to medium-grained sandstones and siltstones. The grains are sub-angular to well-rounded, tabular to spheroidal. Detrital clay within the sandstones is very

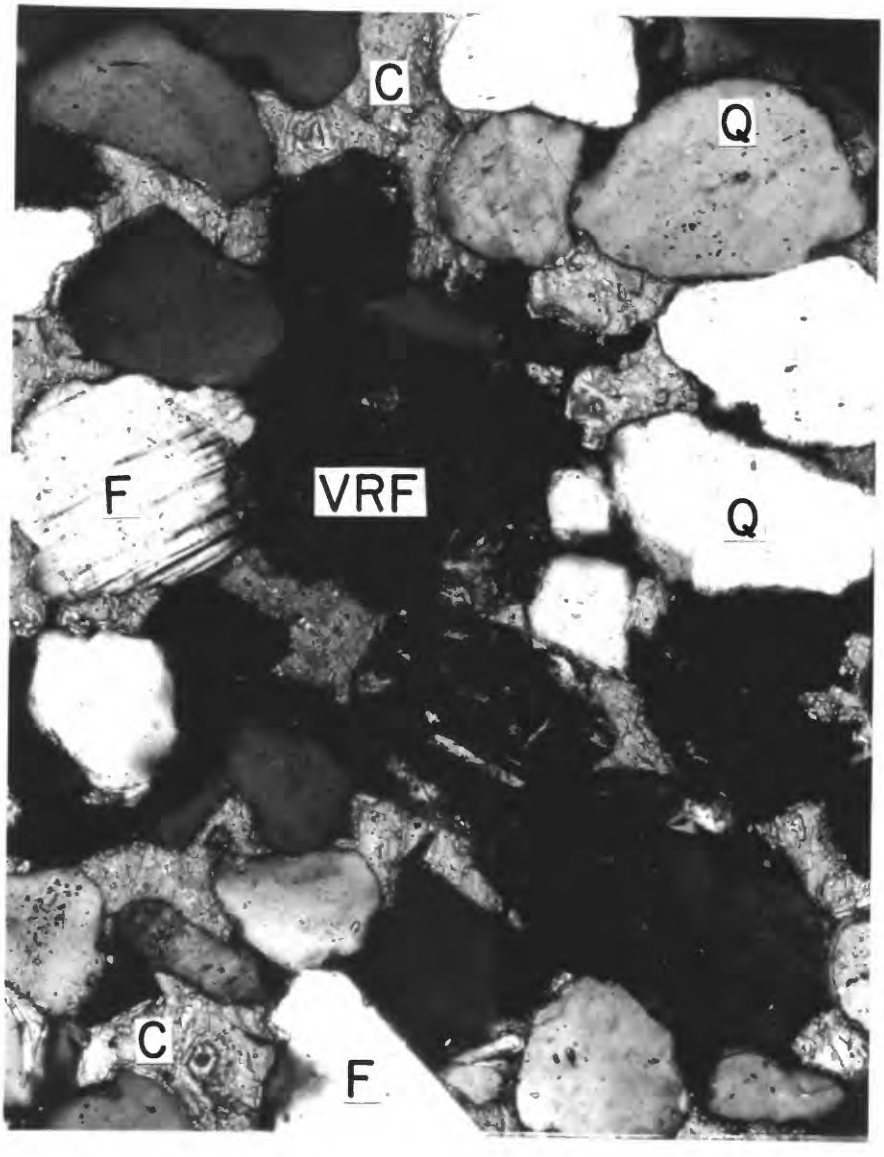

Figure 4.--Photomicrograph of calcite-cemented, barren, arkosic sandstone. Displays quartz (Q), feldspar (F), and 2 large volcanic rock fragments (VRF) in center -- note plagioclase laths in upper VRF. Calcite cement is (C). Sample is from the section 30 mine (sample # NM-S30-A4). Transmitted light view of polished thin section, crossed nichols, field length is 1.0mm.

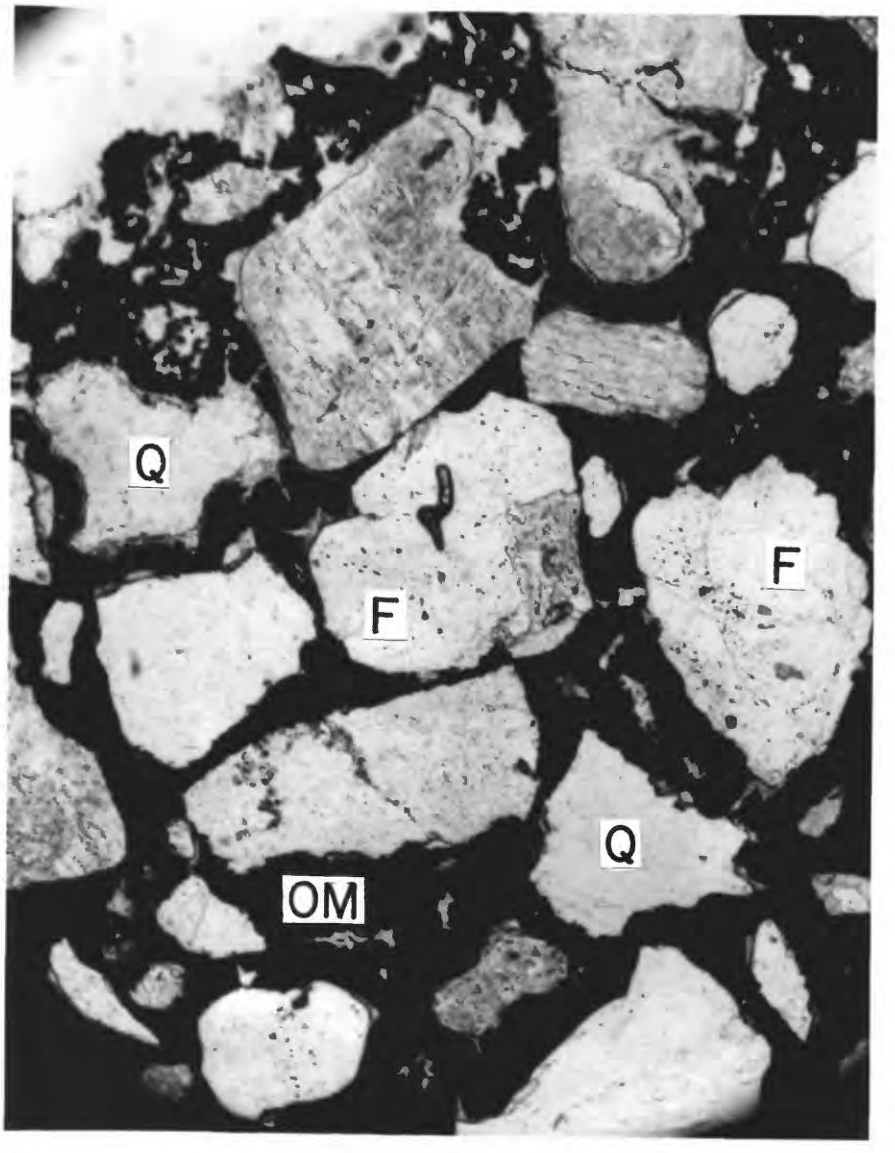

Figure 5.--Photomicrograph showing sand grains and matrix partly replaced by organic matter (O.M.); embayed quartz (Q) and silica overgrowths and feldspar (F). Transmitted light view of polished thin section from the section 30 mine (sample # NM-S30-A7), field length is 2.0mm.

minor. The average grain size range is from 0.10 to 0.45 mm with a mode of 0.20 mm. The sandstones are white or gray to pale greenish gray where reduced and tan or buff to dark maroon-red where oxidized. The sandstones of the Westwater Canyon Member are commonly cross-bedded with abundant scour-and-fill sedimentary structures. Interbedded pale-yellowish-green siltstone and bentonitic mudstone are locally cut by braided channel scours.

Characteristics of the ores of the present study

Prefault versus postfault ore

The uranium deposits of Ambrosia Lake include prefault (also called primary) uranium occurrences and postfault or redistributed ore. Prefault deposits are elongate to tabular masses of authigenic organic material which follow and sometimes cut across scour surfaces, bedding planes, diastems and unconformities (Granger, 1963). There are cases where primary orebodies have been scoured by overlying channel sandstones of the Westwater Canyon Member (Nash, 1968). Primary orebodies may end abruptly along sharp interfaces with barren sandstone or they may feather out along more permeable sandstone layers. Some mudstone conglomerate beds and individual mudstone cobbles are mineralized, whereas the barren conglomerates, which are more tightly bound by carbonate cements, are not.

Prefault ore follows primary sedimentary structures within sandstone beds. Individual ore pods preferentially parallel single channels which may cut across other sandy channels or overbank mudstone units. The more permeable channel lag gravels, common to the stream base, usually contain highly mineralized structured organic material--e.g. logs, limbs, leaves of trees. These uraniferous fossil logs can have uranium content exceeding 15 percent U_3O_8 (Clary et al., 1963).

Prefault uranium orebodies consist of detrital quartz and feldspar, authigenic carbonaceous material (herein termed organics), jordisite, pyrite, titanium phases and uranium, usually reported as coffinite (Granger, 1963). The epigenetic, black organic matter occurs as grain coatings, matrix disseminations, fracture fillings in grains, and, more rarely, as a replacement of detrital grains. Upon closer examination, some of the rounded, detrital-appearing organic masses exhibit fine ghosts of Ti-rich lamellae. These lamellae are remnants of primary titanomagnetite grains which have been chemically attacked by the organic-rich solutions. The detrital, Ti-rich magnetite grains exhibit varying degrees of alteration. The authigenic phases which derive their Ti from the titanomagnetites include anatase, ilmenite, rutile, and an unknown V-Ti mineral. The black, amorphous variety of MoS_2, jordisite, is characteristic of primary ore only. Another mineral common to primary ore is pyrite, which occurs as fine grains, framboids, cement, and as alteration phases.

Postfault ore bodies contain coffinite, uraninite, montroseite, ferroselite, pyrite, marcasite, barite, kaolinite and calcite (Granger, 1963). Their form can include large blocky stacked bodies and vein-like occurrences along post-Dakota age faults. The organic matrix as well as the Mo occurring in the prefault ore is disseminated when the U is remobilized.

Granger (1963) states that pitchblende, which commonly appears in colloform rounded blebs, has been observed only in postfault ore, however. The main U phase is coffinite. Although prefault ore is enclosed by reduced host rocks, postfault ore is enclosed by both oxidized and reduced host rocks. The oxidized sandstones are due to the advance of an oxidizing front through the sandstones. In places, ghost-like remnants of prefault ore are still present within the oxidized sandstones. This observation is especially true in the Section 23 mine. Further discussion of postfault ore will be limited, as this study was primarily involved with prefault mineralogy.

Observed ore characteristics

An unusual feature observed in the Section 23 mine was small ore-filled cylinders, termed ore-rods, extending up from a prefault orebody. Where visible, these rods are from 10 to 15 cm in diameter and from 30 cm to several meters in length. The contact between the outer margin of the ore and the adjacent barren sandstone is knife-sharp. The shape of these ore-filled rods may be due to the way in which the organic matrix was precipitated. Perhaps these are simply small-scale versions of the previously-mentioned sandstone pipes. Similar ore-rods have been observed in the Laguna district (Moench and Schlee, 1967).

Clay galls are intimately mixed with uranium-rich organics. Some of these elongate masses of clay (clay galls) are tan-orange-red in the center with a reduced, green exterior. Squyres (1969) believes that the Morrison sands were originally altered to red beds. Therefore, the clay galls which formed by lateral undercutting of mudstone units when stream channels shifted should also have been an oxidized red at the surface, before reburial. These clay galls are commonly surrounded by small bodies of ore and organics whose exterior margins are sub-parallel to the overall shape of the clay galls. Apparently, the influx of organic-bearing solutions after deposition of the sands caused the reduction of the outer margins of the clay galls and thus produced a green color from ferrous iron. In general, mineralization is concentrated along the base of the channel where the mudstone galls, organic trash, and generally coarser-grained sediments prevail.

Ore characteristics of the Section 30 Section 30-W and Section 23 mines

The Section 30 and 30-W mines are at the intersection of the middle and southern ore trends of the northwestward-oriented Ambrosia Lake ore trend (Clary and others, 1963) (fig. 1). Locally within Section 30 (of the Ambrosia Lake 7 1/2^{o} topographic quadrangle), the Westwater Canyon Member consists of four arkosic sandstone lenses (from top to bottom labeled "A" through "D"). Intercalated between the four sands are shaly mudstone units. The largest primary orebodies are always within the "A" and B" sands. These deposits are more continuous in nature than the smaller and more random orebodies of the "C" and "D" sands. The "A" sand deposits range from 30 to 200 m in width and from 1 to 20 m in thickness (Clary and others, 1963). The trend ore of the Ambrosia Lake mining district is associated with what Clary terms "vegetal matter." Clary and others also note that the organic matter, which they propose was precipitated from humic solutions, is less abundant in the "B" sand. As a direct consequence, fewer uranium deposits occur in the "B"

sand. Thus, the presence or absence of organic matter has been cited as a primary control for prefault ore.

Similar orientations are observed between the long dimensions of ore pods, cross-bed foreset trends, the regional ore trend, and mineralized fossil logs. Each of these are generally oriented northwestward. Exceptions to this are due to syn-depositional folding and intraformational faulting which varied the direction of flow of the humic fluids through the sands (Clary and others, 1963). Local faulting redirected the humic solutions such that the organic masses are not sub-parallel to one another.

Due to the overprint of remobilized postfault ore upon the primary ore deposits, the structure and geochemistry of Section 23 are more complicated. In a "snaking" fashion the post-fault ore of the Section 23 mine loops from the northwest to the southeast. Sub-parallel to the northwestward ore trend is a large syncline within Section 23. Gould and others (1963) believe that oxidizing fluids flowed perpendicular to the northwest-southeast ore trend, resulting in an oxidation-reduction front which is now along the southwestern margin of the ore deposits. Compounding the folding in Section 23 is the Ambrosia dome (a small double-flexure with a diameter of approximately 1 km.) to the north, and a series of post-Dakota faults.

The prefault ore of the Section 23 mine occurs throughout the Westwater Canyon sandstones as continuous, thin, elongate ore layers but the postfault ore occurs as thick, relatively equidimensional masses (Gould and others, 1963). Prefault ore ranges from tens to hundreds of meters in width, and as much as a thousand meters in length (Gould and others, 1963). Prefault ore occurs in organic matter within gray, pyritic sandstones. The Section 23 mine also exhibits primary "S" shaped ore as rolls which trend parallel to the long direction of the overall ore (Shawe and Granger, 1965). The rolls occur at predictable intervals of 20 m to 35 m along the ore-strike direction (Gould and others, 1963). The red and buff oxidized sandstones exhibit sharp reaction interfaces which can be observed against postfault ore. Limonite pseudomorphs after pyrite are present in this highly oxidized dark-red to buff sandstone. In general, the ore deposits of the Section 23 mine were controlled by the higher permeability of the coarser-grained sands, the poorer-sorted sands, the regions of increased fracture density, and the Tertiary oxidation-reduction interface (Gould and others, 1963).

Characteristics of the detrital phases

Cadigan (1967) gives an excellent description of all of the observed detrital and secondary minerals of the Morrison Formation. The detrital phases include quartz, feldspar, clays, volcanic rock fragments, chert fragments, silicified-limestone fragments, zircon, biotite, pyroxene, magnetite, apatite, muscovite, sphene, and epidote. Included at the end of the present report is an appendix which describes each of the samples.

The quartz grains of the different samples display various degrees of attack. Rutilated quartz grains occur in all thin sections but are usually of minor abundance. Some mineral strain is evident in the undulatory extinction present in many of the quartz grains. The highest-grade ore samples show

pronounced embayment of the quartz grains as well as thick overgrowths of secondary silica. Some of these samples exceed 5 percent U_3O_8 and also tend to have the highest organic content. This common occurrence of the U- and organic-rich samples with the more severely corroded detrital grains implies that the organic solutions, the ore solutions, or both, were alkaline. Most of the secondary silica overgrowths are in optical continuity with the quartz grains to which they are attached. Both Cadigan (1967) and Austin (1963) report occurrence of fine bands of organic matrix coating sand grains, which in turn are coated by secondary quartz overgrowths. These fine bands were not observed in any of the 40 polished sections of the present study. The good correlation between the degree of quartz embayment and the organic and uranium content is also present in the low-grade samples. Secondary silica overgrowths and embayments are minor to nonexistent in the detrital quartz of the barren samples.

Several source regions for the detrital feldspar are evident in these samples. Differences in the calcium content in plagioclase and variable feldspar alteration suggest that the feldspars, at least, were derived from more than one source. Plagioclase grains are more strongly altered than alkali feldspar. Sericite, pyrite, epidote, chert, calcite, and organic matter are the principal secondary alteration phases. Cadigan (1967) observed organic matter that has replaced quartz as well as feldspars. Potassium feldspars show highly variable degrees of alteration, ranging from complete replacement to unaltered. Perthitic feldspars, however, are invariably the least altered.

Detrital rock fragments observed are either volcanic or sedimentary, although Cadigan (1967) reported metamorphic rock fragments as well. Volcanic detritus makes up as much as 15 percent of individual thin sections. Recognition of volcanic rock fragments within the thin sections can be difficult because such fragments are highly altered (fig. 4). Pyrite, sericite, clays, and chert commonly appear to have replaced the fragments. Fission-track map studies of 10 of the Ambrosia Lake thin sections showed little detectable U remaining in the altered volcanic fragments. Assuming that volcanic fragments contained a normal uranium content, much of it must have been remobilized and lost. Sedimentary chert and silicified-limestone fragments are of only minor importance in the sandstones. Several large silicified-limestone fragments were found to contain foraminiferal tests.

Extensively altered titanomagnetites locally make up a considerable portion of the arkosic heavy-mineral suite (fig. 6). These grains were deposited as dark-gray to black grains with lighter gray exsolution lamellae consisting of ilmenite. Because the heavy minerals tend to concentrate within higher energy sedimentary regimes, the magnetite content can vary considerably across a stream channel as well as between channels. In fact, highly altered titanomagnetite ghosts are as much as several percent of some of the samples. Because of the high adsorption capacity of the titanium oxides for U, some of the uranium might be expected to have been adsorbed on the authigenic titanium oxides (rutile, anatose, ilmenite) that occur in remnants of titanomagnetite. SEM/EDS and microprobe show, however, that less than 5 percent of the observed titanomagnetites had detectable U.

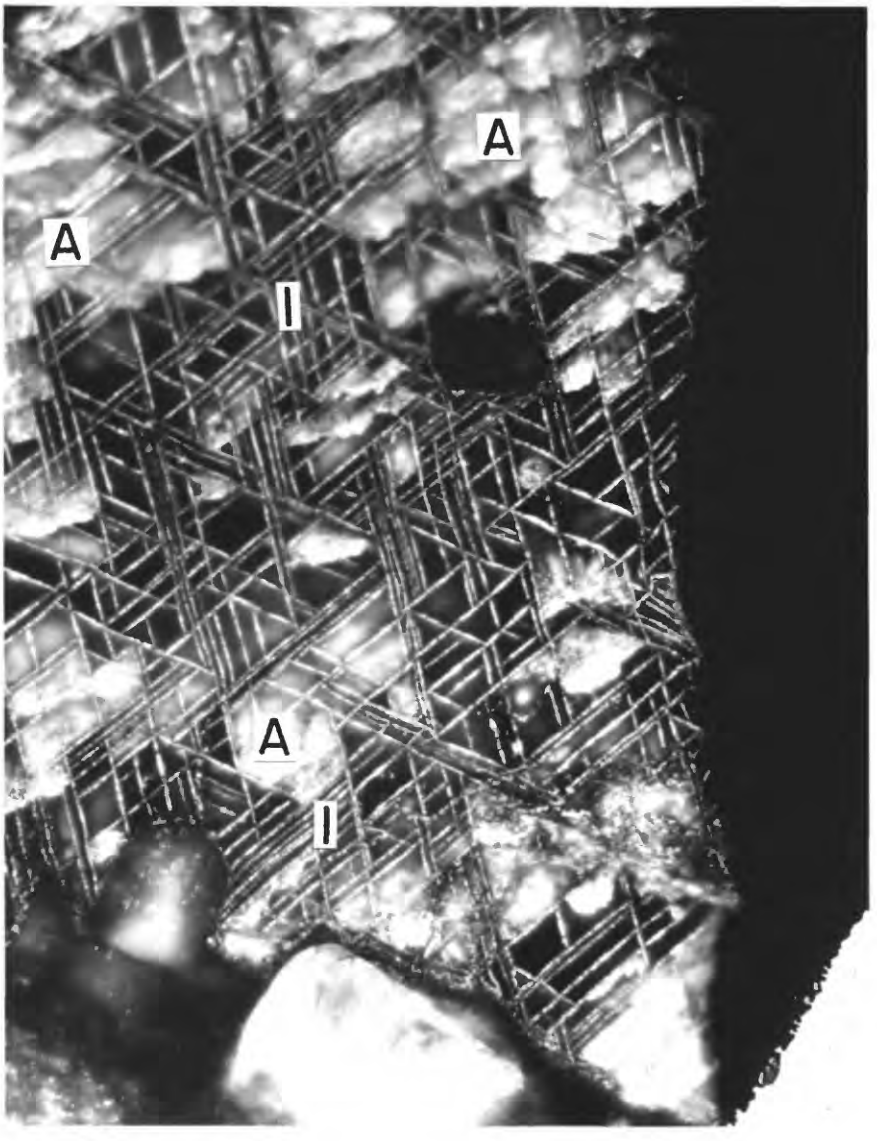

Figure 6.--Photomicrograph of an altered Fe-Ti oxide. Lamellae are ilmenite (I) and the large, brighter, rounded masses are anatase (A). The dark interlamellae voids are silica. Reflected light view of a polished thin section (sample # NM-S30-A5), field length is 160 microns. Sample is from the Section 30 mine.

Both the titanomagnetite grains and their ilmenite lamellae have been chemically altered to several secondary phases. Pyrite, rutile crystals, tiny scattered anatase particles, and an unknown V-Ti phase apparently were precipitated from solutions that remobilized the Fe, Ti, and V from the titanomagnetites. Studies of detrital titanomagnetites by Adams et al. (1978), Reynolds and Goldhaber (1978), and Rhett (1980) and others have shown that these grains serve as excellent indicators of the geochemical history of the host sediments, and as potential geochemical pathfinders. Unaltered magnetite grains are rarely observed in U-mineralized rocks and thus these rocks may give negative anomalies during magnetic surveys (DeVoto, 1978).

Characteristics of the ore-related phases of this study

Diagenetic, authigenic, and epigenetic phases occur in the arkose as grains, matrix fillings, cement, and grain coatings. These phases are pyrite, marcasite, clausthalite (PbSe), several titanium phases (anatase, rutile, ilmenite, and an unnamed V-Ti mineral), clays, non-detrital silica overgrowths, silica dust, chert, very fine grained oxides of Fe and Ti, organic matter, and prefault uranium minerals. These minerals occur as extremely fine grained mixtures of every possible combination. The largest grains of both the clausthalite or the Ti phases range from 10 to 50 microns in diameter. Pyrite occurs as medium-size sand grains. The remaining phases (clays, silica, very fine grained Fe_2O_3 and TiO_2 particles, organics, and prefault uranium minerals) rarely exceed one micron in size. These phases commonly fill the matrix as a dark brown mass, containing all of the minerals.

Pyrite and marcasite

Pyrite and marcasite occur as highly reflective, brass-yellow grains, crystals, cement, or as replacement of detrital minerals. Pyrite also occurs as individual framboids or as framboidal clusters. The majority of the FeS_2 is pyrite; marcasite is only rarely observed and then as a replacement of the inter-lamellar voids of titanomagnetites. The ilmenite exsolution lamellae of the titamomagnetites obviously were more resistant to alteration than the Fe_3O_4 which composes the remainder of the grain. Whether silica, organics, or pyrite replace the titanomagnetites, the lamellae are nearly always present which makes the altered titanomagnetites readily identifiable. Figure 7 shows near-total replacement of a large titanomagnetite grain, with the titania still present as the distinct lamellae which intersect at acute angles. In other altered titanomagnetite grains, pyritic framboids, silica and anatase lamellae fill the relict grains. Figure 8 shows that the framboids had definitely crystallized before the lamellae were reprecipitated because the normally linear lamellae are bent around and tend to be sub-parallel to the curved outer surface of the framboids. Primary ilmenite lamellae are exsolved into distinct bands which cross the titanomagnetite grain's polished surface. Recrystallized lamellae of the V-Ti mineral are shown in figure 8. These lamellae have indistinct edges which thicken and thin. Ramdohr (1969) states that recrystallized exsolution lamellae thicken at the points of intersection and thin elsewhere. Often, recrystallized lamellae are not linear, but due to sedimentary compression during recrystallization curve around opposing objects in their microenvironment. Thus, the intimate spatial association of altered magnetite and diagenetic pyrite and the petrographic

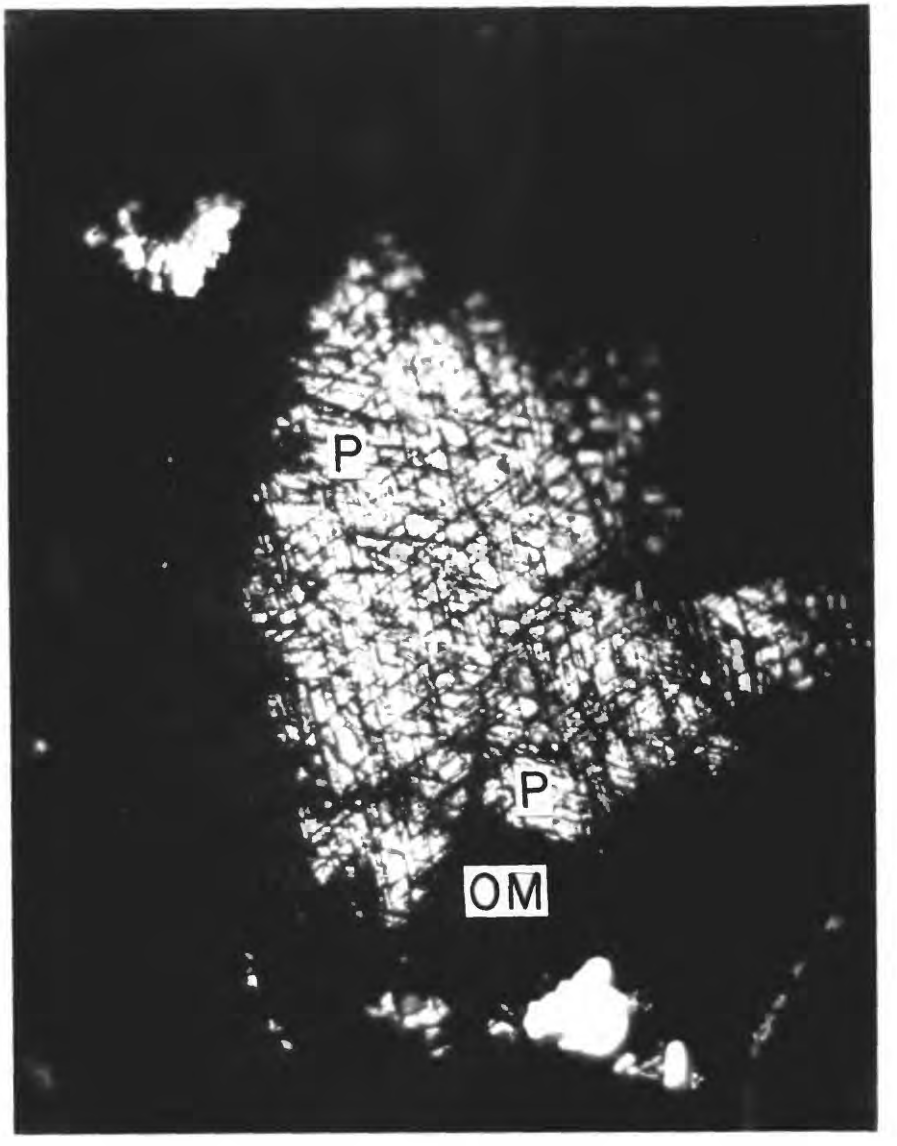

Figure 7.--Photomicrograph of a polished thin section from the section 30 mine. Pyrite (P) replacing an Fe-Ti oxide except for the relict lamellae. The relict lamellae have also been replaced by organic matter. Reflected light view of sample NM-S30-A9, 160 micron field length.

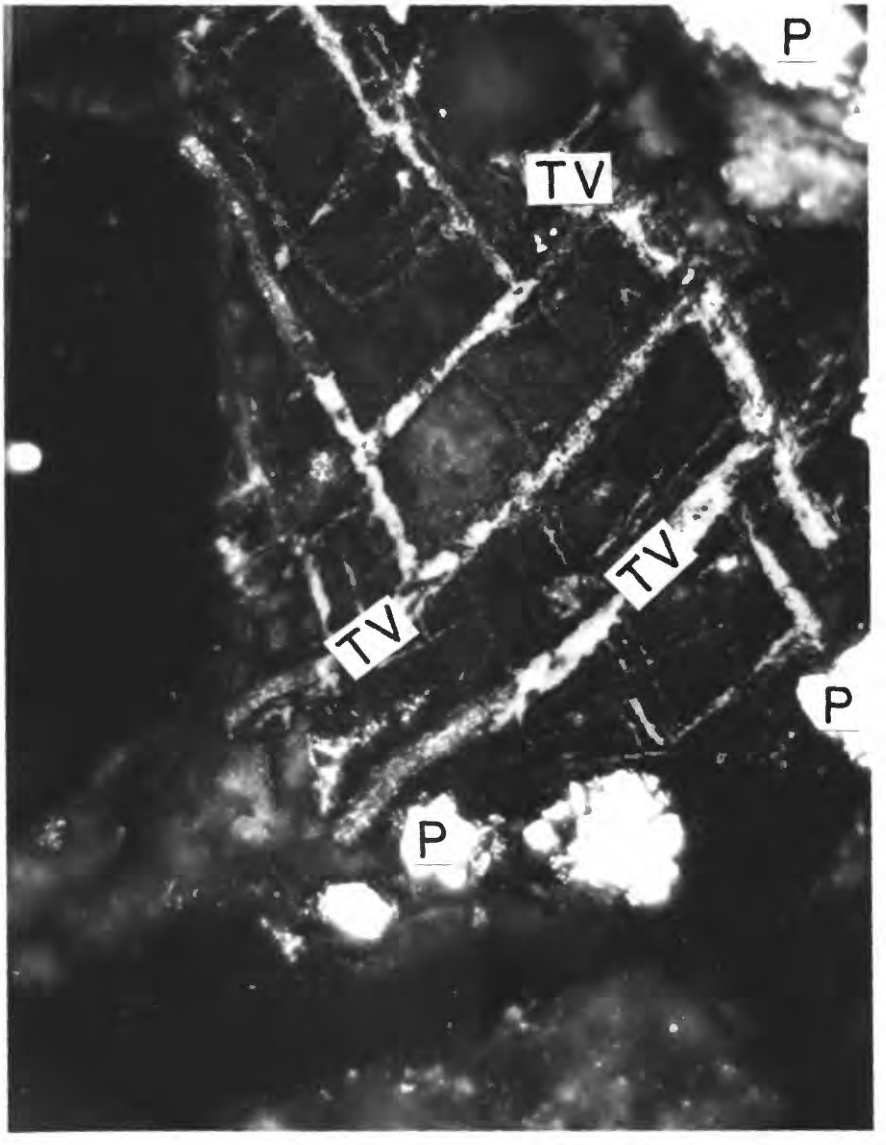

Figure 8.--Photomicrograph of an altered Fe-Ti oxide with the V-Ti mineral (TV) lamellae which bend around pyrite (P) framboids. Dark material between lamallae is silica. Reflected light view of a polished thin section from sample NM-S30-A9, oil immersion, 160 micron field length. Sample is from the Section 30 mine.

evidence for concurrent alteration and pyrite formation suggest that magnetites were a major source of Fe^{+2}.

In some places, pyrite is abundant as distinct grains or as large masses of cement. These regions may also contain pyrite which has replaced volcanic rock fragments, titanomagnetites, feldspars, and organic-rich matrix. The interior of pyrite grains occur as large masses marked by cubic pits, relict Ti lamellae or organic-filled embayments. In postfault-ore suites, the outer margins of pyrite grains commonly are oxidized to limonite. Limonite pseudomorphs also occur after pyrite in postfault, oxidized sandstone. Goldhaber and others (1978) concluded that alternating influxes of reducing and oxidizing fluids may be recognized by the study of secondarily oxidized remnants of pyritized titanomagnetites.

Cubic or octahedral pyrite crystals are randomly scattered in both the organic matrix and in pyrite-rich areas of reduced sandstone. These are the predominant form of pyrite in the ore samples studied. Fine pyrite crystals and framboidal masses within the organic matrix are commonly bordered by a low-reflectance black, carbon-rich layer. Electron microprobe examination indicates that these carbon-rich regions contain very high U concentrations, in some cases exceeding 30 percent. Otherwise, carbon is usually the only element detectable. These forms of pyrite, as well as most of the iron sulfides in general, are nearly pure Fe and S. No Se, Pb, U, or other elements were ever recorded in any of the pyrites analyzed by SEM/EDS or electron microprobe at the 5000-ppm limit of detection.

Clausthalite

The only observed phase with major constituent Pb is the clausthalite. It has an extremely high reflectivity, bright blue-white tint, and an easily polished surface. This PbSe(S) mineral is common in the highest grade ores (fig. 9) but has not been observed in barren or low-grade ore samples (samples with less than 0.3 percent U). The clausthalite grains always appear euhedral, and never display evidence of sedimentary transport or rounding. Because clausthalite grains typically occur as groupings of as many as several hundred 0.1- to 20-micron-size grains within the organic matrix, clausthalite is undoubtedly authigenic and not detrital.

Qualitative analyses by SEM and microprobe show the clausthalite has a variable composition. Ramdohr (1969) states that nearly total solid solution is possible between galena and clausthalite. The highest-grade ore samples (samples with greater than 0.3 percent U) from Ambrosia Lake typically show Pb with predominant S and minor Se. Less commonly, clausthalite occurs only as Pb and Se. Other observed metals of lesser abundance are Fe, V, and Zn. Because the optical characteristics of galena are similar to those of clausthalite, the range in the galena-clausthalite solid solution was not discernable by reflected light properties.

As mentioned above, clausthalite is most abundant within those organic-rich samples displaying the highest U content. Davidson (1963) reported a similar trend in Paleozoic sandstone-type U deposits in the United States, noting that clausthalite has a positive correlation with uranium content. His

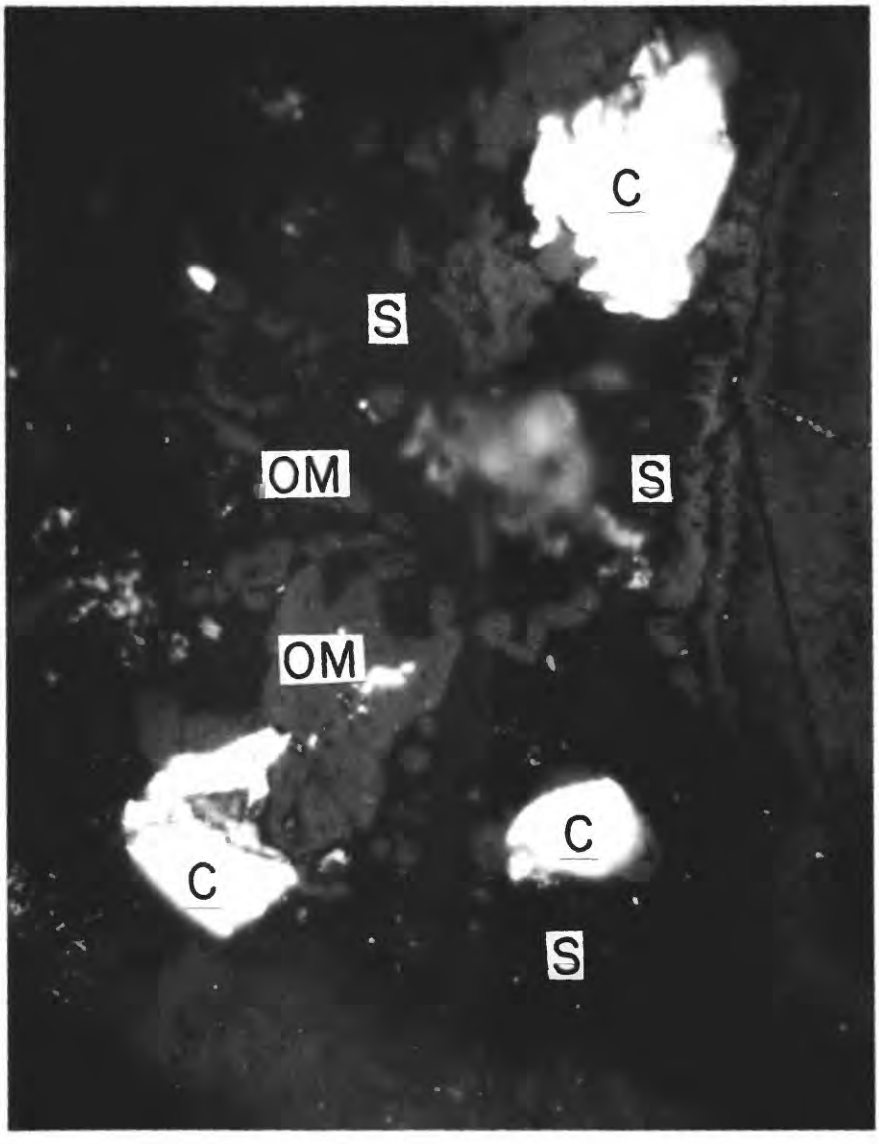

Figure 9.--Photomicrograph of bright, large masses of clausthalite (C), mixed with round blebs of organic matter (OM) which is medium gray, both within silica (S) cement. The silica is dark gray to black. Note the colloform texture of the organics. To right is zoned (light and dark gray) organic matter. Reflected light view of a polished thin section from sample NM-S30-A9, oil immersion, 160 micron field length. Sample is from the Section 30 mine.

study also showed a high correlation of U with V and Cu. If the Pb is predominantly radiogenic, the Pb of the clausthalite was probably derived from the U of the ores.

Titanium phases

By far the most interesting aspect of this study is the wide range of secondary Ti minerals which have precipitated. Optically distinct phases include anatase, rutile, a dark V-Ti oxide, and ilmenite. Other Ti-bearing authigenic phases include various mixtures of the above minerals as well as sub-micron, highly reflective spheroids of Ti and Fe oxides scattered throughout the matrix. Because many of the samples initially contained at least 3 or 4 volume-percent titanomagnetites, the Ti-bearing magnetites seem the most likely source of most of the secondary Ti phases. Another interesting observation concerns the mutual occurrence of these secondary phases. When the predominant secondary phase is anatase, there is usually little uranium, organic matter, pyrite, rutile, or V-Ti phase present. A high concentration of anatase within a sample is usually accompanied by a matrix of ilmenite, Fe oxides, clays, and little else. The high-grade samples, on the other hand, commonly contain the V-Ti mineral, rutile, pyrite, and organic matter with only minor anatase.

Anatase is a polymorph of both rutile and brookite. In the Ambrosia Lake ores, anatase appears in polished section as very bright, tan-yellow to white grains. In places, the bright-white color in reflected light is accompanied by a translucent appearance in transmitted light with a blotchy appearance. The strong internal reflections within anatase result in a blue and pink sheen to the surface. This sheen consists of submicron particles reflecting white light as blue and pink spots. Usually, the dark brown color of the organic-rich matrix is accompanied by this blue-pink sheen, probably indicating the presence of finely divided anatase.

The most common form of anatase is extremely fine grains. These sub-micron spheres are usually combined into larger masses which have replaced altered titanomagnetite grains, as fine rims around relict titanomagnetites (filled by silica, organic matter, rutile and/or ilmenite), or simply as scattered masses within the matrix (fig. 10). Owing to the significantly lower solubility of Ti than Fe in the presence of the humate-bearing solutions, much of the Fe was apparently selectively remobilized and carried away from the titanomagnetites. This Fe is now present as nearby pyrite grains. Partial solution and redistribution of the Ti is indicated by the occurrence of anatase-filled titanomagnetites, curved ilmenite lamellae, and scattered rutile and V-Ti grains. The inter-lamellar voids among ilmenite lamellae that cross the surface of the titanomagnetites may exhibit translucent anatase mixed with quartz. The quartz/anatase ratio of these fillings ranges from 10 to 0.1. Altered titanomagnetites with a fine anatase rim are also common. Within the anatase rim, various mixtures of silica, epigenetic organic matter, ilmenite, rutile, pyrite/marcasite, clays, and clausthalite are present. Figures 11 and 12 show two titanomagnetites partly replaced by organic matter. One of the examples (fig. 11) shows concentric, alternating bands of silica, the V-Ti mineral, and organic matter. Anatase is also found as randomly scattered concentrations of small spheres with Fe oxides and clays frequently intermixed. In fact, most of the matrix for the barren and low-grade samples consists of secondary Fe and Ti oxides, silica,

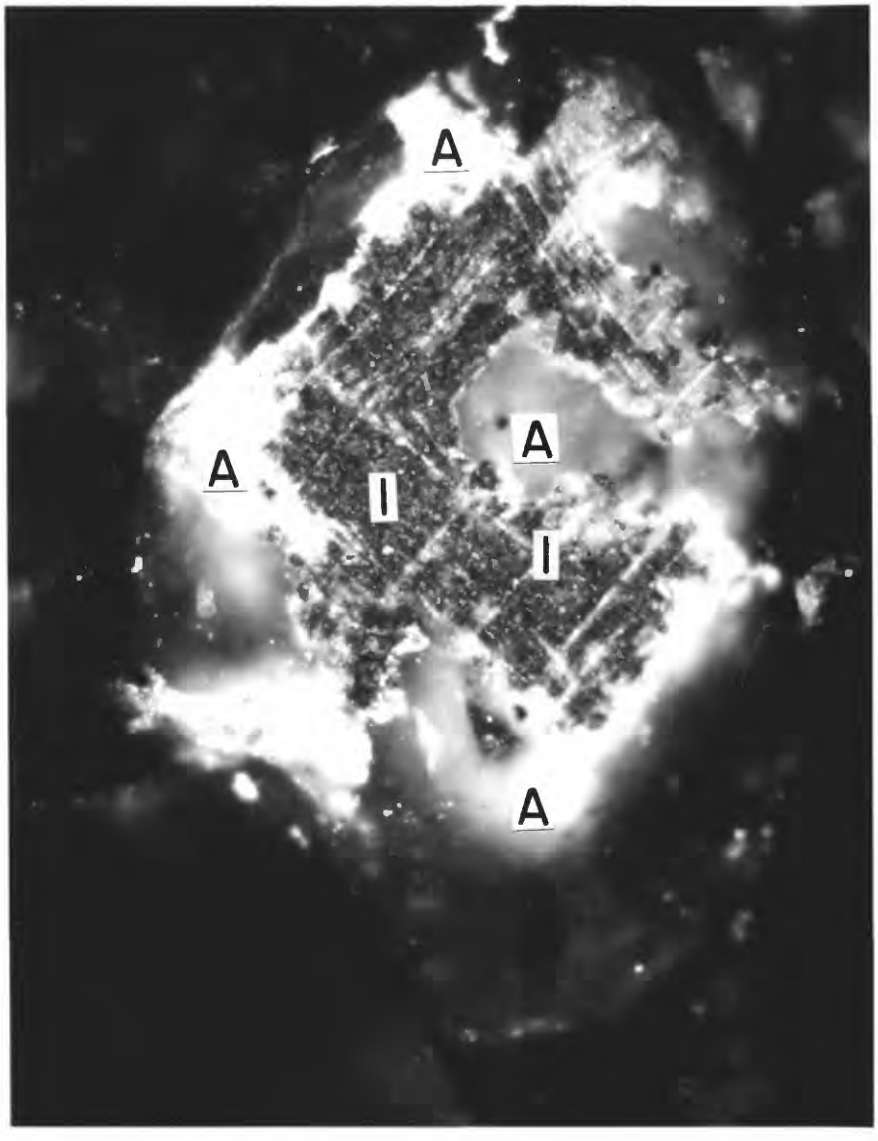

Figure 10.--Photomicrograph of an altered titanomagnetite relict with bright anatase (A) lamellae and anatase rim. The darker, spotted material filling in between the white anatase lamellae is ilmenite (I). The surrouonding, dark gray to black material is chert and organic matter. Reflected light view of a polished thin section from sample NM-S30-A9, oil immersion, 160 micron field length.

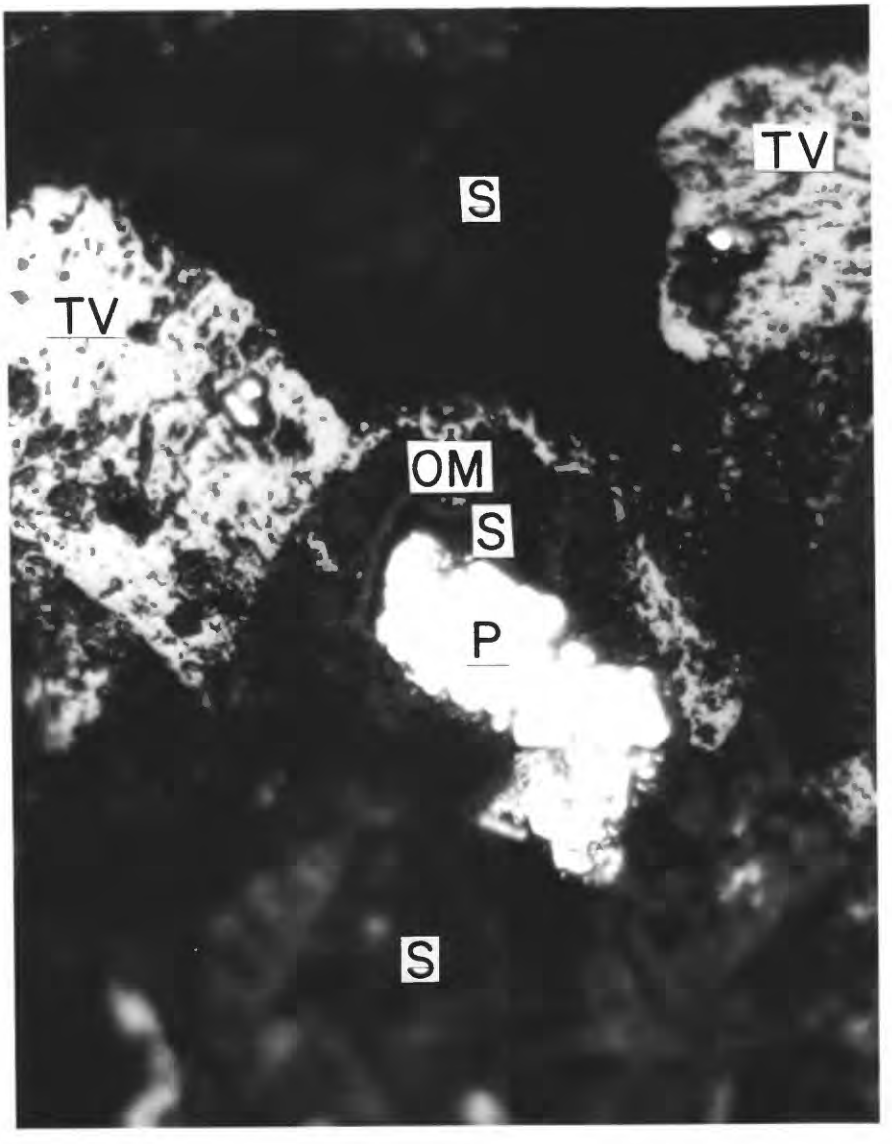

Figure 11.--Photomicrograph of a strongly altered titanomagnetite grain. Now present are the Ti-V mineral (TV), pyrite (P), silica (S) and organic matter (OM). To the immediate upper right of the centermost pyrite grain is alternating bands of: silica- organics- silica- organics- TiV. Reflected light view of a polished thin section from sample NM-S30-A9, oil immersion, 160 micron field length.

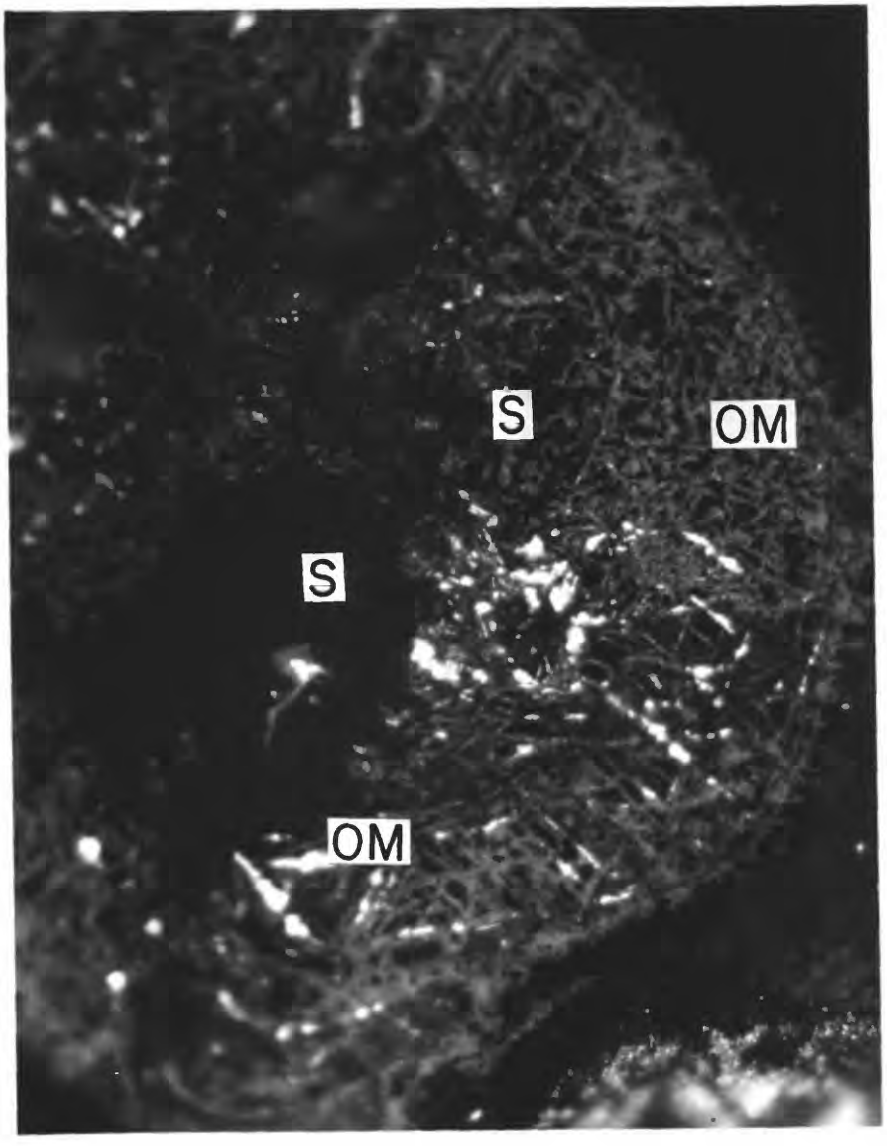

Figure 12.--Photomicrograph of an altered titanomagnetite grain with the highly reflective, lamellae relicts now totally replaced by organic matter (OM). Within the inter-lamellae voids is silica (S). Notice that some of the replaced lamellae are not linear. Reflected light view of a polished thin section from sample NM-S30W-A2 of the Section 30 W mine. Oil immersion, 160 micron field length.

and clays. The apparent limited solubility of Ti during influx of the humate solutions is also seen in the occurrence of Ti oxide particles concentrated within the organic trash of channel lag gravels. Anatase spheroids are commonly coprecipitated with clausthalite inside fossilized tree fragments. During the burial and compaction of the organic trash, connate and epigenetic solutions carried Ti and Pb into the dissolving cell structures. These epigenetic metals were apparently precipitated as anatase and clausthalite.

A second example of an authigenic Ti phase is ilmenite. During cooling of the magma source of the magnetites, primary ilmenite lamellae exsolved from the titanomagnetites. Some of these primary ilmenite lamellae are still present in the relict titanomagnetites. Since initial crystallization, these detrital grains have been weathered, transported, deposited, and altered (figs. 13, 14 and 15). The ilmenite appears moderately reflective, blue-white to gray. Thus, ilmenite occurs both as primary linear lamellae which criss-cross the surface of titanomagnetite grains, or as secondary ilmenite masses which totally replace titanomagnetites. These large ilmenite masses commonly have an anatase rim. In many samples, the only evidence which indicates that a rounded mass of pyrite or organic matter is a replaced titanomagnetite grain is the partial lamellae still present. In general, ilmenite is not a common secondary Ti phase.

Rutile probably is to be a secondary phase due to its euhedral to subhedral form and its common occurrence as small, distinct grains within the organic matrix. It is yellow-brown to tan, moderately reflective (less than anatase but greater than the ilmenite) and polishes poorly. The pink-blue sheen of anatase is also present within and bordering much of the rutile. Rutile does not show the extremely fine-grained character of anatase, but instead appears as larger, homogeneous grains of relatively pure TiO_2. SEM/EDS studies confirm Ti as the major element with variable but minor V, Fe, Mn, and more rarely U.

Rutile was precipitated as 1 to 50 micron diameter grains scattered in the organic matrix, and as finely radiating crystal-splays within relict titanomagnetites. These euhedral crystals are definitely authigenic Ti phases. As the photomicrograph in figure 16 shows, the rutile crystals grew inward from the outer anatase rim. This relict titanomagnetite was altered in the mineral sequence: anatase (as the rim), rutile crystals, and silica (which filled the interior). The presence of rutile as fine, euhedral to subhedral grains throughout the matrix also suggests some remobilization of Ti to points moderately distant from the proposed titanomagnetite source (figure 17). One might expect a 1:1 correlation between the concentration of altered titanomagnetites and the occurrence of rutile (if the Ti was not remobilized for distances greater than 2 to 3 cm). A considerable amount of Ti was definitely released from the large titanomagnetite grains, now totally replaced by sulfides, silica, and organic matter.

The final example of authigenic Ti is as an unnamed V-Ti mineral. The mineral has a low reflectance (lowest of all the authigenic Ti minerals), appears dull gray to gray-brown, and exhibits no visible anisotropism or internal reflections. The polished surface of these grains ranges from smooth to heavily pitted with a generally shredded texture. Of major importance is the composition of this phase. This gray mineral consists predominantly of V and Ti (as oxides) in about equal concentrations, and possibly is the first

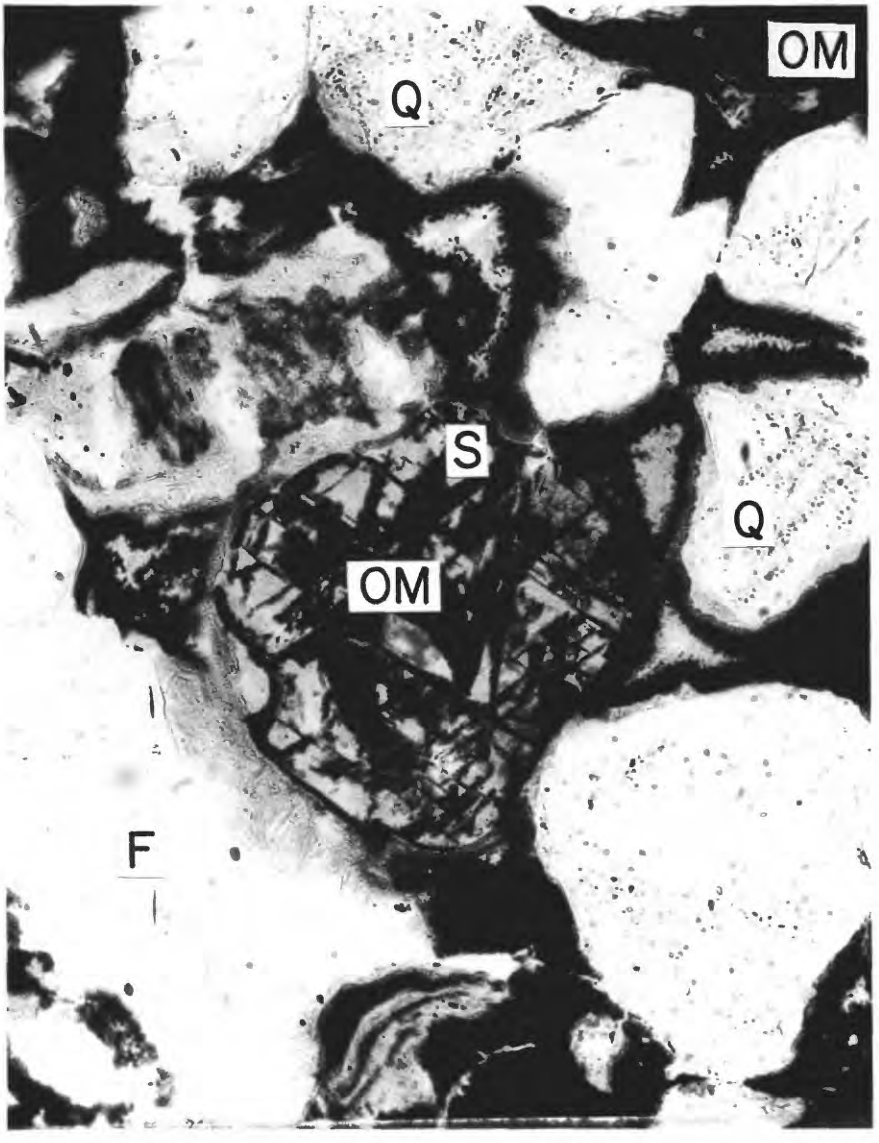

Figure 13.--Photomicrograph of an altered titanomagnetite, now showing predominant O.M. replacing lamellae and O.M. filling pore space. There is minor ilmenite mixed in with the organic matter (OM), but is not recognizable in this transmitted light view. Detrital grains are quartz (Q) and feldspar (F). Field length is 0.48mm. Sample no. NM-S30-A5, from the Section 30 mine.

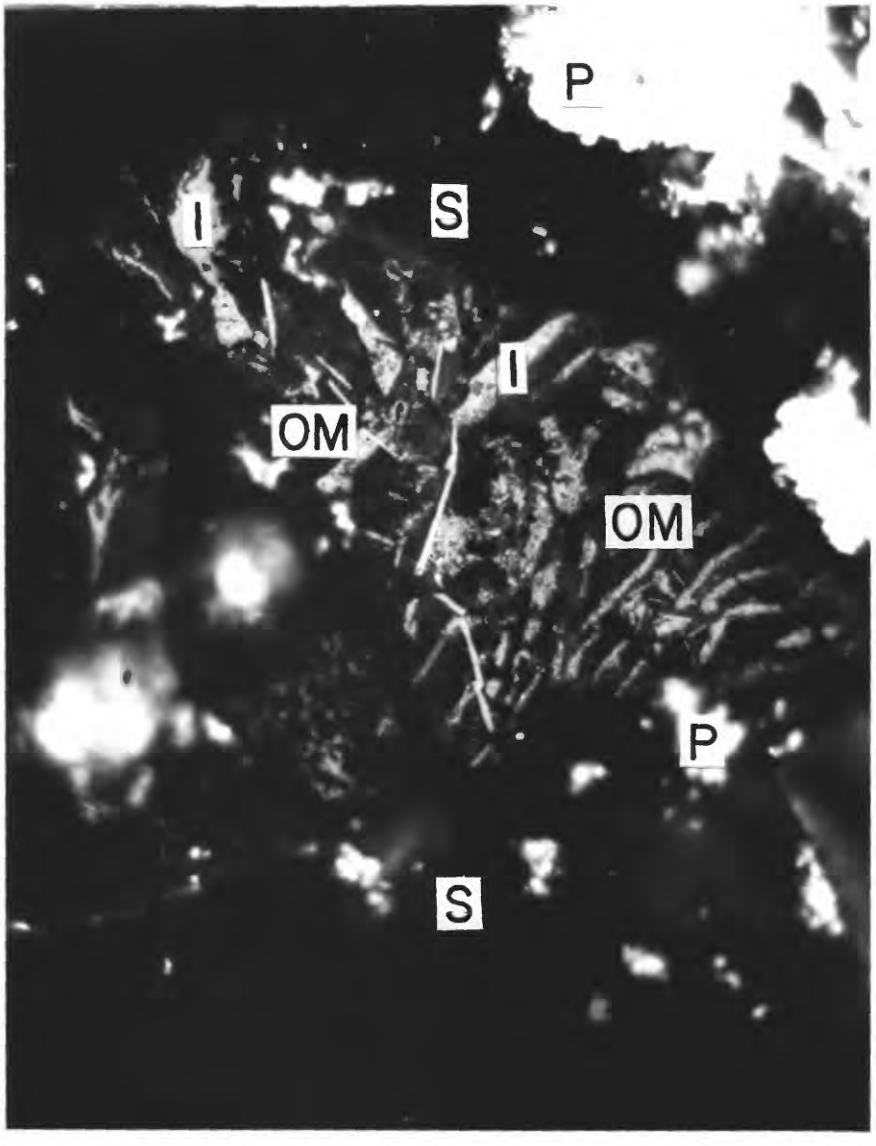

Figure 14.--Photomicrograph of recrystallized ilmenite (I) and organic matter (OM) filling a relict titanomagnetite. The ilmenite forms straight, non-intersecting lamellae and the O.M. fills in the voids. To upper right are 2 pyrite grains, and to lower left is a mass of anatase (A). Black material filling in between the grains is silica (S). Reflected light view of a polished thin section from the Section 30 mine, sample no. NM-S30-A9, oil immersion, 160 micron field length.

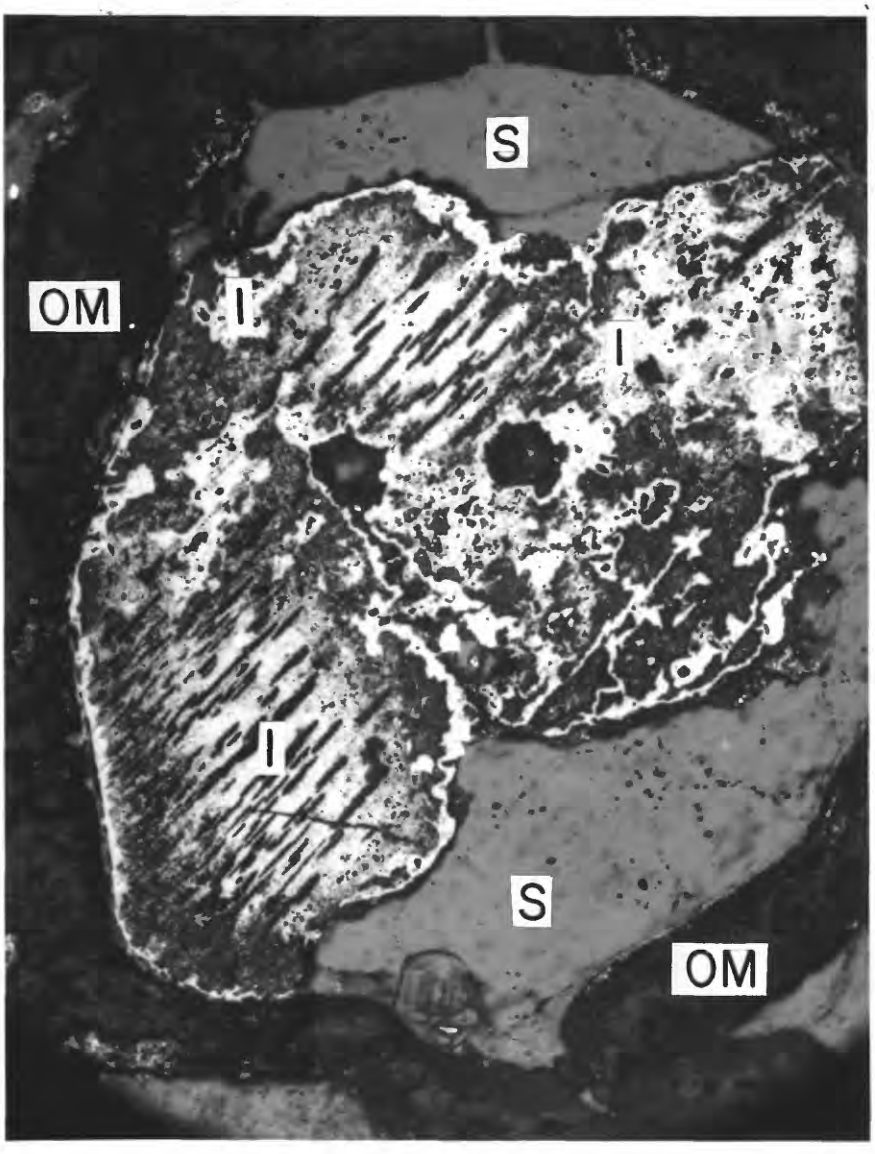

Figure 15.--Photomicrograph of an extremely large titamomagnetite relict, now replaced by secondary ilmenite (I) and minor silica (S). Note the relict lamellae patterns still visible in the ilmenite. Surrounding the grain is zoned (dark to light gray-brown) organic matter (OM). Reflected light view of a polished thin section from the Section 30 mine, sample no. NM-S30-A7, oil immersion, 0.48mm field length.

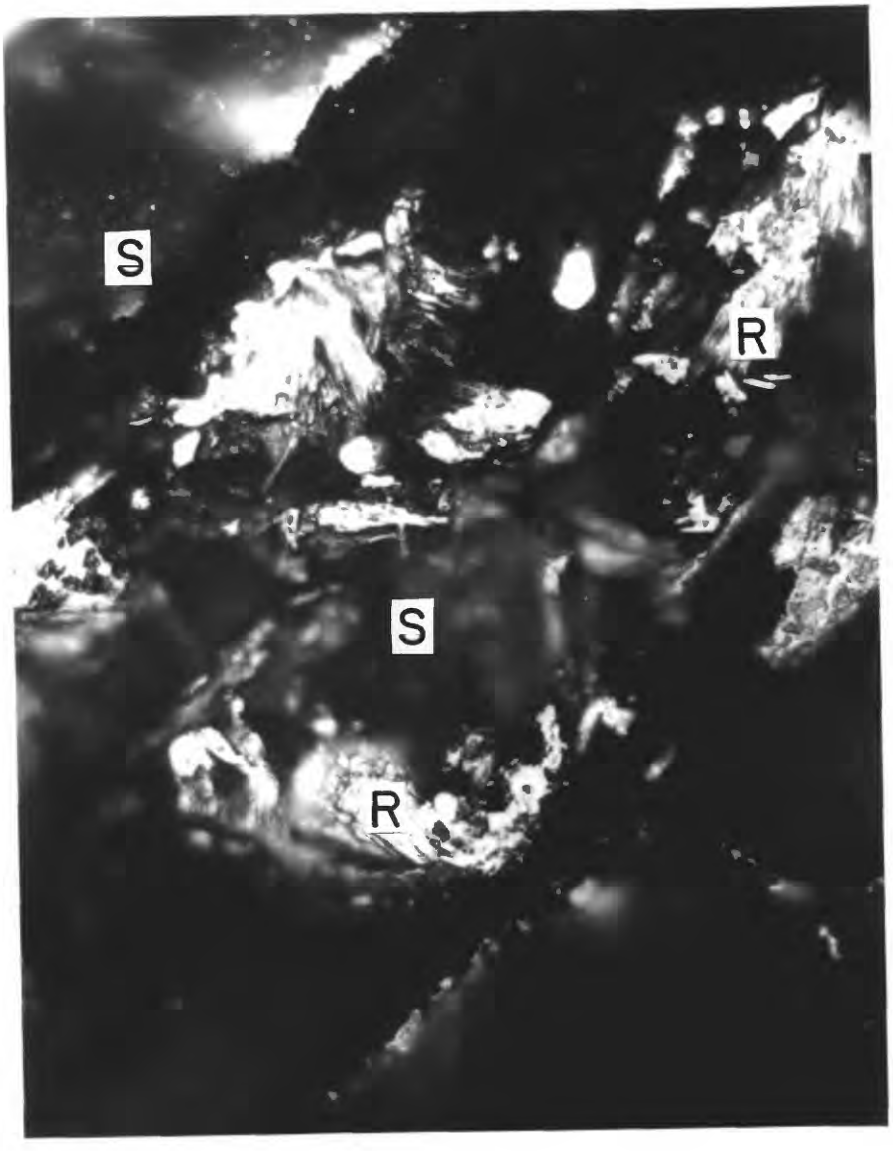

Figure 16.--Photomicrograph of an altered titanomagnetite grain. The bright, radiating crystal splays are rutile (R), with silica (S) filling the internal voids and silica surrounding the relict grain. The rutile crystals are a bright gray-white color, with orange-red internal reflections. Reflected light view of a polished thin section. Section 30 mine, sample no. NM-S30-A10, oil immersion, 160 micron field length.

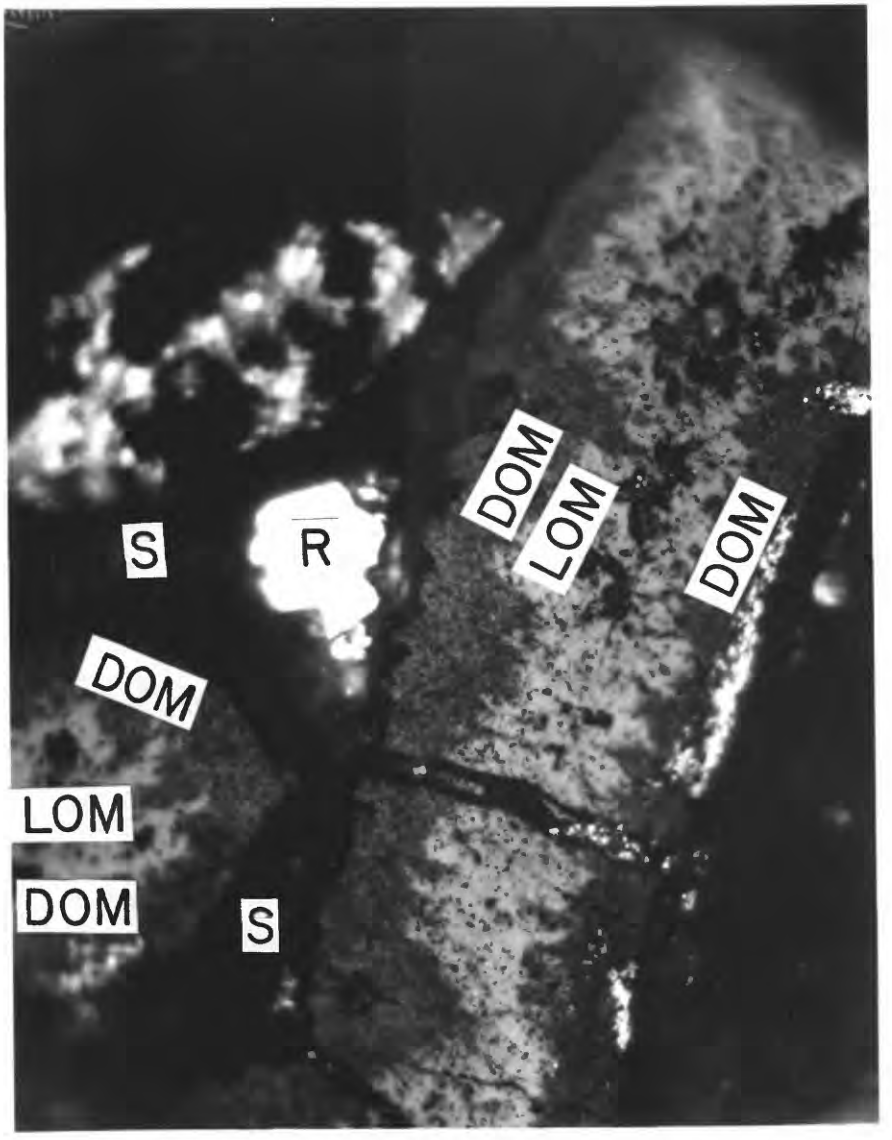

Figure 17.--Photomicrograph of a single rutile (R) crystal within silica (S) and organic matter--matrix. This rutile crystal was not near any visible titanomagnetite relicts. The organic matrix is zoned: with the darker organic matter (DOM) along the detrital grain boundary and lighter organic matter (LOM) within the core of the organics. Reflected light view of a polished thin section from the Section 30 mine, sample no. NM-S30-A7, oil immersion, 160 micron field length.

reported occurrence of a prefault V mineral in Ambrosia Lake. Minor Fe, U and Si are commonly observed with the SEM/EDS but may be present as impurities of fine clay or silica particles. The U and Si are probably coffinite present within or adsorbed on this phase. The V-Ti mineral is observed rarely as relict lamallae and most commonly occurs as distinct grains scattered through the matrix. Several occurrences of the V-Ti mineral as total replacements of titanomagnetite can also be seen (fig. 18 and fig. 11). SEM/EDS and microprobe study show V and Ti to be the major cations. Only one V-Ti mineral, schreyerite, is recorded in the mineralogical literature. Schreyerite is monoclinic, with the composition $V_2Ti_3O_9$.

The petrographic observations of this section of the report indicate that during and after deposition of the sandstones and their detrital titanomagnetites, significant alteration occurred. The most common pattern during this alteration was significant remobilization of Fe, partial sulfidization of some of the Fe in situ, and dissolution of the Ti, most of which reprecipitated in place. A small portion of the dissolved Ti was transported throughout the sediment, resulting in the disseminated anatase spheres, rutile grains, and V-Ti grains within the matrix. Dissolution of the Fe from the titanomagnetites left inter-lamellae voids which were subsequently filled by pyrite-marcasite, organic matter, silica, and secondary Ti phases. Replacements by pure pyrite or pure organic matter were observed, whereas mixtures of the above are most common.

Organic matter

The most significant elemental correlation involving the prefault ores of the Grants mineral belt is the strong correlation between weight percent of U and weight percent of organic carbon. In prefault ore, most of the uraniumexists intimately mixed in some form with the black, amorphous carbonaceous matter. This epigenetic organic matter occurs as grain coatings, matrix disseminations, fracture fillings, and more rarely as replacements of the detrital grains (fig. 19). Some controversy exists over the nature and source of the organic matter. Because of the age and the concomitant radiation damage to the organic matter contained in the sandstones, a humic vs. hydrocarbon origin for these organics remains unresolved (Leventhal, 1980; Squyres, 1980). A mixture of humic and fulvic acids derived from decaying plants may be the most likely source of the epigenetic organic matter (Squyres, 1980; Granger and others, 1961). SEM/EDS study indicates that organic matter occurs as nearly pure amorphous carbon with variable amounts of impurities of Si, Al, Fe, K, V, U, and S present. Of major importance is the observation that much of the organic matrix is chemically and texturally zoned. This zonation is recognized petrographically. Another type of U-bearing organic matter also occurs as carbonized chips, branches, and trunks of plants deposited with the sandstones.

In reflected light the organic matrix is typically brown to gray-brown. Increased concentrations of jordisite in the organic matrix imparts a dark blue to black color. Associated Fe-bearing clays and secondary Fe oxides give a reddish-brown variation. Fe stain is found immediately adjacent to grain margins, between grains, and with the organic portion of the matrix. Anatase, indicated by its blue and pink sheen, is also found distributed throughout the organic matter. Variability in the apparent brightness of the organics is a

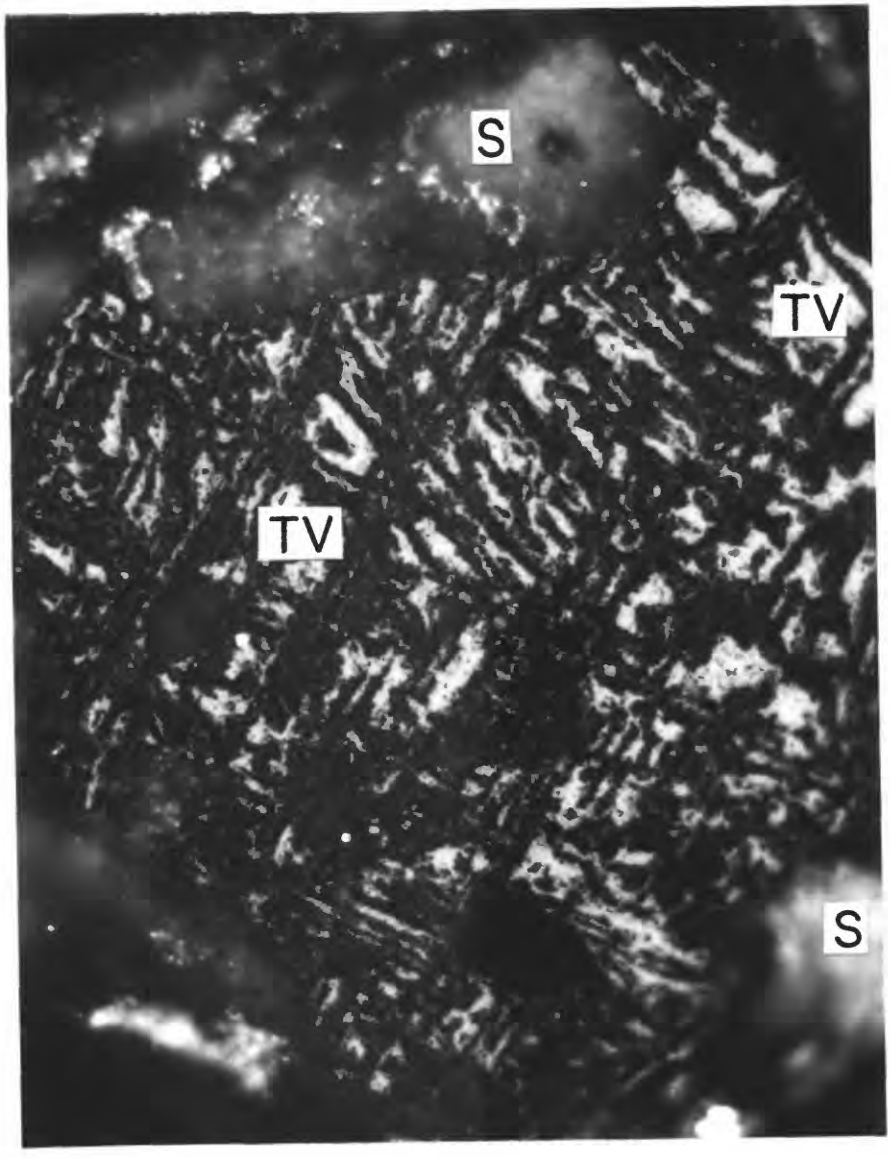

Figure 18.--Photomicrograh of a relict titanomagnetite grain, now totally replaced by the new, un-named V-Ti mineral. Note the relict lamellae patterns are still present. The bright masses above and below the grain are silica (S). The brightness of the silica is due to its many internal reflections. Reflected light view of a polished thin section from the Section 30 mine, sample no. NM-S30-A9, oil immersion, 160 micron field length.

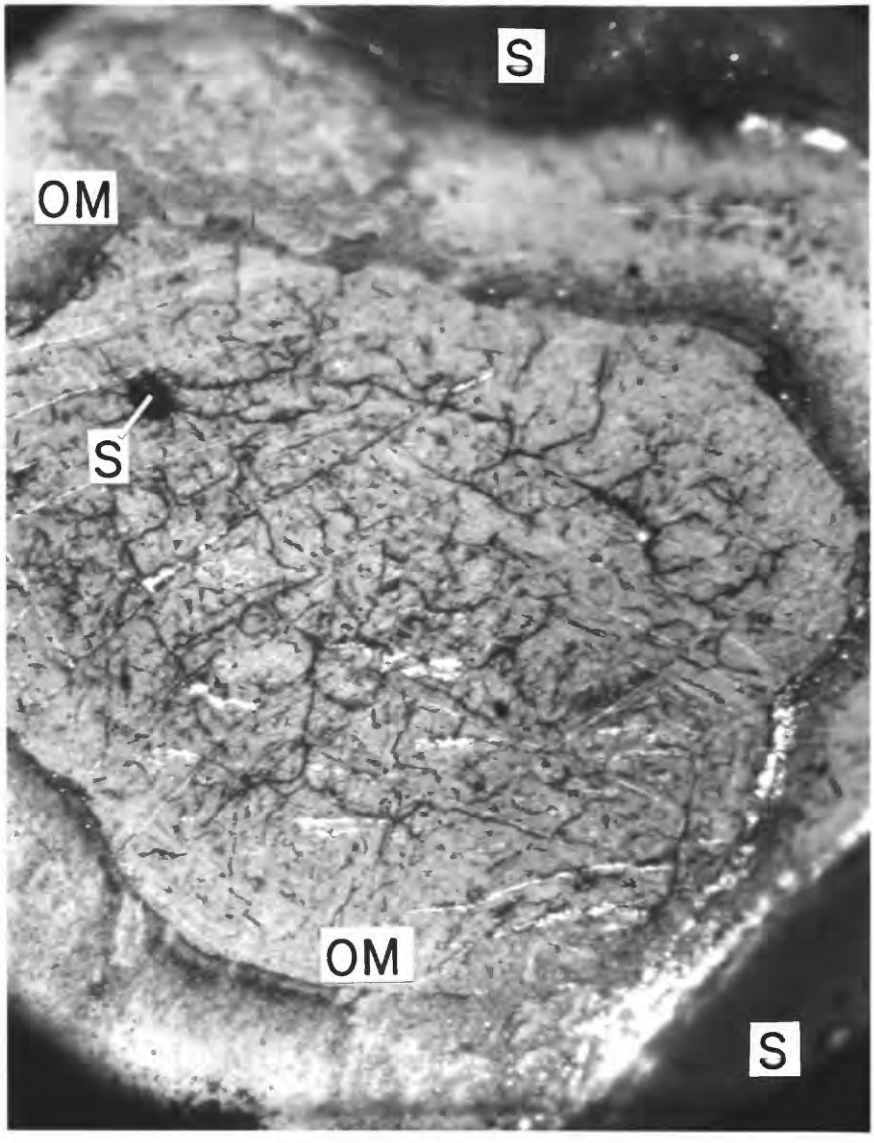

Figure 19.--Photomicrograph of a detrital titanomagnetite grain, now almost totally replaced by organic matter (OM) and minor silica (S) (as the dark material). Note that the organics did not replace the Ti-rich lamellae. Reflected light view of a polished thin section from the Section 30 mine, sample no. NM-S30-A10, oil immersion, 160 micron field length.

result of the pitted surfaces of the matrix. Darker regions which tend to concentrate along the matrix-detrital grain contacts are principally a result of the deeply-pitted surface of the matrix (fig. 20). Figure 20, however, shows an unusual feature of the zoned organics which is observed only with the SEM. Apparently because of the oblique incidence of the electron beam of the SEM onto the surface of the polished thin section, the dark-light nature of the zoned organic matter is opposite to that observed through the petrographic microscope. In figure 20, the contrast of the dark-light zoning of the organic matter is quite evident. Typically, from the boundary of a detrital grain (fig. 21) inward to the core of the matrix, the color and brightness of the matrix vary. Immediately adjacent to the detrital grain, a <1- to 10-micron band of clays, silica and Fe and Ti oxides occurs. Adjacent to the first layer is a dark-gray to dark-brown, heavily pitted band of organic matter. The color and texture of the organics vary further in the innermost region of organics (which fill the core of the pore space) which is a light gray-brown and has a smooth surface. Rarely the center of the organic matrix will show silica-filled pockets.

The organics occur as replacement for detrital grains and as open-space fillings. Altered titanomagnetites, feldspars and volcanic rock fragments are visable in various stages of replacement by the organic matter. Many of the pieces of biotite observed have ragged edges with organic matrix filling the inter-planar spaces between the mica sheets. Cadigan (1967) reports total replacement of both detrital quartz and feldspar in the Morrison Formation samples that he studied. The highly sutured quartz of some of the organic-rich samples from these ores should therefore be kept in mind. When present as open-space filling, the organic matter commonly appears rounded or bleb-like (fig. 22). These organic matter occurrences lead the impression that organic matter-chert-pyrite mixtures were folded in and around the detritus as a soft, plastic mass (Moench, 1963; Squyres, 1980). Surface cracks regularly extending from the lighter core of the matrix outward to the darker, matrix-grain, contact appear to be desiccation cracks. There is no evidence that the cracks are due to applied grain stress. In some cases, chert-filled pockets found within the lighter matrix contains 1- to 10-micron spheres of organics. These rounded, organic blebs were apparently insoluble in the silicate matter and appear to have separated from the chert. "Grape-like" clusters of organic blebs are also common. Distinctly colloform bands of alternating layers of silica and organics were observed in organic-rich ores. As noted above, the outer edges of the matrix are usually pitted and the zoned light-dark matrix parallels the apparent folds within the matrix. This organic-rich matrix clearly was folded, squeezed, and compressed following precipitation. The organics of the low-grade ore samples do not regularly have these rounded and folded textures. The matrix of these samples consists of a mixture of organic matter, clay, chert, and metallic oxides. Many of the samples with less than 0.3 percent U_3O_8 show little observable organic matter (Table I). Apparently the uranium-organic matter correlation breaks down in low U samples. The uranium is not totally contained within or held by the organic-bearing matrix. In general, the zoned or rounded organics are a minor occurrence, relative to the more common textureless mixtures of clay, silica, metallic oxides, and organic matter that occur in lower grade samples.

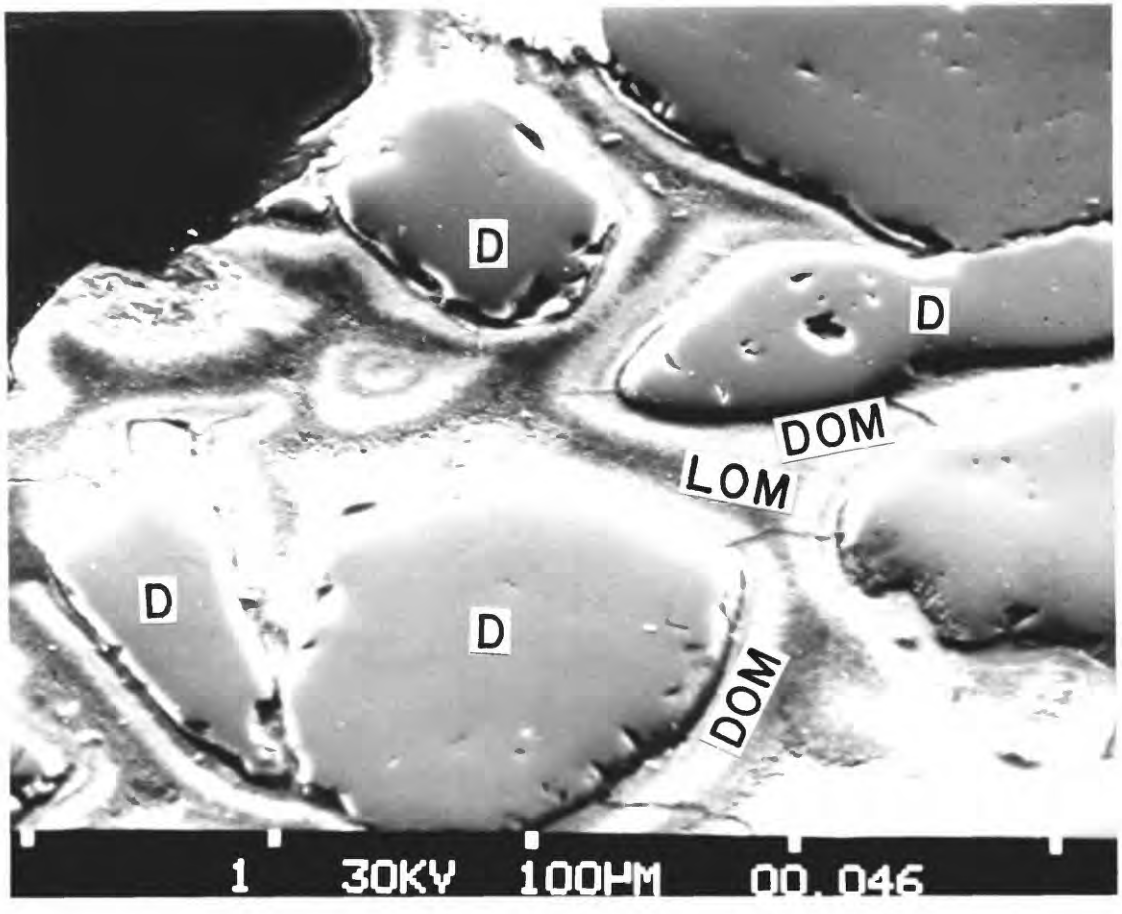

Figure 20.--Photomicrograph of highly zoned organic matter (OM) from sample NM-S30-A10 of the Section 30 mine. This photo was taken with the SEM which causes the apparent reflectivity to appear opposite of that seen through a reflecting light microscope. Therefore the high U organic ban (immediately along the grain boundaries) appears light gray on the SEM, while the inner organics (low in U) appear dark gray. Note the extra zone of high U (labeled #1) in the center of the large matrix region. Also note the minor folding (labeled F) apparent along some grain boundaries. This photo is at 200 magnification. Detrital grains are labeled D.

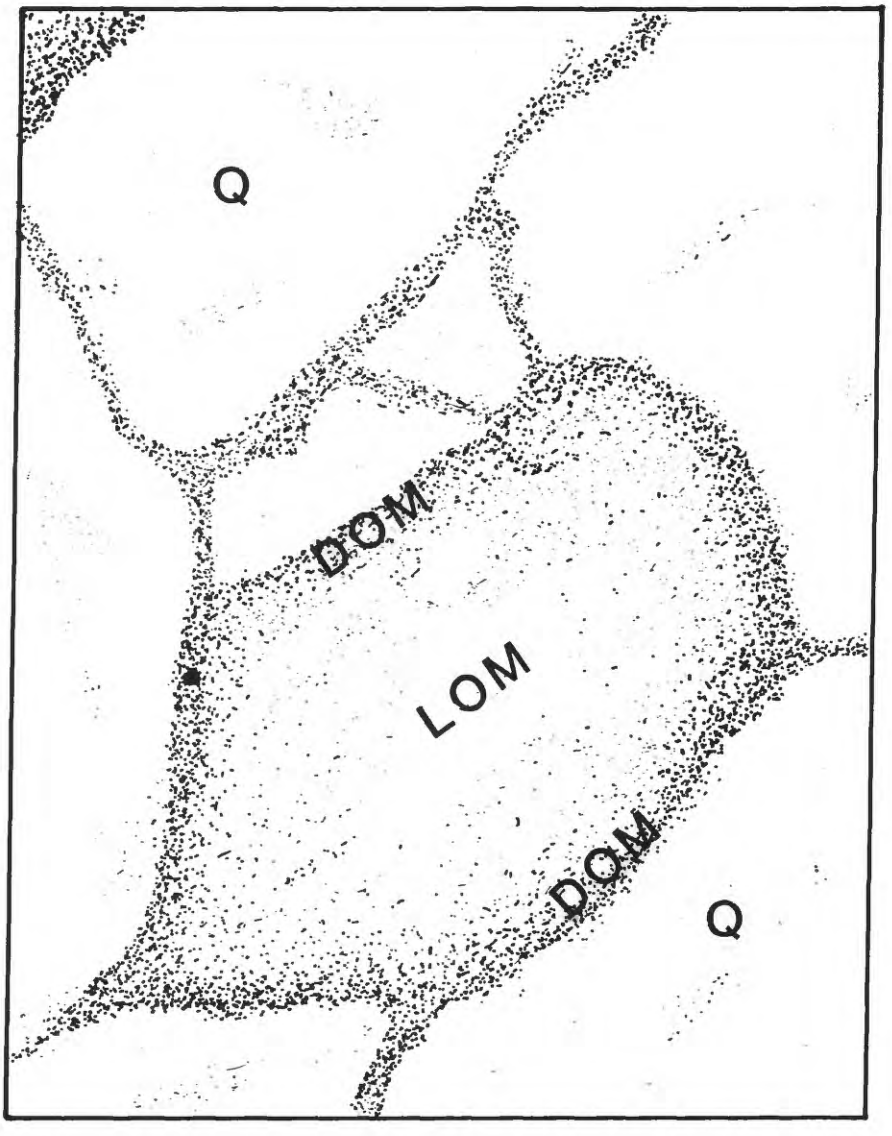

Figure 21.--Diagram of zoned organics as matrix filling the pore space between detrital grains. Note the quartz (Q), the dark organics (DOM) along grain margin and light organics (LOM) making up the core of the pore space. Metallic oxides and clays commonly occur immediately along the grain margins.

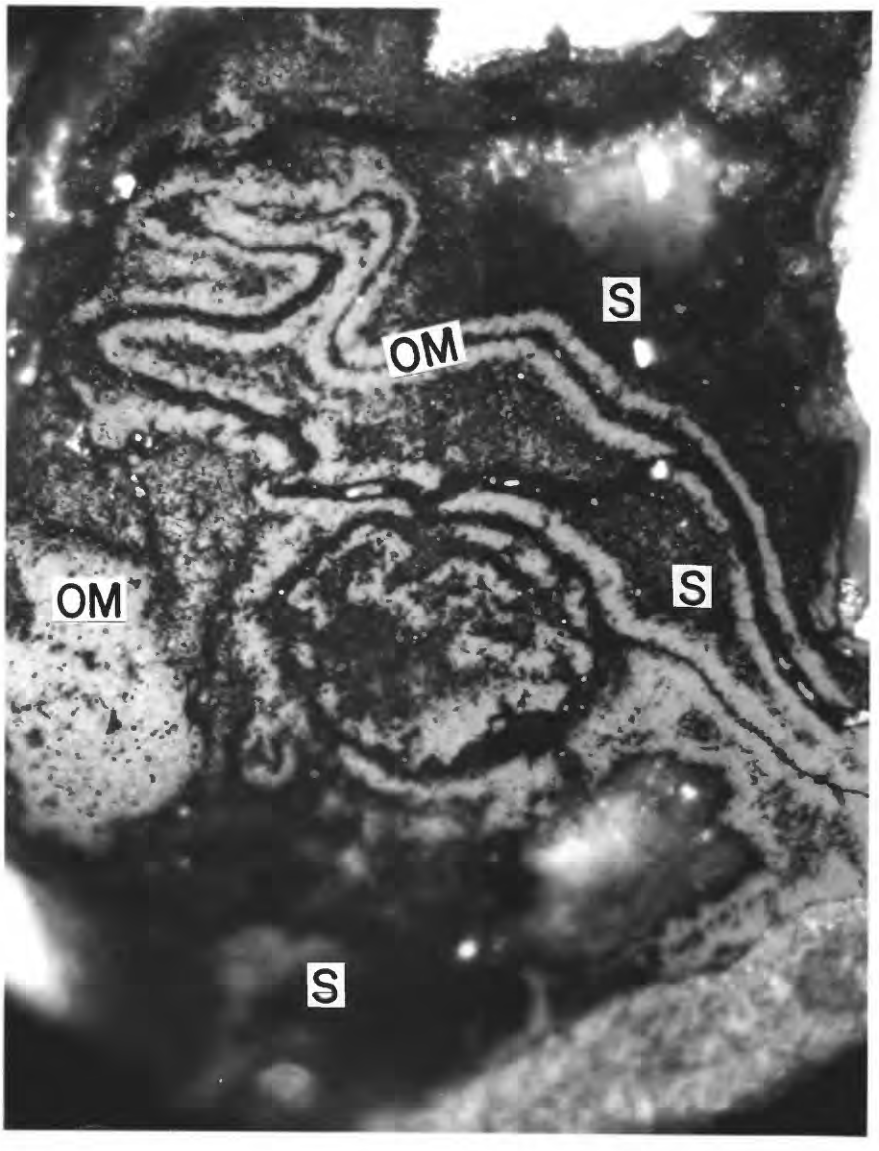

Figure 22.--Photomicrograph of zoned, dark and light organic matter (OM). Note the collapsed and folded texture of the organics. To lower right is a bright mass of silica (S) with strong internal reflections, while the surrounding silica is a mixture of dark and light material. Reflected light view of a polished thin section from the Section 30 mine, sample no. NM-S30-A8, oil immersion, 160 micron field length.

Interestingly, the petrographically observed zonation of darker matrix along the grain boundary and lighter matrix within the matrix core is mirrored by a similar chemical zonation. Microprobe and SEM/EDS analysis consistently showed that the darker, outer zone of the matrix is higher in the associated elements Si, Al, Fe, and V. The inner matrix contains no detectable amounts of these elements. X-ray maps observed on the microprobe also show that most of the U in these zoned organics is also concentrated within the darker, outer zone. Concentrations exceeding 5 percent U_3O_8 were recorded for the thin band of pitted matrix immediately adjacent to grain margins. One dark band has greater than 30 percent U_3O_8. Movement of the microprobe beam away from the detrital grain margin to a point 50 microns within the organic matrix, in some cases indicate areas in the matrix core with uranium concentrations as low as 0.5 percent U_3O_8. Little S was found, so the observed elements were probably present as oxides, complexed to the organics or adsorbed on clays. Adams and others (1978) suggest that considerable Al, Si, and Fe can exist stably complexed to organic humic molecules.

The chemical and petrographic zonation of the organic matter is evident in figures 23 and 24. Figure 23 is a 300X magnification of a triangular region of matrix. The three grains which enclose the matrix are quartz or feldspar grains. Figure 24 is an X-ray map for U of the matrix in figure 23. This photo shows the location of the U in the organics as small white dots. High concentrations of white dots are equivalent to high concentrations of U. When one considers common interference effects of other elements (one K peak on the SEM is close to the main U peak) and the fact that detrital quartz and feldspar obviously hold little U but appear to in the photo, there should be fewer U dots within the detrital grains (at the limit of detection of the SEM). Subtraction of this background density of dots from the photo would reduce the number of dots from the central matrix region. Thus, less apparent U would appear in the matrix core. This essential consideration further emphasizes the strong apparent concentration of U along the grain boundaries.

A geochemical zonation of U is again evident in figures 25 and 26. Figure 25 is a 300X magnification (SEM photomicrograph) of a matrix-filled pore space. Remembering that the outer, light-colored matrix photographed on the SEM is actually the dark organic matter viewed through a petrographic microscope, one observes from Figure 26 that this outer matrix margin is U-enriched. The core of this pore space is observed to be U-deficient.

An organic fixative for uranium which may have served as a source for some of the epigenetic organic matter is detrital carbonaceous debris buried with the sandstones. Whole trees and grain-size fragments of branches and limbs were observed in both high- and low-grade ores. Five of the Section 30 mine samples were collected within and around a 15-m-long, 2-m-diameter uranium-bearing, carbonaceous tree trunk. Cadigan (1967) reports that many trees preserved in the Morrison Formation are petrified. Thus, much of the humic material derived during partial petrification of trees in and near the Section 30 mine may have been solubilized and remobilized to nearby locations. Observations of the uranium-rich tree trunk in the Section 30 mine showed two readily distinguishable types of organic matter. Along the entire outer margin of the tree trunk is a thin band of organic matter, ranging from 5 to 15 cm in thickness along the length of the tree and up to as much as several meters into the ends of the tree. This shiny organic band appeared to encroach deeper into the ends of the tree trunk along preferred pathways. The

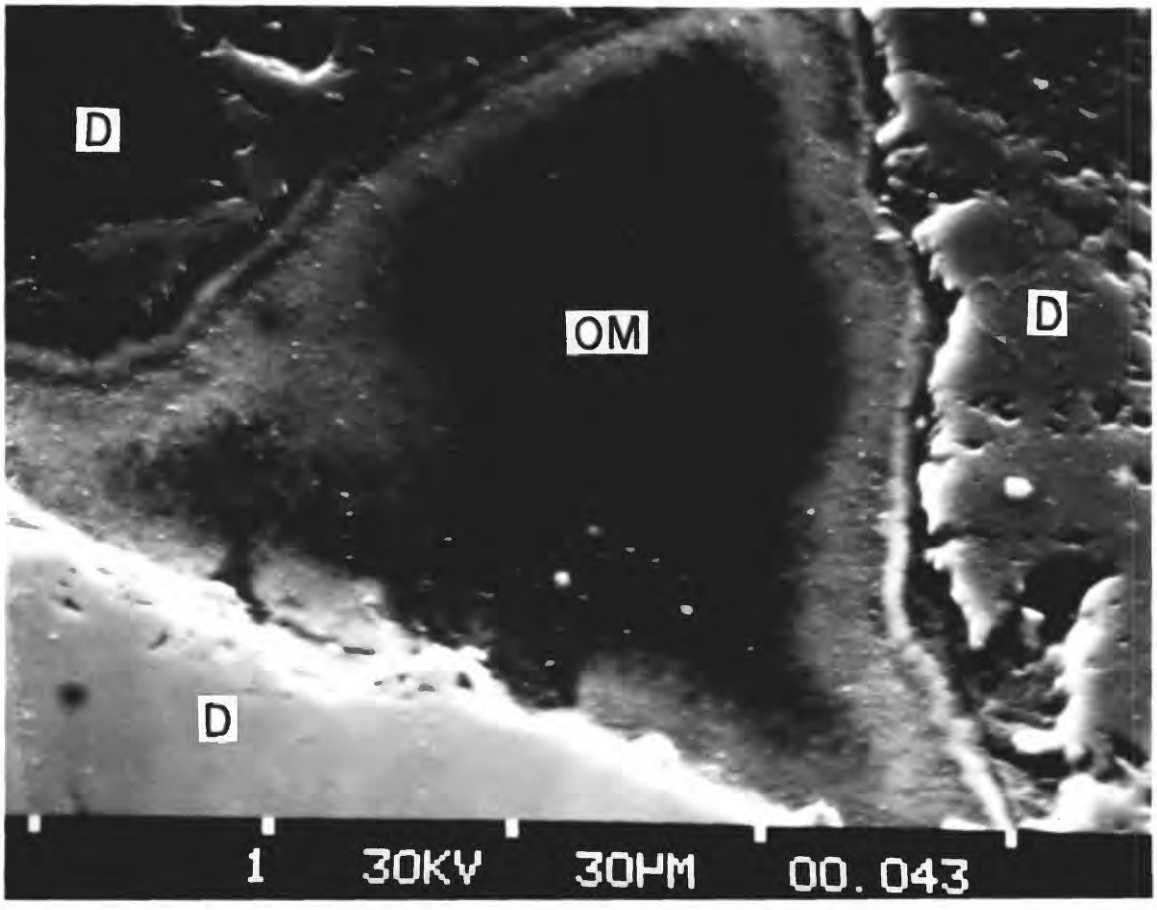

Figure 23.--SEM photomicrograph at 300X of a highly zoned region of matrix (OM). Note the strong light and dark banding. The dark/light nature of the organic matter is opposite the real appearance as seen in a petrographic microscope. Detrital grains are labeled D. This is sample NM-S30-A10 from the Section 30 mine.

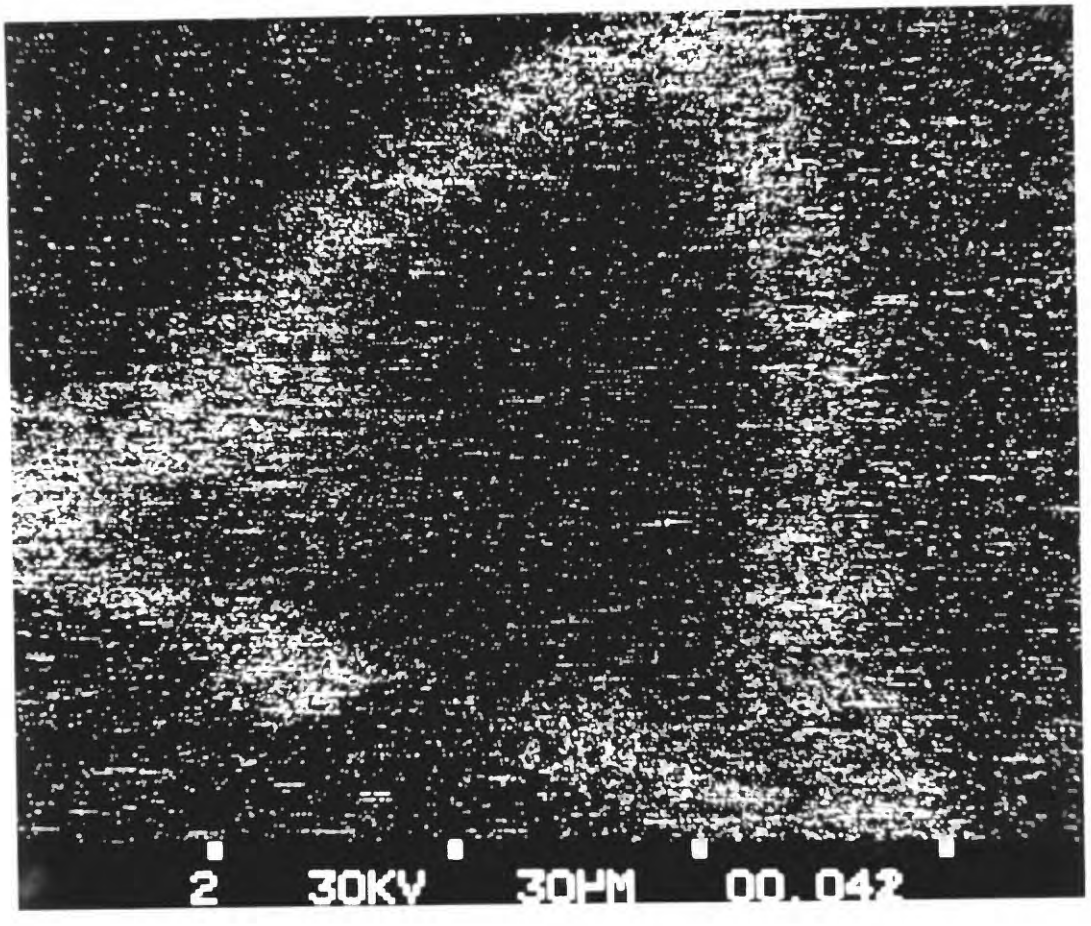

Figure 24.--X-ray fluorescence map for U. This is the exact same view of sample NM-S30-A10 seen in figure 23. White dots reflect U concentration. Anomalous white dots appear throughout the photo because of interference effects resulting in a non-zero background.

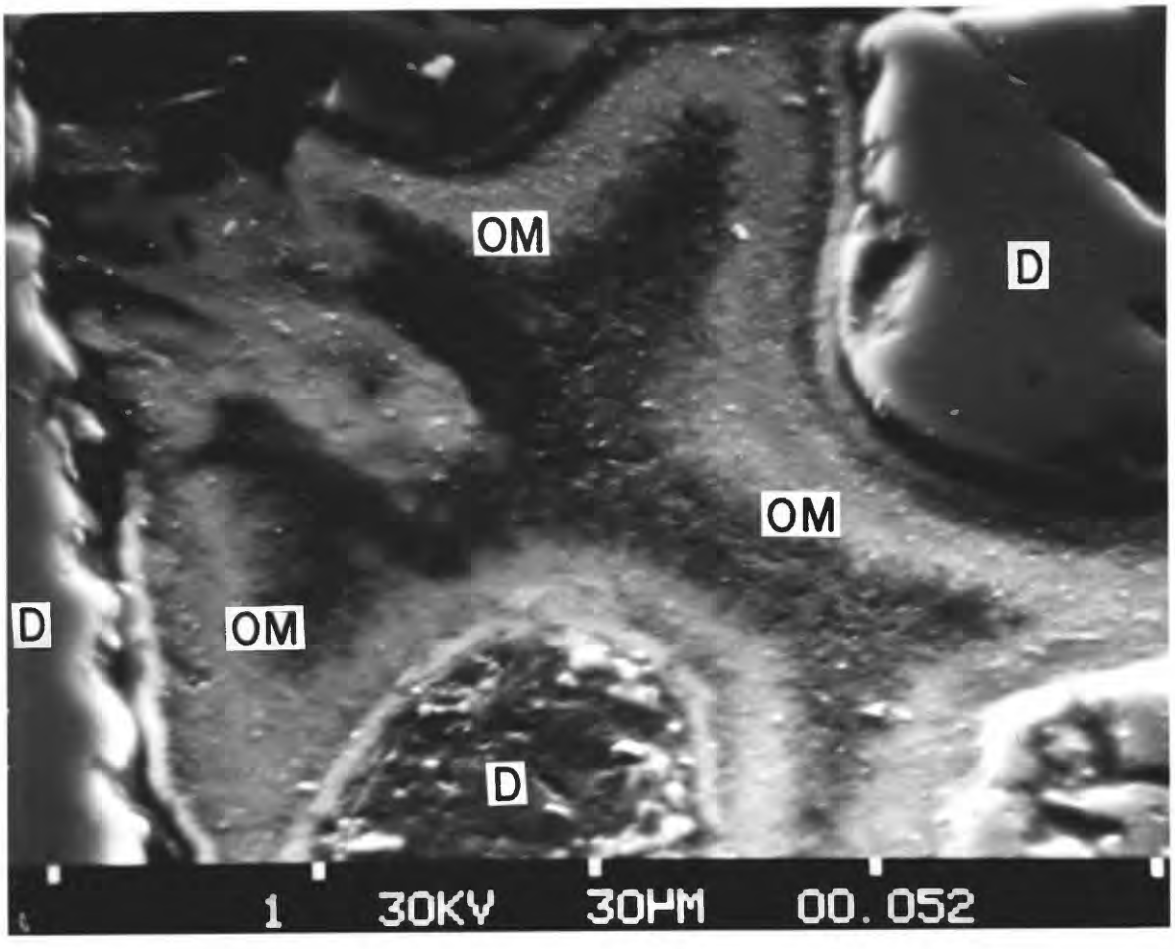

Figure 25.--SEM photomicrograph at 300X of a highly zoned and partially compressed region of organic matrix (OM). Note the light and dark banding. Detrital grains are labeled D. This is sample NM-S30-A10 from the Section 30 mine.

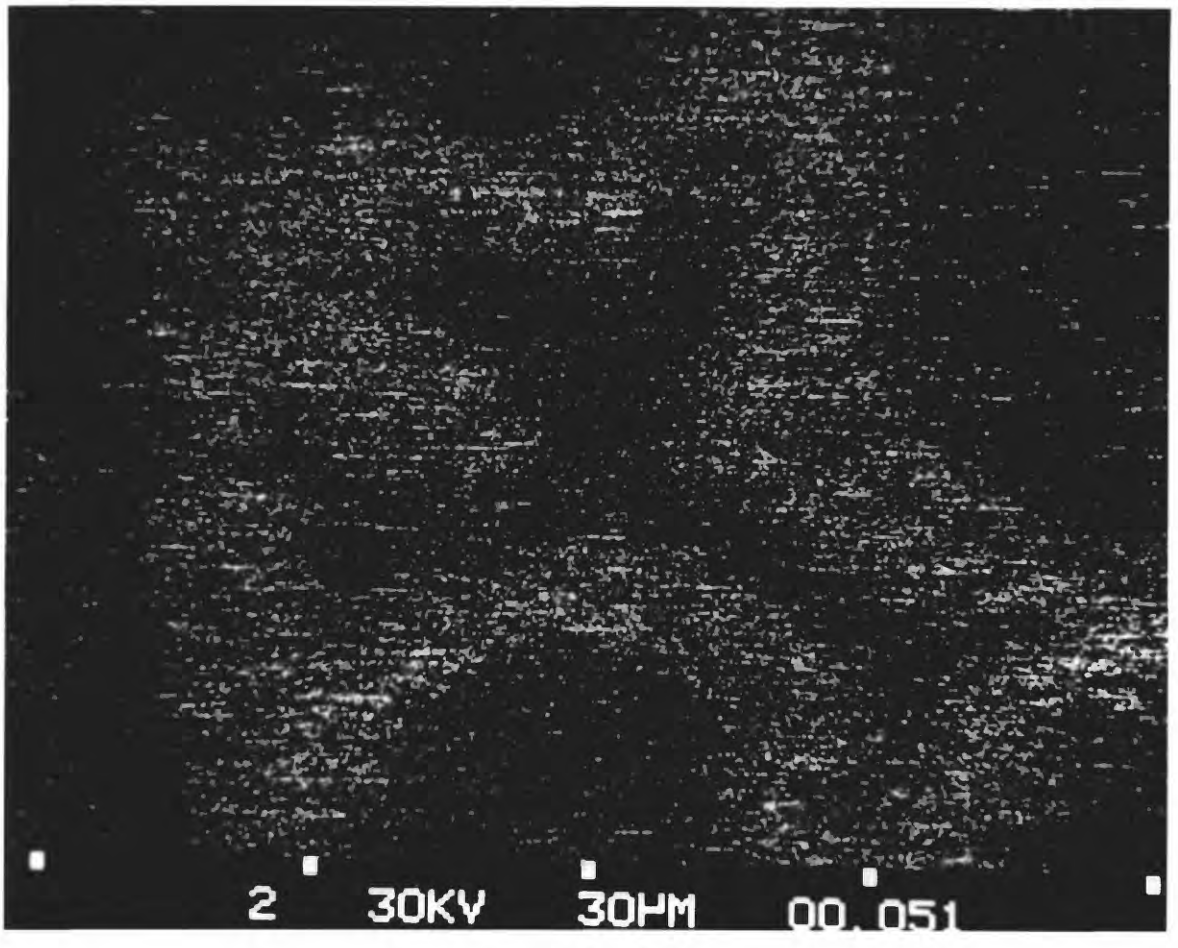

Figure 26.--X-ray fluorescence map for U. This is the exact same view of sample NM-S30-A10 seen in figure 25. White dots represent U concentration. The U is enriched along grain boundaries.

remaining organics of the fossil log are duller and coarser grained (termed flat-black organics). Several thin sections taken from the shiny material show the organic matter to consist also of the two organic types on a smaller scale. Each thin section shows both the highly reflective and the flat-black organics as thin (1 mm to 4 mm) sub-parallel bands extending in all directions through the fossil material. Fission-track maps and SEM/EDS analysis of these polished thin sections show extremely high concentrations of U and lesser amounts of Si, Al, K, V, and Fe in the shiny bands. The adjoining flat-black organics are relatively lacking in the above elements. Under reflected light, the shiny organics display little or no cell structures, whereas the inner flat-black organics are predominantly cellular. In some instances, these relict cells were flattened or crushed during burial and now appear in states of partial dissolution. A zone of solution movement extends across the fossil log. Due to the textural and chemical differences between these two fossil organic types, the outer margin of the tree trunk probably was partly dissolved by a U-bearing solution, the result being a softer, shinier, and finer organic remnant.

Other matrix phases

Besides organic matter, chert, and pyrite, variable amounts of clay, silica dust, and Fe and Ti oxides are also common in the ore matrix. These observations are true for the highest grade, organic-rich samples. The low-grade and barren samples, however, contain clays, silica dust, and metal-oxide particles as the dominant matrix material. Granger (1962) and Squyres (1980) report montmorillonite to be the dominant clay, with minor chlorite, illite, and kaolinite. A study by Riese (1980) at the Mt. Taylor mine showed chlorite as the major clay within the ore zone, although montmorillonite dominated elsewhere. Ore-zone clays are usually reported to contain considerable V.

Bright and translucent silica as rosette-shaped grains is observed in every thin section. At times, silica dust makes up a considerable portion of the matrix. As seen in figure 27, these fine (sub-micron to 25 microns) individual silica crystals are distinguished from chert cement principally by their tendency to occur as distinct, isolated phases within the matrix. The chert cement, on the other hand, usually occurs in larger masses of individual crystals. Silica dust appears as bright yellow-white rosettes; with anatase it makes up the majority of the matrix of the barren samples. Riese (1980) also distinguishes fine silica crystals as a phase separate from chert cement. The final members of the sub-micron matrix phases include scattered Fe and Ti oxides. These phases tend to be finely intermixed with the clays and silica.

Uranium-bearing phases

Clary and others (1963) and Granger (1963) report that the dominant prefault ore mineral is coffinite. Granger (1963) also states that no uraninite has ever been observed in prefault ores, however, a high-grade sample from the Section 30 mine displayed two small, optically distinct, grains of light pink coffinite near an oblong mass of clausthalite. The coffinite was of moderate to high reflectance (somewhat less than the clausthalite) and had a smooth, homogeneous surface. The coffinite and

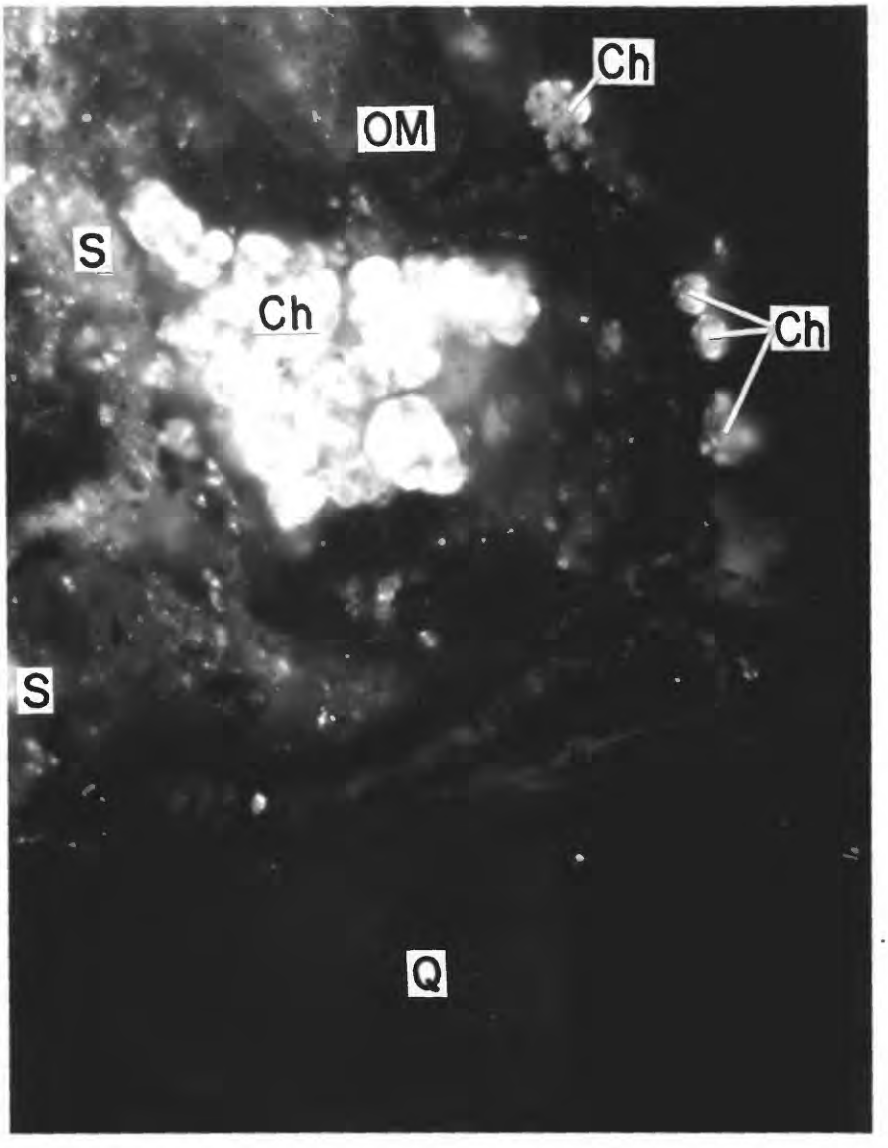

Figure 27.--Photomicrograph showing a reflected light view of the many internal reflections of the chert rosettes (Ch) versus the darker silica (S) matrix. These chert roses are distinct, large grains of pure silica, but highly reflective. To upper right and along bottom are detrital quartz (Q) grains. The fine, light gray bands are organic matter (OM)--visibly folded and compressed. From a polished thin section of sample NM-S30-A7 of the Section 30 mine, oil immersion, 160 micron field length.

clausthalite were joined along a sharp contact. SEM/EDS analysis of the coffinite showed U and Si. No other elements were present at the near one-half percent limit of detection.

Several of the high-grade ore samples were studied by means of X-ray mapping. Microprobe element scans of zoned, organic matrix showed high U concentrations along the matrix-grain contacts. In addition, elemental maps show that Si, Al, U, Fe, and V are concentrated in the darker organic margin. Rarely S, Al, and K show a weak zonation. Similar elemental scans for Si in the same regions indicate a distinctly poor point by point correspondence between the abundance of U and Si. Apparently, much of the U in the dominantly organic samples is not present as coffinite, as this would require a 1:1 correspondence. There is some weak correlation, but, in general, the Si concentrations located more to the center of the matrix and have a much larger degree of dispersal compared with the U-rich margins.

Fission-track maps also show anomalous U concentrations within the cement and matrix of organic-poor sandstones. Figures 28 and 29 show an organic-poor region of matrix with considerable U present. The extremely fine grained U (sub-micron) is most likely adsorbed on matrix phases such as clays, Fe_2O_3 and TiO_2. Apparently, high content of organic matter is not a necessary pre-requisite for low-grade sandstone mineralization, and that U-bearing solutions were present in this area far from any known ore. Fission-track maps also showed a strong association of U with the silica dust. Locally, increased concentrations of U were observed in matrix dominantly composed of silica dust.

Two final important observations regarding the distribution of U in the Ambrosia Lake prefault ores are the absence of significant U, a) in organic matter immediately adjacent to deep cracks or fissures, and b) within titanomagnetite relicts. As mentioned above, the folded and compressed organic matter is commonly marked by deep cracks, interpreted to be the result of drying of the plastic, organic mass. Many of these cracks are filled by chert, but SEM/EDS and fission-track studies show no tendency for U to concentrate within them. The grain-bordering bands of darker uraniferous matrix in many instances cross the mouth of these cracks. But even in these cases, no U is localized within the surface rupture. No U was observed (at the 0.5-percent detection limit) within titanomagnetite relicts, either. Of the hundreds of titanomagnetite relicts studied, only rarely was U ever observed, and when observed, U was adsorbed to the outside of the anatase rim which surrounded the titanomagnetite grain. Langmuir (1978) concludes that fine-grained titania has as a considerable capacity to adsorb any U present in solution. Even when the lowest-grade U samples were irradiated with a neutron dosage that allowed detection of less than 1 ppm U, no U was ever observed within the Ti-rich relicts of titanomagnetite grains. Because the organic-bearing solutions are presumed to be the altering agent of the titanomagnetites and no U was found within titanomagnetites, the altering solutions probably were not U-bearing. The presence of U only on the outside rim of the relict titanomagnetites implies that the U was introduced after the organics had entered the sandstones, altered the titanomagnetites, and precipitated the organic mass. The lack of U within the shrinkage cracks suggests that U mineralization preceded the dewatering of the organic mass.

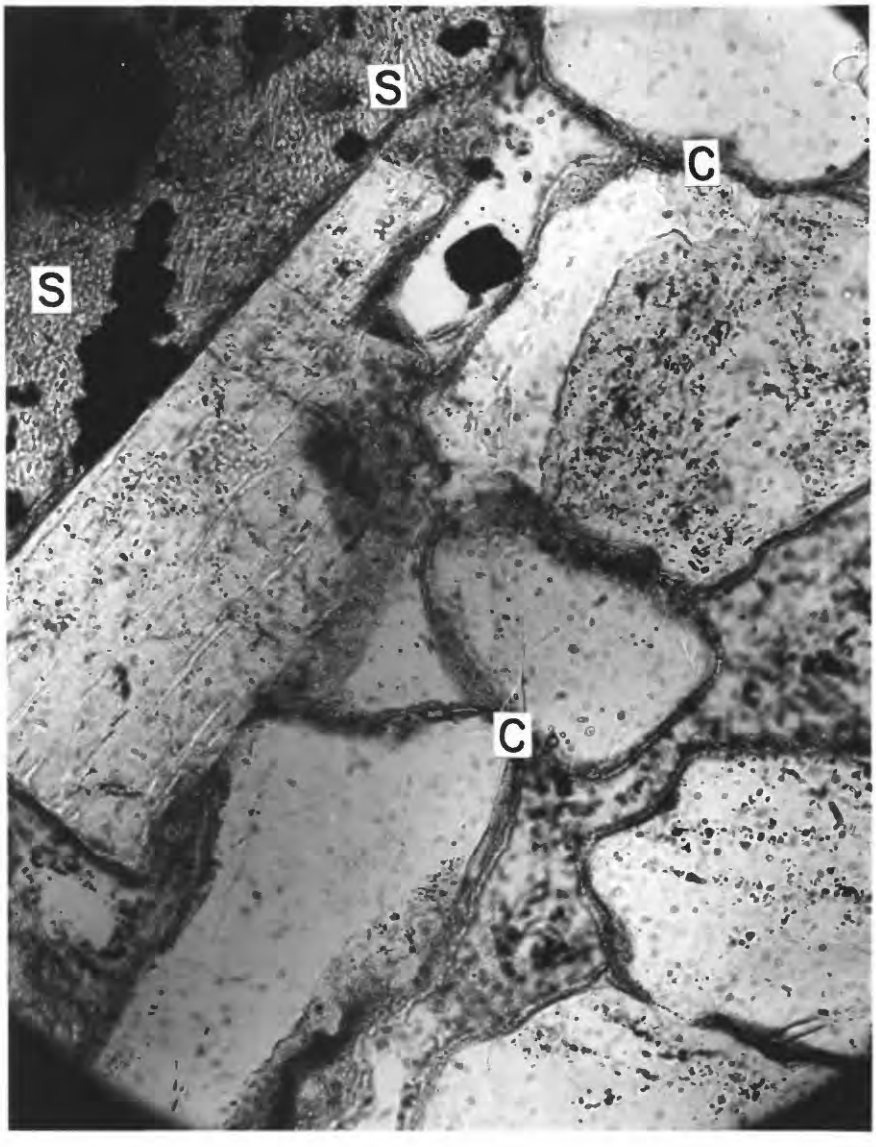

Figure 28.--Photomicrograph of a low organic content ore sample (.07% organic carbon). High magnification view of organic - free matrix which consists of silica (S), clays(C) and iron/titanium oxide particles (too fine to recognize in photo). Transmitted light view of a polished thin section, sample no. NM-S23-A1. Ore sample from Section 23 mine, 0.48mm field length.

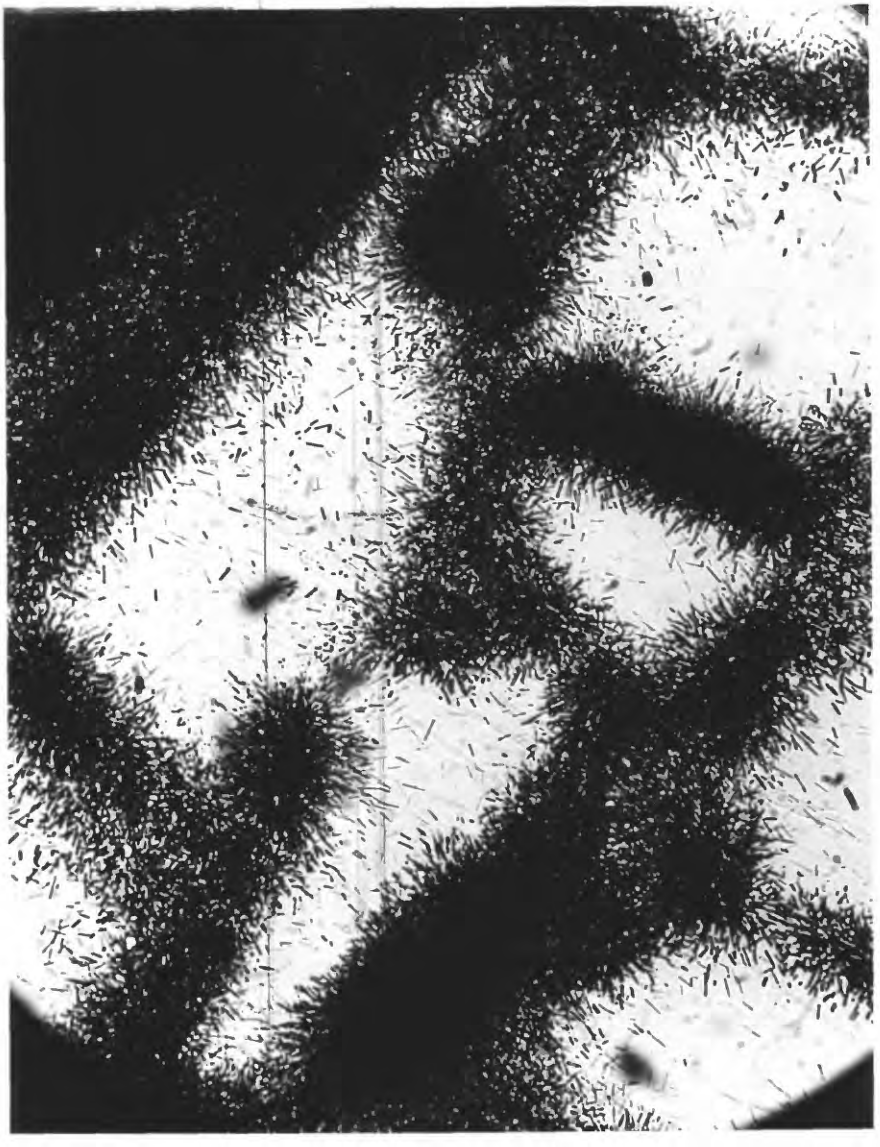

Figure 29.--Fission track map of low-grade ore sample (seen in Figure 28) with 4700 ppm U and only 0.07% organic carbon. The dark areas are high fission track concentrations which correspond to uranium in matrix. Note uranium concentrations outline detrital grains. Transmitted light view of muscovite detector, field length is 0.48mm.

DISCUSSION

Even though the sandstone-type U ores of the Grants mineral belt have been studied for more than 30 years, there is still considerable controversy concerning the source of the U as well as of the Mo, V, and Se, the method of U transport, and the time of U deposition. The hypothesized sources of the U include hydrothermal solutions (Laverty and others, 1963), the granite sources of the arkosic sediments of the mineral belt, and the interbedded volcanic detritus. The transportation of U invariably involves complexes of some type. Carbonate, sulfate, fluoride, phosphate, and organic complexes are possible if their concentrations as well as the pH are appropriate. The epigenetic solutions which carried the organic matter also may have transported the U. The results of this study, however, show that this hypothesis is unlikely. A final consideration arising from this study are petrographic observations that place limits on the time of formation of each of the epigenetic phases. Instead, these petrographic observations indicate that U must definitely have been introduced to the sediments after the organic matter precipitated but before the plastic organic mass had been highly compressed and dewatered.

Metals and their Source

The most likely source for the U is the volcanic detritus of the Morrison Formation. The bentonitic shales of the Morrison attest to significant contents of volcanic material deposited with the sandstones. Zielinski (1982) studied partially altered bentonite of Miocene age and concluded that low-temperature alteration of silicic ash to montmorillonite under oxidizing conditions can liberate major fractions of contained U. In addition, experimental leaching of volcanic glass by aerated alkaline solutions can liberate U, Se, Mo, alkali elements, silica, Zn, As, and Cu (Goodell and Trentham, 1980; Zielinski, 1982).

Some U also may have come from the granitic source regions of the arkosic sediments. Because large ion lithophile (LIL) elements such as U concentrate in the melt during magmatic differentiation, the early crystallizing minerals are lower in U than the fine-grained matrix or late crystallizing minerals. Much of this U is released during weathering processes. Szalay and Samsoni (1969) states that some of the U deposited during the cooling of a granitic pluton is deposited along grain boundaries, within microfractures, and along cleavage planes. Some of this U would be dissolved and carried away with the first weathering solutions to contact freshly exposed parts of the pluton. However, U incorporated in relatively insoluble accessory minerals such as zircon or sphene should not be as readily available for mobilization during weathering or during subsequent transport and deposition of arkosic material.

The detrital titanomagnetites are the probable source of V for the V-rich clays and the unnamed V-Ti mineral. With an ionic radius of 0.61 A for V^{+3} and a radius of 0.64 A for Ti^{+4}, substantial V can be structurally incorporated into titanomagnetites (Wedepohl, 1978). The close spatial association of altered titanomagnetites with abundant authigenic V-Ti oxides, and their similar ionic radii support the idea that the titanomagnetites served as a source for both elements.

Paragenetic model for uranium deposition

During Middle to Late Jurassic time, the source areas of the Morrison Formation were in New Mexico, Utah, and Arizona (Cadigan, 1967; Green, 1975; Granger and others, 1980). The Morrison was deposited on a continental outwash plain within a coalescing alluvial fan complex by braided and meandering streams. Variable sedimentary energy regimes are observed in the dominant cross-bedding, strong scour-and-fill features, and the many overbank-type mudstone units. Squyres' (1980) belief that at least some of the Westwater Canyon Member originally altered to red beds is supported by my observation of the many red-brown and orange clay galls which have been since chemically reduced and show an outer layer of pyritic gray-green clay. The bentonitic clays of the upper Brushy Basin and lesser amounts of bentonitic clay in the Westwater Canyon and Recapture Members prove that considerable volcanic material was deposited with the Morrison sandstones. The general paleoenvironment of the Late Jurassic can be characterized as wet, oxidized, and humid with lush vegetal growth. Overbank flooding deposited clays which buried plants that later released humic acids to the sediments (Squyres, 1980).

During the accumulation and early burial of the Morrison sediments, diagenetic chemical changes began in the sands and muds. Early compaction and burial of the newly deposited host sediments was accompanied by formation of early sulfides, silica overgrowths, and some authigenic clays, as well as detrital clay flocculation. The sands were probably heavily waterlogged (i.e. below the regional water table) and highly permeable at this stage. Because the sediments were deposited in a braided-river environment, some of the finest clays should have remained in suspension as the sands accumulated. Some clay particles eventually flocculated, presumably along the outer surfaces of detrital grain boundaries. Early sulfides would result from combination of dissolved ferrous iron and bacterially reduced sulfate species. Much of the pyrite cement, the framboids, and the fine euhedral pyrite grains probably are diagenetic. Most of the large pyrite masses are clean with little to no included organics, clays or silica. Some of the sulfide cement, however, does have organic inclusions and is therefore of a later depositional period. Euhedral crystals usually indicate nucleation and growth in an uninhibited environment. The well-crystallized pyrite grains probably formed in water-saturated, organic-free sediments. Pyrite framboids are more rarely observed. These framboids are locally replaced by the organic matter of the matrix. Finally, the minute quantities of silica in solution tended to precipitate along the surface of quartz grains. In many of the samples, the optically continuous quartz overgrowths were apparently coprecipitated with the first humate-rich materials.

The entrance of the epigenetic, organic-bearing solutions and precipitation of the organic matrix occurred soon after deposition of the sediments. Fitch (1980) reports an intraformational scour surface, within the Johnny M mine in Ambrosia Lake, which truncates an ore-bearing pod of organic matter. This and the primary sedimentary ore controls (trend ore commonly follows paleochannels) show that the organics were deposited with the sediments. Downstream flow of streams and rivers induces a similar hydraulic underflow in the underlying sediments. Squyres (1969) reported that remobilization of solubilized organics (possibly humic material) is

substantial within and along channel bottoms. The organic trash carried by the braided streams and the organic matter buried during flooding released soluble organics to ground waters. These waters apparently followed the downstream flow, within the underlying sediments.

Humic acids are soluble in alkaline to neutral solutions, and are speculated to transport significant quantities of iron, silica, and aluminum (Adams and others, 1978). The passage of alkaline, humic material bearing waters through the arkose probably caused considerable alteration of quartz and feldspars, resulting in increased concentrations of Si and Al within the solutions. The observed correspondence between the degree of detrital grain pitting, embaying, and suturing and the organic content of the samples is compatible with the proposed geochemistry of the ground waters. More humic material would be soluble in the more alkaline groundwaters, and the more alkaline ground waters would cause the greatest corrosion of detrital grains. Therefore, the samples highest in organic carbon should be the most severely altered. SEM/EDS analysis showed Si, Al, K, Fe, and V concentrated within the organic matrix. The K was most likely derived from potassium feldspars and the Fe and V from titanomagnetites.

Reducing, organic-rich alkaline porewaters also dissolved the Fe, Ti, and V from the titanomagnetites probably by complexation with dissolved organics. Each of the three elements were remobilized to varying degrees. Iron is apparently the most soluble of the three and was often transported to considerable distances. This effect can be seen in the most common occurrence of titanomagnetite relicts which are void of any Fe or Fe sulfides. Often the Ti of the titanomagnetites was reprecipitated in place, as secondary ilmenite or anatase lamellae, as secondary ilmenite or anatase masses which filled the entire relict titanomagnetite grain, or as rutile crystals bordered by an anatase rim. Some remobilization of Ti produced the scattered rutile crystals, V-Ti crystals, and the fine specks of Fe and Ti oxides. Assuming that titanomagnetites were a source of V, V was also remobilized and precipitated as V-rich clays. Because titanomagnetite grains were observed with pyrite and marcasite filling the inter-lamellar voids, some sulfide ion must have been present within the humic solutions. With such an abundance of organic matter, some portion of it was probably metabolizable by sulfate-reducing bacteria. The general effects of the alteration of titanomagnetites by the organic-bearing solutions are Ti-rich phases remaining as lamellae with silica, organic matter, and Fe sulfides filling the interior of the relict titanomagnetites.

Precipitation of dissolved or colloidal humic acids from ground waters requires a reduction in pH, increased temperature, increased concentration of large polyvalent cations (increased salinity), and/or time. When local, organic-rich alkaline porewaters reacted with volcanic ash and detrital silicates, the salinity was increased by cations which were added to the solutions. Any large-radius, polyvalent cations increase the rate of colloidal humate precipitation. Actually, the precipitation process may have been combined flocculation-precipitation of dissolved and colloidal organic matter. Squyres (1980) reports that organic matter appeared to have been precipitated as an organic gel. The rate of flocculation of a colloidal gel

increase with heat, agitation of the solution, or increased salinity (fig. 30). Because many of the samples high in organic matter have rounded, bleb-like, and banded forms of organics and silica, the organic matrix of these samples may have precipitated as a gel. Evidence of the plastic deformation of the organic matter in the sediments is clearly preserved in many of the samples of this study (fig. 28). The humic porewaters reacted with the detrital minerals, and SEM/EDS analysis has shown Si, Al, K, V, Fe ,and U to be commonly present in the organic matrix. Therefore, the increasing salinity and particularly the increasing concentration of polyvalent cations may have initiated precipitation of the organics.

Organic lenses precipitated as a plastic mass within water-saturated sediments. The typically rounded, bleb-like textures, the folded and compressed appearance, and the apparent drying cracks indicate that the organics were deposited as a soft, hydrous mass which was subsequently compressed, folded, and desiccated. Intermixed and banded silica and organic matter in the matrix show that silica coprecipitated with the organics. This observation is also true for the secondary quartz overgrowths on quartz and the organic matrix.

Sometime after the organic matter was deposited, slightly oxidizing solutions bearing U, Se, and Mo passed through the sediments. Because the organic matter and the pyrite were not destroyed, the solutions could not have been highly oxidizing. Before and during the U mineralization event, sufficient permeability had to exist within the organic-impregnated sediments to allow homogeneous U enrichment on a large scale. Within orebodies of all sizes, nearly all of the organic matter is mineralized. It is only on a microscale that a non-homogeneous distribution of U is observed. In the high-grade samples, U is always observed to be selectively concentrated on the outer margin of the organics, between the core of the organic matrix and the detrital grains (fig. 30). Fe, V, and Si also displayed this type of zoned concentration. Apparently, a thin band of pore-water existed between the plastic organic mass and the enclosing detrital grains. This water-filled space allowed sufficient permeability for the diffusion and flow of U-bearing waters in and around the organics. The observed lack of a correlation between U and Si during X-ray fluorescence mapping indicates that not all of the U is present as coffinite. Much of the U is or was directly adsorbed to the organics in the high-grade samples and adsorbed to organic matter, clays, and authigenic Fe and Ti oxides in the low-grade samples as UO_2. Leventhal (1980) and Schmidt-Collerus (1979) stress that U uptake by organic matter is predominantly by chelation and complexing to the organics outer surface, (functional groups) rather than by simple ion exhange or electrostatic adsorption. Schmidt-Collerus believes that adsorption is too dependent on a chemically-stable environment to be an important bonding mechanism. Uranyl ions, transported as carbonate complexes $UO_2(CO_3)_2$ are, upon contact with the outer organic surface, bonded to this surface and perhaps simultaneously reduced to the less soluble U(IV) form.

Because U was not observed within the silica- and organic matter-filled voids or along the surface of Ti-rich lamellae within titanomagnetite grains, the U could not have come into the sediments with the humic solutions. The humic solutions were the direct cause for the alteration for the titanomagnetites, but if the U had been transported as humic complexes, the

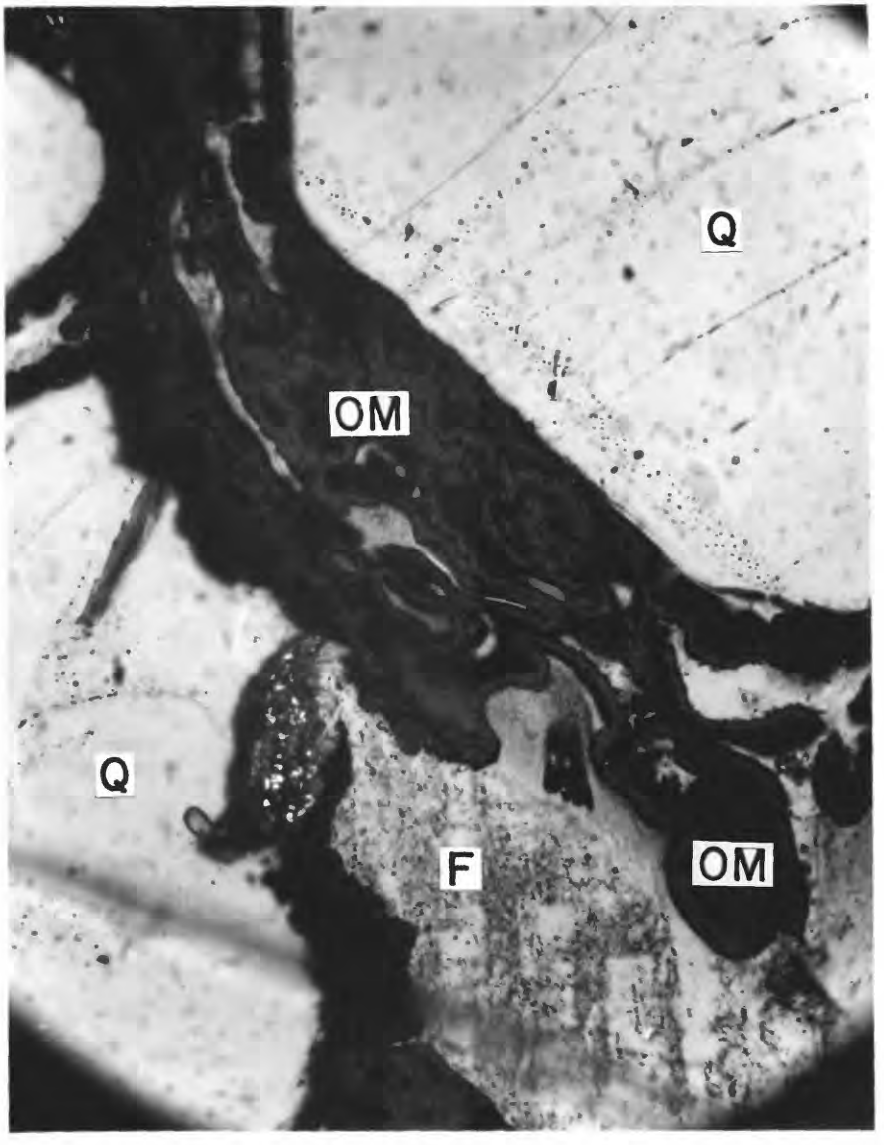

Figure 30.--Photomicrograph of collapsed, folded and highly zoned (dark and light) organic matrix. The organics are a dark to light, grayish-brown. Note that the organic matter immediately along the detrital grain -- organic matrix boundary is dark. The light organic matter commonly fills the core of the organic matrix. Detrital quartz (Q) and feldspar (F) surround the folded organics. Reflected light view of a polished thin section from the Section 30 mine, sample no. NM-S30-A7, oil immersion, 8.0mm field length.

highly adsorptive authigenic Ti-oxides surely would have captured some U during the alteration event. SEM/EDS and microprobe observation of hundreds of titanomagnetite relicts did not indicate any detectable U held within a titanomagnetite grain. Only rarely was U observed on the outside of the common anatase rim, which apparently sealed the titanomagnetite well before the mineralization event.

Petrographic evidence also indicates that the U was introduced to the sediments and bonded to the organic matrix before the sediments were greatly compacted and while the matrix was still hydrous. X-ray fluorescence maps showed U to be concentrated on the outer surface of the organic matrix. U was also selectively concentrated in darker matrix regions which originally had been the matrix surface, but during compaction of the sediments were apparently complexly folded and deformed (fig. 30). No matter how tight or complex the folding of the dark and light colored organic matter, the concentration of U, Si, Fe, and V still follows the original dark matrix outer surface. In rare instances, the dark matrix is so tightly folded into the lighter gray organic matrix that it is difficult to imagine how the uraniferous solutions could have selectively passed into the darker, folded region to precipitate U. Significant diffusion of U, Si, Fe, and V is unlikely because of the presence of the preservation of the zoned organic matrix. Once the metals were deposited along the outer surface of the organics they apparently moved no further. Detailed study of the apparent desiccation cracks within the organic matrix shows that the U was deposited before the matrix had dried because no U was ever observed within the cracks. If mineralization occurred after drying and cracking of the zoned matrix, one would expect some U to be present within these cracks.

After the U chelated to the organics and lesser amounts of U were adsorbed to the clays, silica, and Fe-Ti oxides, the sediments were further cemented and compacted. The organic matrix began folding and dewatering as Cretaceous and Tertiary sedimentation continued. Final cementation by calcite and chert filled some of the desiccation cracks within the matrix and also filled open pore spaces within the very core of the matrix space. This stage of cementation was definitely established before the oxidizing, postfault waters passed through the sediments. Formation of clausthalite probably continued through this period. Assuming that most of the Pb in the clausthalite is radiogenic, there must have been significant diffusion of Pb through the matrix to common centers of clausthalite nucleation. The concentration and distribution of Se and S are important here. The Pb has diffused at least far enough to precipitate with Se and S.

After deposition of the prefault ores, the Grants mineral belt was severely faulted and eroded (Kelley, 1963). During this time, highly oxidizing ground waters entered the sediments from the south and west. The organic matter was destroyed, pyrite oxidized to limonite, jordisite dispersed to form broad Mo haloes, and U reprecipitated near the redox interface, particularly along faults. These postfault orebodies formed large, equidimensional masses (Granger, 1963). Postfault ore deposition includes successive events of remobilization. No single, definite period of postfault ore formation has been defined based on geology or geochronology.

SUMMARY AND CONCLUSIONS

The prefault U deposits of the Ambrosia Lake District generally are intimate mixtures of U and organic matter. Minor amounts of U exist intermixed with clays, fine silica particles, and Fe and Ti oxides of the matrix. Observation of polished thin sections and polished sections of prefault ore samples from the Section 30, Section 30 W and Section 23 mines established the following paragenetic sequence:

1) the organic matter was precipitated as a hydrous, plastic mass;

2) the influx of organic-rich reducing, alkaline groundwaters remobilized significant Fe, V, and Ti from the detrital titanomagnetites, resulting in secondary anatase, pyrite-marcasite, rutile, ilmenite, and a new V-Ti mineral;

3) another set of ground waters which were more oxidizing and U-bearing allowed complexing and chelation of U to the exposed, water-saturated, outer surface of the organic matrix; and thus U was definitely precipitated after deposition of the main, organic mass;

4) much of the precipitated U was chelated to the organic material and adsorbed to clays, silica, and Fe and Ti oxides of the matrix, rather than simply present as coffinite; and

5) U precipitation was followed by aging, compaction, folding and dewatering of the plastic interstitial matrix.

REFERENCES

Adams, S. S., Curtis, H. S., Hafen, P. L., and Hossein, S. N., 1978, Interpretation of post-depositional processes related to the formation and destruction of the Jackpile-Paguate uranium deposit, northwest New Mexico: Economic Geology, v. 73, no. 8, p. 1635-1654.

Austin, S. R., 1963, Dissolution and authigenesis of feldspars, in Geology and mineral technology of the Grants uranium region, C. A. Rautman, compiler: New Mexico Bureau of Mines and Mineral Resources, Mem. 38, p. 107-115.

Berglof, W., 1970, Absolute age relationships in selected Colorado Plateau uranium ores: PhD. thesis, Columbia Univ., distrib. by University Microfilms.

Brookins, D. G., 1980, Geochronologic studies in the Grants Mineral belt, in Geology and mineral technology of the Grants uranium region, C. A. Rautman, compiler: New Mexico Bureau of Mines and Mineral Resources, Mem. 38, p. 52-58.

Cadigan, R. A., 1967, Petrology of the Morrison Formation in the Colorado Plateau region: U.S. Geol. Survey Prof. Paper 556, 113 p.

Chenowith, W. L., and Learned, E. A., 1979, Stratigraphic section, Ambrosia Lake area McKinley and Valencia Counties, New Mexico: New Mexico Bureau of Mines and Mineral Resources, Mem. 38, p. 401.

Clary, T. A., Mobley, C. M., and Moulton, Jr., G. F., 1963, Geological setting of an anomalous ore deposit in the Section 30 mine, Ambrosia Lake area, in Geology and technology of the Grants uranium region, V. C. Kelley, compiler: New Mexico Bureau of Mines and Mineral Resources, Mem. 15, p. 72-79.

Davidson, 1963, Selenium in some oxidized sandstone-type uranium deposits: U.S. Geol. Survey Bull. 1162-C, 33 p.

DeVoto, R., 1978, Uranium geology and exploration: Colorado School of Mines--Lecture Notes and References, 396 p.

Fitch, D. C., 1980, Exploration for Uranium deposits, Grants Mineral belt, in Geology and mineral technology of the Grants uranium region, C. A. Rautman, compiler: New Mexico Bureau of Mines and Mineral Resources, Mem. 38, p. 40-51.

Galloway, W. E., 1980, Deposition and early hydrologic evolution of Westwater Canyon wet alluvial-fan system, in Geology and mineral technology of the Grants uranium region, C. A. Rautman, compiler: New Mexico Bureau of Mines and Mineral Resources, Mem. 38, p. 59-69.

Goldhaber, M. B., Reynolds, R. L., and Rye, R. O., 1978, Origin of a South Texas roll-type uranium deposit: II. sulfide petralogy and sulfur isotope studies; Economic Geology, v. 73, p. 1690-1705.

Goodell, P. C., and Trentham, R. C., 1980, Experimental leaching of uranium from tuffaceous rx: Bendix Field Engineering Corp., U.S. Dept. of Energy, 160 p.

Gould, W., Smith, R. B., Metzger, S. P., and Melancon, P. E., 1963, Geology of the Homestake-Sapin uranium deposits, Ambrosia Lake area, in Geology and technology of the Grants uranium region, V. C. Kelley, compiler: New Mexico Bureau of Mines and Mineral Resources, Mem. 15, p. 66-71.

Granger, H. C., Santos, E. S., Dean, B. G., and Moore, F. B., 1961, Sandstone-type uranium deposits at Ambrosia Lake, New Mexico--an interim report: Economic Geology, v. 56, no. 7, p. 1179-1209.

Granger, H. C., 1962, Clays in the Morrison Formation and their spatial relation to the uranium deposits at Ambrosia Lake, New Mexico: U.S. Geol. Survey Prof. Paper 450-D, p. D15-D20.

Granger, H. C., 1963, Mineralogy, in Geology and technology of the Grants uranium region, V. C. Kelley, compiler: New Mexico Bureau of Mines and Mineral Resources, Mem. 15, p. 234-243.

Granger, H. C., and Warren, C. G., 1979, The importance of dissolved free oxygen during formation of sandstone-type uranium deposits: U.S. Geol. Survey Open-File Report 79-1603, 22 p.

Granger, H. C., Finch, W. I., Kirk, A. R., and Thaden, R. E., 1980, Genetic-geologic model for tabular humate uranium deposits, Grants mineral belt, San Juan Basin, New Mexico: U.S. Geol. Survey Open-File Report 80-2018-C.

Green, M. W., 1975, Paleodepositional units in upper Jurassic rocks in the Gallup-Laguna uranium area, New Mexico: U.S. Geol. Survey Open-File Report 75-610, 13 p.

Green, M. W., 1981, Origin of intraformational folds in the Jurassic Todilto Limestone, Ambrosia Lake uranium mining district, McKinley and Valencia Countries, New Mexico: U.S. Geol. Survey Open-File Report, no. 82-69.

Hilpert, L. S., and Moench, R. H., 1960, Uranium deposits of the southern part of the San Juan Basin, New Mexico: Economic Geology, v. 55, no. 3, p. 429-464.

Hilpert, L. S., 1963, Regional and local stratigraphy of uranium-bearing rocks, in Geology and technology of the Grants uranium region, J. C. Kelly, compiler: New Mexico Bureau of Mines and Mineral Resources, Mem. 15, p. 6-18.

Kelley, V. C., 1963, Tectonic setting, in Geology and technology of the Grants uranium region, V. C. Kelley, compiler: New Mexico Bureau of Mines and Mineral Resources, Mem. 15, p. 19.

Langmuir, D., 1978, Uranium solution-mineral equilibria at low temperatures with applications to sedimentary ore deposits: Mineralogical Association of Canada Short Course Notes, v. 3, 521 p.

Laverty, R. A., Ashwill, W. R., Chenoweth, W. L., and D. L. Norton, 1963, Ore processes, in Geology and technology of the Grants uranium region, V. C. Kelley, compiler: New Mexico Bureau of Mines and Mineral Resources, Mem. 15, p. 191-204.

Leventhal, J. S., 1980, Organic geochemistry and uranium in Grants Mineral belt, in Geology and mineral technology of the Grants uranium region, C. A. Rautman, compiler: New Mexico Bureau of Mines and Mineral Resources, Mem. 38, p. 75-85.

McLaughlin, Jr., E. D., 1963, Uranium deposits in the Todilto Limestone of the Grants District, in Geology and technology of the Grants uranium region, V. C. Kelley, compiler: New Mexico Bureau of Mines and Mineral Resources, Mem. 15, p. 136-149.

Miller, D. S., and Kulp, J. L., 1963, Isotopic evidence on the origin of the Colorado Plateau uranium ores: Geol. Soc. of America Bulletin, v. 74, p. 609-630.

Moench, R. H., 1963, Geologic limitations on the age of uranium deposits in the Laguna district, in Geology and technology of the Grants uranium region, V. C. Kelley, compiler: New Mexico Bureau of Mines and Mineral Resources, Mem. 15, p. 157-166.

Moench, R. H., and Schlee, J. S., 1967, Geology and uranium deposits of the Laguna district, New Mexico: U.S. Geol. Survey Prof. Paper 519, 117 p.

Nash, J. T., 1968, Uranium deposits in the Jackpile sandstone, New Mexico: Economic Geology, v. 63, p. 737-750.

Perry, B. L., 1963, Limestone reefs as an ore control in the Jurassic Todilto Limestone of the Grants district, in Geology and Technology of the Grants uranium region, V. C. Kelley, compiler: New Mexico Bureau of Mines and Mineral Reosurces, Mem. 15, p. 150-156.

Pierrot, R. M., 1979, Chemical and determinative tables of mineralogy: Masson Publishing USA, Inc., p. 167.

Ramdohr, P., 1969, The ore minerals and their intergrowths: Pergamon Press, Oxford, 1174 p.

Reynolds, R. L., and Goldhaber, M. B., 1978, Recognition of oxidized sulfide minerals as an exploration guide for uranium: U.S. Geol. Survey Jour. Research, v. 6, no. 4, p. 483-488.

Rhett, D. W., 1980, Heavy mineral criteria for subsurface uranium exploration, San Juan Basin, New Mexico, in Geology and mineral technology of the Grants uranium region, C. A. Rautman, compiler: New Mexico Bureau of Mines and Mineral Resources, Mem. 38, p. 202-207.

Riese, W. C., 1980, The Mount Taylor uranium deposit San Mateo, New Mexico: Ph. D. Thesis, University of New Mexico, 588 p.

Santos, E. S., 1970, Stratigraphy of the Morrison Formation and structure of the Ambrosia Lake district, New Mexico: U.S. Geol. Survey Bull. 1272-E.

Saucier, A. E., 1980, Tertiary oxidation in Westwater Canyon Member of Morrison Formation, in Geology and mineral technology of the Grants uranium region, C. A. Rautman, compiler: New Mexico Bureau of Mines and Mineral Resources, Mem. 38, p. 116-121.

Schlee, J. S., 1963, Sandstone pipes of the Laguna area, New Mexico: Jour. Sed. Petrology, v. 33, no. 1, p. 112-123.

Schmidt-Collerus, J. J., 1979, Investigations of the relationship between organic matter and uranium depoists: University of Denver, Denver Research Institute, no. 2513, 192 p., Report to U.S. Atomic Energy Commission.

Shatkov, G. A., Shatkova, L. N., and Gushchin, Ye. N., 1970, The distribution of U, Th, F, Cl, Mo, and Nb in liparites and acid volcanic glasses: Geochemistry International, v. 7, p. 1051-1063.

Shawe, D. R., and Granger, H. C., 1965, Uranium ore rolls--an analysis, Economic Geology, v. 60, no. 2, p. 240-250.

Squyres, J. B., 1969, Origin and depositional environment of uranium deposits of the Grants Region, New Mexico: PhD Thesis, Stanford University, 228 p.

_____ 1980, Origin and significance of organic matter in uranium deposits of Morrison Formation, San Juan Basin, New Mexico, in Geology and mineral technology of the Grants uranium region, C. A. Rautman, compiler: New Mexico Bureau of Mines and Mineral Resources, Mem. 38, p. 86-97.

Szalay, A. and Samsoni, Z., 1969, Investigation of the leaching of Uranium from crushed magmatic rock: Geochem. Intl., v. 6, p. 613-623.

Taggart, J. D., Lichte, F. E., Wahlberg, J. S., 1981, Methods of analysis of samples using XRF and ICP. in Mt St. Helens, USGS Prof. Paper 1250, p. 683-92

Wedepohl, K. H., ed., 1978, Handbook of Geochemistry: Springer-Verlag, Berlin, p. 23-A-1 to 23-O-1.

Wylie, E. T., 1963, Geology of the Woodrow Breccia Pipe, in Geology and technology of the Grants uranium region, V. C. Kelley, compiler: New Mexico Bureau of Mines and Mineral Resources, Mem. 15, p. 177-181.

Zielinski, R. A., 1981, Mobility of uranium and other elements during alteration of airfall ash to montmorillonite: a case study. (Abs), 29th Annual Meeting Rocky Mountain Section, Amer. Assoc. of Petroleum Geologists, Albuquerque, N.M., p. 56.

_____ 1982, Experimental leaching of volcanic glass: implication for evaluation of glassy volcanic rocks as sources of uranium: In Amer. Assoc. of Petroleum Geologist Studies in Geology , No. 13, Uranium in Volcanic and Volcaniclastic Rocks, p. 1-13.

Zielinski, R. A., Peterman, Z. E., Stuckless, J. S., Rosholt, J. N. and Nkomo, I. T., 1981, The chemical and isotopic record of rock-water interaction in the Sherman Granite, Wyoming and Colorado: Contrib. Mineral and Petrol., v. 78, p. 209-219.

APPENDIX

Field notes and petrographic descriptions

Sample No.	
NM-S30W-A1	
NM-S30W-A2	Section 30 West mine
NM-S30W-A3B	
NM-S30-A4	
NM-S30-A5	
NM-S30-A6	
NM-S30-A7	Section 30 mine
NM-S30-A8	
NM-S30-A9	
NM-S30-A10	
NM-S23-A1	
NM-S23-A2	Section 23 mine
NM-S23-A4	
NM-S23-A5	

Sample no.: NM-S30W-A1

Field notes: Dense, black, prefault sandstone ore, little calcite cement. Inclusions of mudstone galls with orange-red centers and green, outer margins. Sample site - 318,220 N 526,465.

Petrography:

Quartz - makes up 30 to 45 percent of thin sections; 25 percent of quartz grains show secondary silica overgrowths with high relief; inclusions are minor to heavy; minor embaying; minor rutilated quartz.

Feldspars - makes up 25 to 30 percent of thin sections, plagioclase, K-spar, and perthite display weak to strong alteration; perthites are generally the least altered; seicite, epidote, pyrite, calcite, chert, and iron oxides replace feldspars.

Other minerals - rounded chert fragments, pyrite, titanomagnetites, volcanic rock fragments comprise from 5 to 15 percent of thin section.

Organics - are dark gray-brown, heavily pitted; cracked; some organics replace titanomagnetites; organic cement minor and calcite as main cement; within organics are framboidal pyrite and clausthalite grains.

Description - medium-grained (average grain size is 0.45 mm), moderately sorted, arkosic sandstone; grains spheroidal to equant; rounded to sub-rounded; calcite, organic matter, chert, and pyrite as cement; minor clay.

Sample no.: NM-S30W-A2

Field notes: Dense, black, prefault sandstone ore. Many included clay galls with a red interior and a reduced, green, exterior. Sample site - 318,265 N 526,405.

Petrography:

Quartz - makes up 50 percent of thin sections; quartz grains are strained and cracked with undulatory extinction; contains some(?) silica overgrowths with some secondary silica filling fractures in the quartz; inclusions in quartz are few to many; contains only minor amounts rutilated quartz.

Feldspars - make up 25 to 35 percent of thin sections; minor overgrowths; plagioclase, K-spar, perthite and micrographically intergrown K-spar and quartz less altered than other feldspars; chert, sericite, epidote, pyrite replace feldspars.

Other minerals - pyrite, garnet, chert grains, biotite, zircon, titanomagnetites, volcanic rock fragments comprise approximately 1 percent of thin section.

Organics - occur as matrix and replacing titanomagnetites and as inclusions filling pyrite cement; rutile crystals are randomly scattered in matrix; silica cement and organic matrix are intimately mixed; organic matrix is highly zoned and often colloform.

Description - medium-grained (average grain size is 0.35 mm), poorly to moderately sorted, arkosic sandstone; grains spheroidal to tabular to equant, sub-angular to rounded; organics, chert and pyrite as cement; minor clay.

NM-S30W-A3B

Field notes: Dense, black, prefault sandstone ore, major quantities calcite present as crystals in sandstone. Minor quantities clay galls present with red to yellow interior and green exterior. Clay galls give higher β counts (higher radiation) than nearby sandstone ore. Sample site - 319,471 N 521,617.

Petrography:

Quartz - makes up 50 to 70 percent of thin sections; most quartz grains have inclusions; has minor fractures; rutilation; and secondary silica overgrowths.

Feldspar - makes up 15 to 30 percent of thin sections; most feldspars are unaltered to lightly altered; perthites are least altered; minor grains of micrographically intergrown K-spar and quartz; sericite, calcite, chert, epidote and pyrite replace feldspars.

Other minerals - chert fragments, pyrite, clacite, biotite, zircon, apatite, titanomagnetites, volcanic rock fragments make up 1 to 2 percent of thin sections.

Organics - minor organics as cement/matrix; along outside rim of organic matrix with detrital grains is dusty clay and silica; cracks within matrix are common; V-Ti mineral present in matrix.

Description - fine grained (average grain size 0.16 mm), well-sorted, sub-arkosic sandstone; grains are sub-angular to sub-rounded, spherical to tabular; much calcite cement, minor chert, organics and pyrite cement.

NM-S30-A4

Field notes: Poorly cemented, barren white sandstone. No visible ore or molybdenum sulfides. Sample site - 3800 halvage drift, 3801 stope. This barren sample collected as far from ore as possible.

Petrography:

Quartz - makes up at least 60 percent of thin sections; secondary silica overgrowths are very minor to non-existent; fluid and crystal inclusions in quartz are variable (minor to major); no observed embayments.

Feldspar - makes up approximately 20 percent of thin sections; K-spar, plagioclase, and perthites display minor to complete alteration; many perthitic feldspar grains are present; chert, epidote, sericite, and opaques replace feldspars.

Other minerals - rounded chert fragments, biotite, pyrite, zircon, titanomagnetites. Many pyrite framboids.

Organics - no visible organics.

Description - very fine grained (the average grain size is 0.12 mm), well-sorted, arkosic sandstone; grains are mostly elongate, sub-rounded to rounded; predominantly with calcite cement.

NM-S30-A5

Field notes: Dense, black, highly radioactive prefault ore; mixed sandstone ore and fragments of uranium-bearing carb. trash. Blue and green molybdenum oxides present. Sample collected within 1 meter of a highly mineralized tree trunk (approximately 12 meters long and up to 2 meters in diameter). Sample site - 9401 level; 320,000 N 529,610.

Petrography:

Quartz - makes up 45 to 60 percent of thin sections; thick overgrowths of secondary silica are common; light to heavy inclusions within quartz; moderate rutilated quartz; little fracturing of quartz grains; little embaying of quartz.

Feldspar - makes up 20 to 40 percent of thin sections; alteration of K-spar, plagioclase, and perthite ranges from minor to complete; some feldspars appear "eaten-away;" some perthites are unaltered; sericite, biotite, chert, organics, epidote, and iron oxides replace feldspars.

Other minerals - chalcedony, clausthalite, rounded chert grains, zircon, titanomagnetites, biotite, pyrite (as cement, grains and framboids), rutile.

Organics - as cement/matrix filling and as rounded, detrital pieces of organic trash. Organic matrix is highly zoned, colloform textured, and cracked. Much rutile, clausthalite, pyrite intimately mixed with organics. The organic trash shows rutile and clausthalite within the fragments. Organic matrix makes up 10-20 percent of section.

Description - fine-grained (average grain size is 0.16 mm), well-sorted, arkosic sandstone; grains equant to elongate; sub-rounded to angular; organics and chert as cement.

NM-S30-A6

Field notes: Highly radioactive, mineralized tree material. Both "shiny" and "flat" black organic matter in sample. Much pyrite intimately mixed with the uranium-rich, organics. Sample site - 9401 level; 320,000 N 529610.

Petrography:

This sample is not sandstone.

Minerals - Pyrite and marcasite, rutile, chert, and clausthalite.

Organics - This sample commonly shows fossil cell structures in varying states of alteration. Many cells contain pyrite and chert fillings. Some of the cells have been partially dissolved and have subsequently collapsed. Strong differences in reflectance are readily observed. Many white to orange, fine micro-spheroids appear scattered throughout the organic matter. Sulfide framboids are rarely observed.

NM-S30-A7

Field notes: Dense, black prefault sandstone ore. This high-grade sample was collected approximately 1 meter from fossilized tree trunk, across ore stope. Sample collected 2 meters from contact of ore-bearing, black sandstone with white, U-poor sandstone. Sample site-9401 level; 320,000 N 529610.

Petrography:

Quartz - makes up 35 to 60 percent of thin sections; most quartz grains contain inclusions; little strained or fractured quartz; many quartz grains are embayed and secondary silica overgrowths are common; minor rutilated quartz.

Feldspar - makes up 25 to 40 percent of thin section; many feldspars are highly altered; some have secondary overgrowths. Alteration: sericite, epidote, muscovite, pyrite, organic matter.

Other minerals - zircon, chert fragments, secondary Fe and Ti oxides, titanomagnetites, volcanic rock fragments make up 2 to 3 percent of thin sections, clausthalite.

Organic - Matter is highly zoned (darkest along grain boundary - lighter in the central interior of matrix regions); is red-brown to brownish-black in strong, transmitted light; colloform textures is apparent; finely intermixed with pyrite, clausthalite and rutile; silica commonly fills cracks ("shrinkage" cracks?) within the organic matter.

Description - fine-grained (average grain size is 0.3 mm), moderately-well to well-sorted, arkosic sandstone; grains are tabular to spheroidal, sub-angular to sub-rounded, some clay mixed with matrix, predominant cement is organic matter with minor silical filling of fractures.

NM-S30-A8

Field notes: Dense, black, prefault sandstone ore. Highly radioactive. Near contact of barren, white sandstone with black, uranium-bearing sandstone. Heavy calcite cement. Sample site - 9401 A level; 320,000 N 529,610.

Petrography:

Quartz - makes up 50 to 55 percent of thin sections; strong embaying of quartz grains; minor secondary silica overgrowths; variable inclusion content; minor rutilated quartz.

Feldspars - makes up 30 to 35 percent of thin sections; minor pieces of micrographically intergrown K-spar and quartz; perthite generally less altered than plagioclase and K-spar; sericite, epidote, chert, organic matter, and pyrite replace feldspars.

Other minerals - biotite, pyrite, secondary titanium and iron oxides, zircon, epidote, chert, fragments, titanomagnetites, and volcanic rock fragments (make up at least 2 percent of thin sections), silicified limestone fragments.

Organics - highly zoned organic matrix with finely intermixed pyrite, rutile, ilmenite, and V-Ti oxide; organics commonly appear colloform. Considerable organic matter as cement.

Description - fine grained (average grain size is 0.24 mm), well sorted to moderately sorted, arkosic sandstone; grains elongate, tabular and spheroidal; rounded to sub-rounded; organics, calcite and chert as cement; very little clay in matrix.

NM-S30-A9

Field notes: Medium-grade, well-cemented, black, prefault sandstone ore. Collected less than 40 cm from contact of white, barren sandstones and black, sandstone ore. Bright blue-green molybdenum oxides concentrated within barren sandstone, immediately along contact. Sample collected 3 meters along line S70^{o}E from NM-S30-A8, and also within 3 meters of fossilized, ore-bearing tree trunk. Sample site - 9401 A level; 320,000 N 529610.

Petrography:

Quartz - makes up 40 to 55 percent of thin sections; considerable embayed quartz grains with silica overgrowths common; much strained quartz; minor to major inclusions in quartz; only minor rutilated quartz.

Feldspars - make up 30 to 35 percent of thin sections; some feldspars show corroded edges; perthitic feldspars are most common and usually the least altered; in general--the feldspars display considerable alteration; biotite, iron oxides, epidote, pyrite, and silica replace feldspars.

Other minerals - zircon, sedimentary chert grains, pyrite/marcasite, hundreds of secondary iron and titanium oxide grains, titanomagnetites, pyroxene, and volcanic rock fragments.

Organics - make up 5 to 10 percent of thin sections; strongly to weakly zoned as matrix (darkest along grain boundaries); intimately mixed with pyrite, marcasite, secondary titanium oxides and minor clay; replaces titanomagnetites; show shrinkage cracks, some are chert filled.

Description - fine grained (average grain size is 0.20 mm), moderately sorted, arkosic sandstone; grains elongate, tabular and spheroidal; angular to sub-angular; predominant organic matter as cement, minor chert cement (with finely intermixed clay).

NM-S30-A10

Field notes: Dense, black prefault sandstone ore. Ore samples about 30 centimeters below contact of ore and barren sandstone. Sample site - 9401 A level; 320,000 N 529610.

Petrography:

Quartz - makes up 40 to 45 percent of thin sections; most grains are strained; inclusion content is highly variable; secondary silica overgrowths are common.

Feldspars - makes up 30 to 40 percent of thin sections; most K-spar and plagioclase moderately to highly altered; most feldspar is perthitic; most perthites are less altered; sericite, pyrite, organic matter, epidote and biotite replace feldspars.

Other minerals - clausthalite, zircon, serpentine, pyrite, secondary iron and titanium oxides, biotite, rounded chert fragments volcanic rock fragments make 1 to 5 percent of thin sections and titanomagnetites.

Organics - very highly zoned matrix; shrinkage cracks and colloform textures apparent in organics; pyrite, clausthalite, rutile, V-Ti mineral, and ilmenite are intimately mixed with matrix; some matrix shows high clay content.

Description - fine grained (average grain size is 0.22 mm), moderately to well sorted, arkosic sandstone; grains oblate, spheroidal and elongate; sub-angular to sub-rounded; chert and organics as cement and main matrix component.

NM-S23-A1

Field notes: Highly weathered, crumbly, oxidized post-fault sandstone ore. Ore shows low radiation count in mine. Much calcite and kaolinite as small, distinct masses in sandstone. Sandstone is white; associated sandstones at sample site are cross-bedded fine to very coarse grained, white, yellow, orange, and red. Sample site - 36E 800N.

Petrography:

Quartz - makes up 50 to 55 percent of thin sections; secondary silica overgrowths are minor to moderate; quartz is highly strained; minor fluid inclusions.

Feldspars - make up 25 to 40 percent of thin sections; most feldspar is perthitic; some show secondary overgrowths; alteration ranges from moderate to strong; epidote, sericite, chert, and pyrite replace feldspars.

Other minerals - biotite, zircon, pyrite, secondary iron and titanium oxides, titanomagnetites, chert grains, and volcanic rock fragments.

Organics - no organics are optically recognized; many secondary titanium oxides, pyrite, and clay make up most of the matrix.

Description - fine grained (average grain size of 0.20 mm), moderately sorted, arkosic sandstone; grains elongate, tabular and spheroidal; angular to sub-rounded; main cement is silica, with calcite also predominant.

NM-S23-A2

Field notes: Strongly bedded, fine-grained, gray-white, barren sandstone. Visible kaolinite blebs. Sample site is 40 feet NW of site 36E, 800N.

Petrography:

Quartz - makes up 60 to 65 percent of thin sections; grain borders show high relief; undulatory extinction in quartz grains common; moderate fluid inclusions.

Feldspars - make up approximately 25 percent of thin section; alteration highly variable--some feldspars are totally replaced while some unaltered grains occur; perthitic feldspar common; sericite, pyrite and chert replace feldspars.

Other minerals - rounded chert fragments, pyrite, titanomagnetites, anatase, rutile, biotite, and volcanic rock fragments are approximately 5 percent of thin sections.

Organics - no optically discernible organics are present.

Description - medium-grained (average grain size is 0.30 mm), moderately-well sorted, barren, arkosic sandstone; grains are spheroidal to tabular, sub-rounded to rounded; very strong chert cement content, minor calcite.

NM-S23-A4

Field notes: Heavy, black, primary ore. This sample was taken from a small pod (approximately 1 meter by 1.3 meters). Minor, secondary mine oxidation coat the mine walls. Sample site - 50E, 1400N.

Petrography:

Quartz - makes up 50 to 80 percent of thin sections; grain borders show very strong relief; embayments and silica overgrowths on grain margins are moderate; in places much clay occurs along grain margins; inclusions and strained quartz grains are moderate.

Feldspars - makes up 15 to 25 percent of thin sections; wide range in degree of feldspar alteration; some micrographically intergrown K-spar and quartz present; sericite, epidote, chert, clays, and iron oxides replace feldspars.

Other minerals - biotite, pyroxene, chert, muscovite, zircon, pyrite, titanomagnetites, and volcanic rock fragments which make up about 2-3 percent of the thin sections.

Organics - light to medium gray, dusty matrix and ament; pyrite framboids present in matrix; organics closely associated with pyrite; colloform textures along boundaries with grains.

Description - very fine grained (the average grain size is 0.09 mm), well sorted, arkosic sandstone; grains are oblate, equant and spheroidal, sub-angular to sub-rounded; organics, chert and calcite as cement.

NM-S23-A5

This sample was donated by Bill Harrison (of United Nuclear-Homestake Partners). The sample is from the "B1" sand of the Westwater Canyon. Replaced by organic matter high in carbon and by uranium, this sample was originally a dinosaur bone. This fact is verified by the high P and Ca content.

The original cells are fossilized with cell interiors filled by mixtures of calcite and pyrite. Fission track maps show no detectable U within the cells. The cells themselves are bound together by a bone/organic matter/uranium/pyrite/anatase mixture. Some of the fossilized cells show evidence of pressure collapse.